

HOKKAIDO SUMMER INSTITUTE 2024

HOKKAIDO UNIVERSITY



Magnetic spectroscopy experiments as a probe of the microscopic electronic properties of materials

<https://hokkaidosummerinstitute.oia.hokudai.ac.jp/en/courses/CourseDetail=G006>

ANDREJ ZORKO 

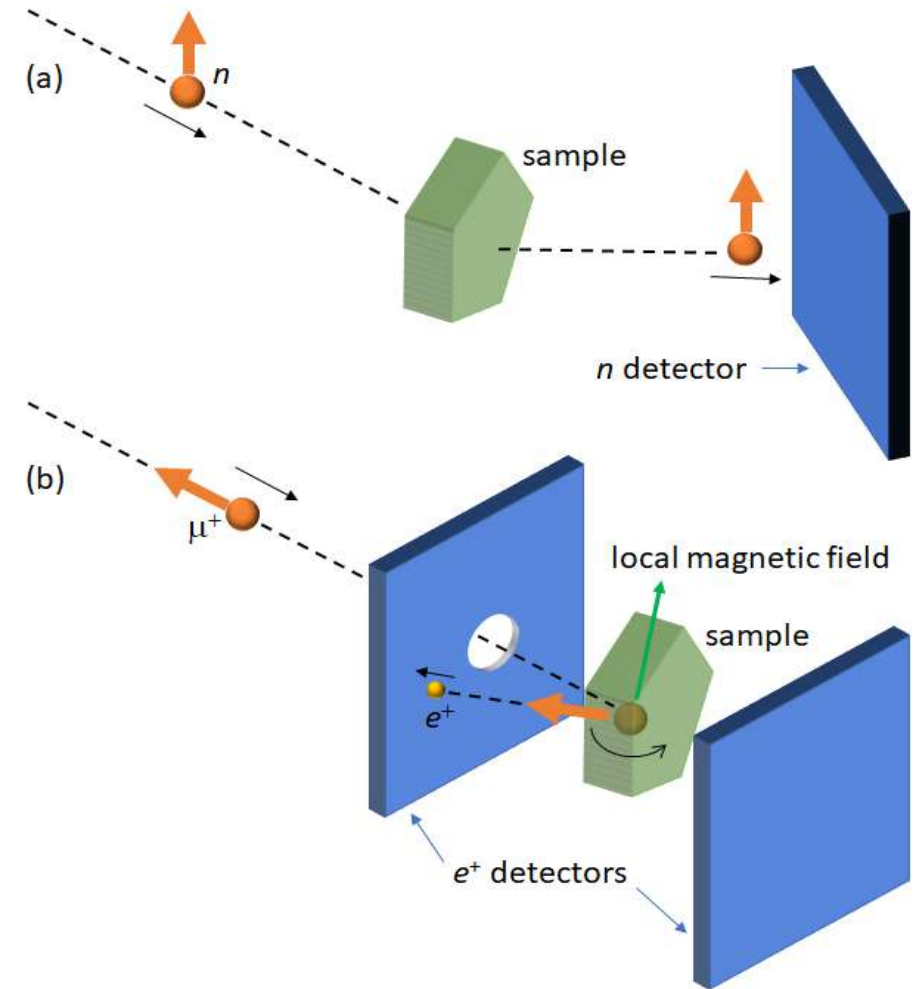
 JOŽEF STEFAN INSTITUTE, LJUBLJANA, SLOVENIA

 FACULTY OF MATHEMATICS AND PHYSICS, UNIVERSITY OF LJUBLJANA, SLOVENIA

Sapporo, 29. July – 2. August 2024

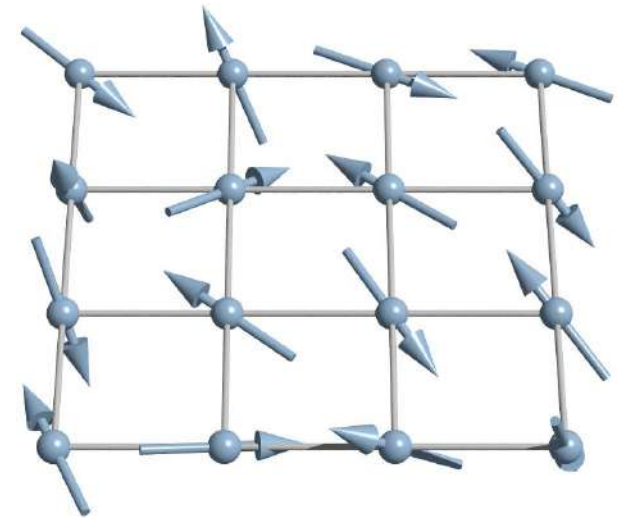
Outline

- Introduction to magnetism
- Probing magnetism: conventional bulk and scattering techniques
- Local probes of magnetism
- Electron spin resonance (ESR)
- Nuclear magnetic resonance (NMR)
- Muon spectroscopy (μ SR)
- Summary: strengths, limitations and complementarity of local probes



Outline

- Introduction to magnetism
- Probing magnetism: conventional bulk and scattering techniques
- Local probes of magnetism
- Electron spin resonance (ESR)
- Nuclear magnetic resonance (NMR)
- Muon spectroscopy (μ SR)
- Summary: strengths, limitations and complementarity of local probes



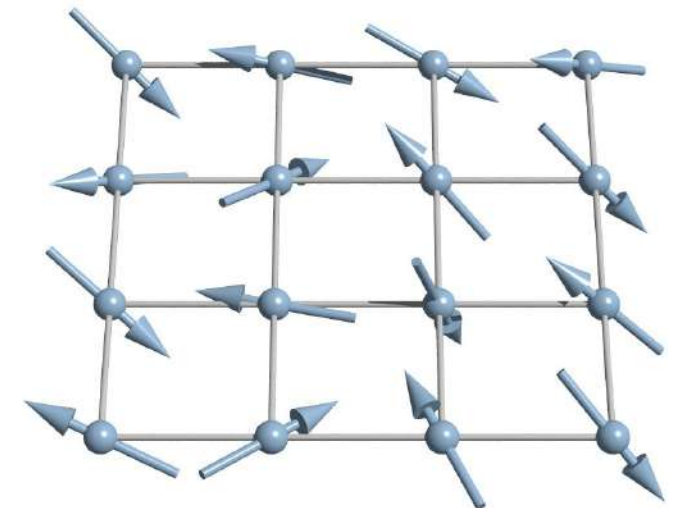
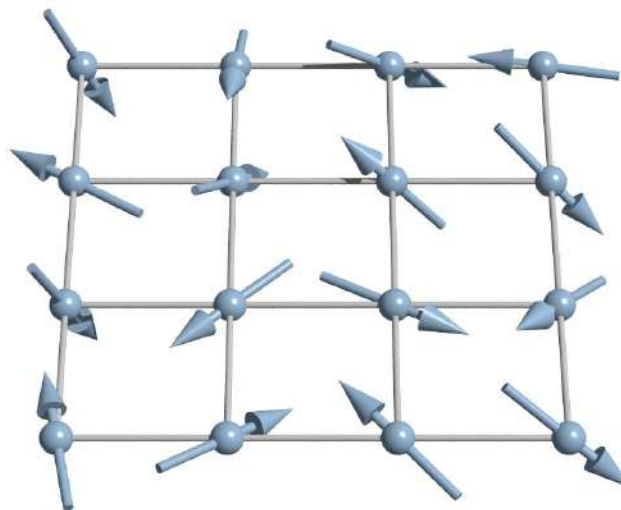
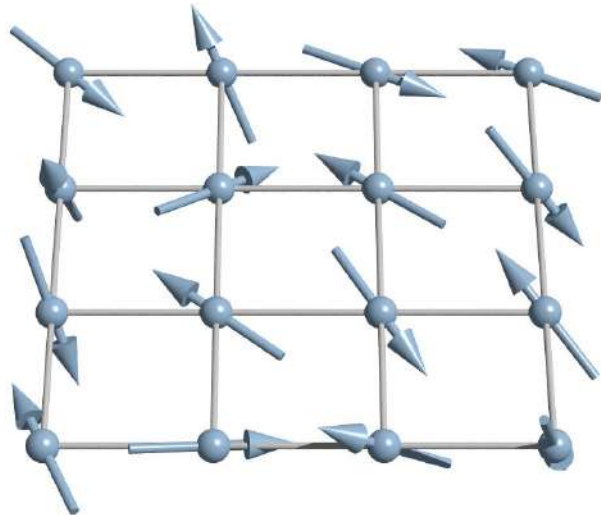
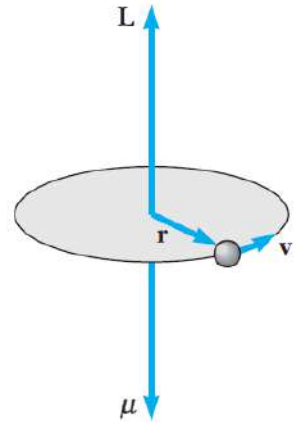
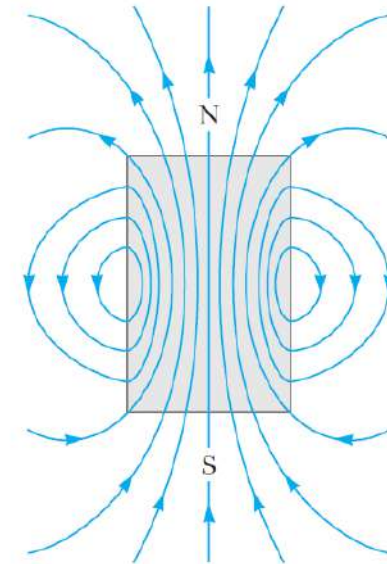
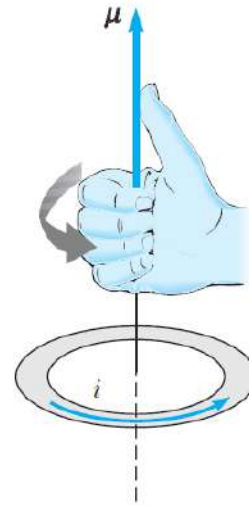
Introduction to Magnetism

□ Magnetic moments:

$$\vec{\mu} = \vec{\mu}_o + \vec{\mu}_s = -\frac{\mu_B}{\hbar}(\vec{L} + g\vec{S})$$

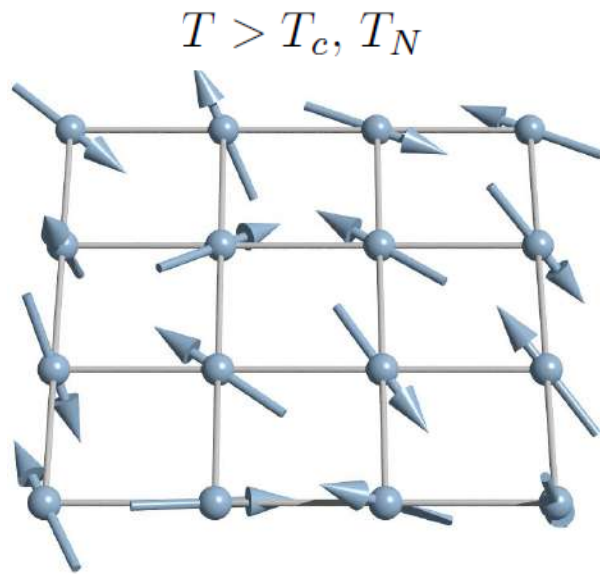
$$\mu_B = \frac{e_0\hbar}{2m_e} = 9,27 \times 10^{-24} \text{ Am}^2$$

□ Electric insulators: localized moments

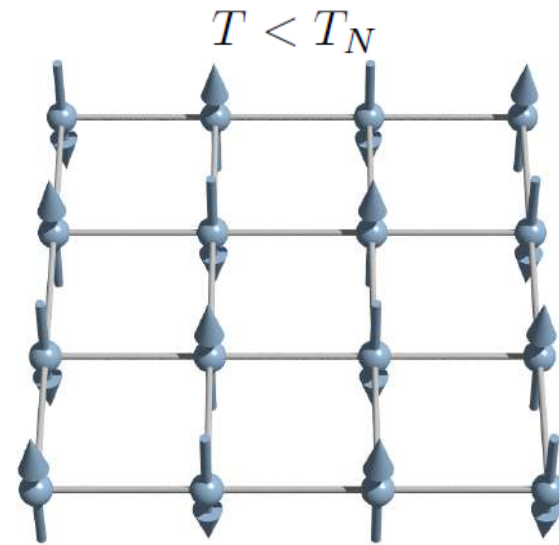


The Many Faces of Magnetism

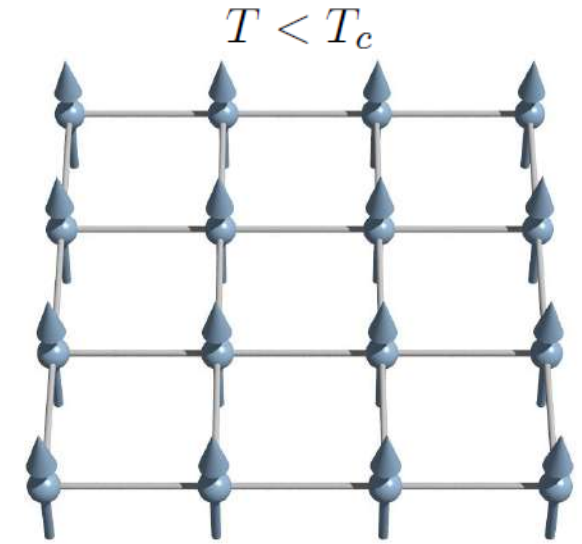
□ Exchange interactions: $\mathcal{H} = J \sum_{(i,j)} \vec{S}_i \cdot \vec{S}_j$



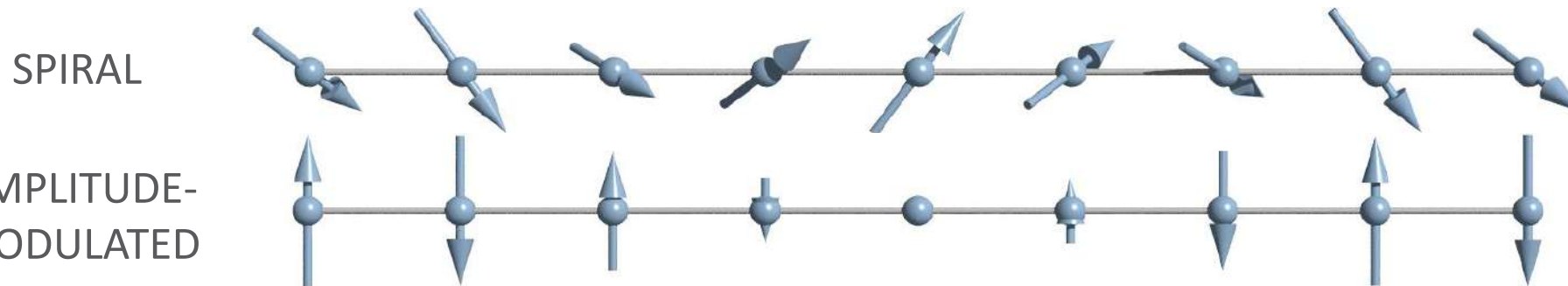
PARAMAGNET



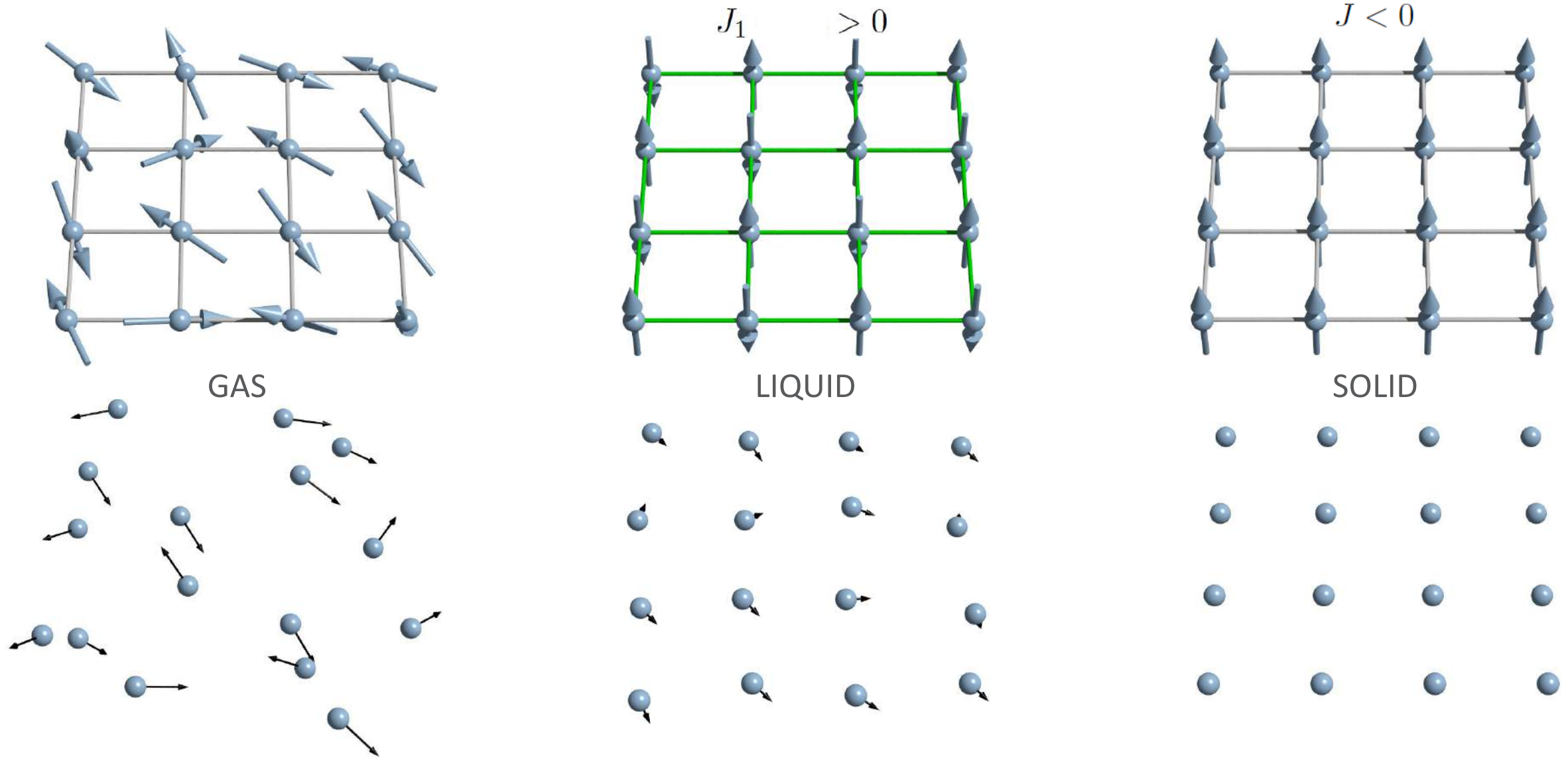
ANTIFERROMAGNET: $J > 0$



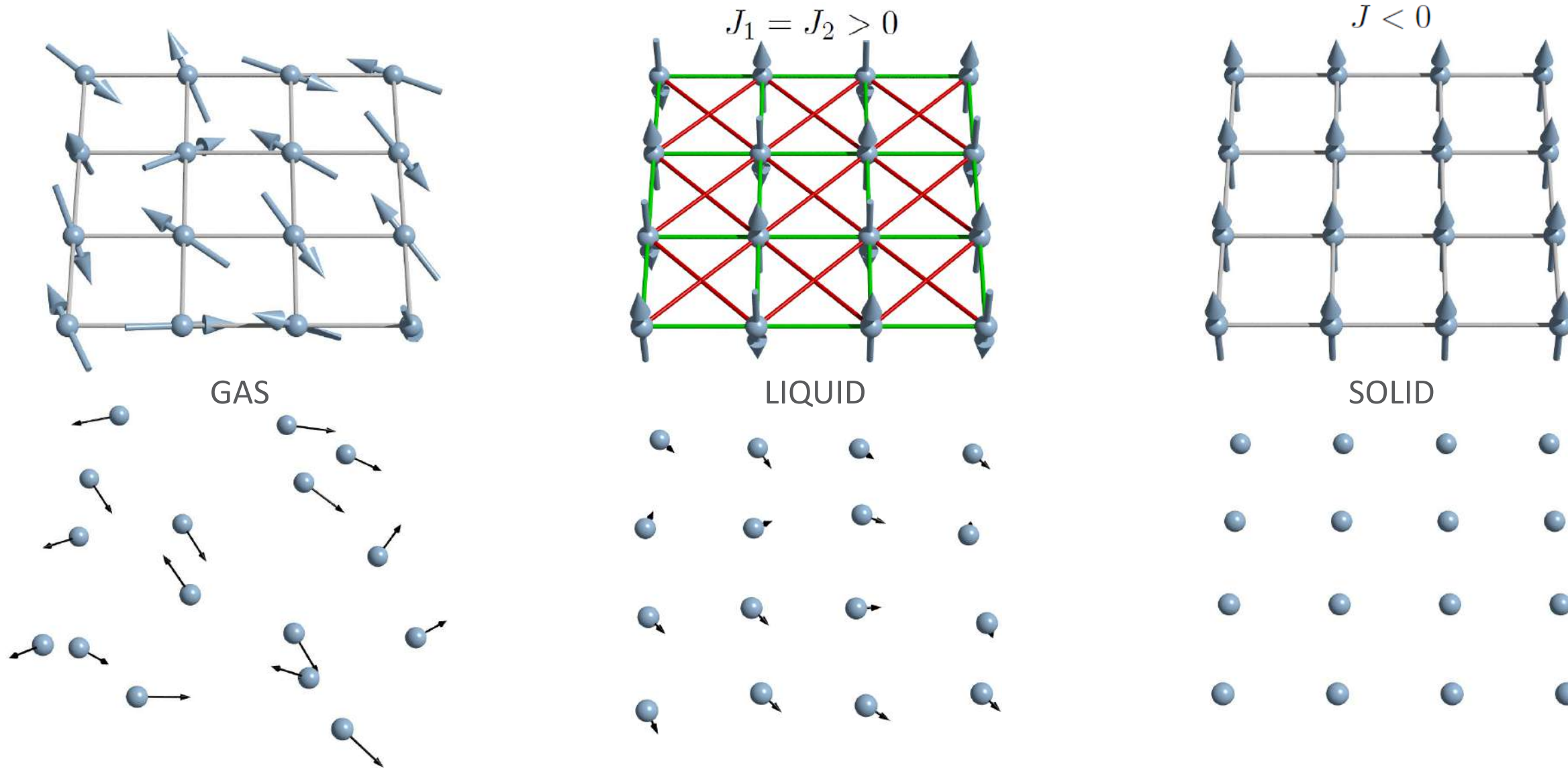
FERROMAGNET: $J < 0$



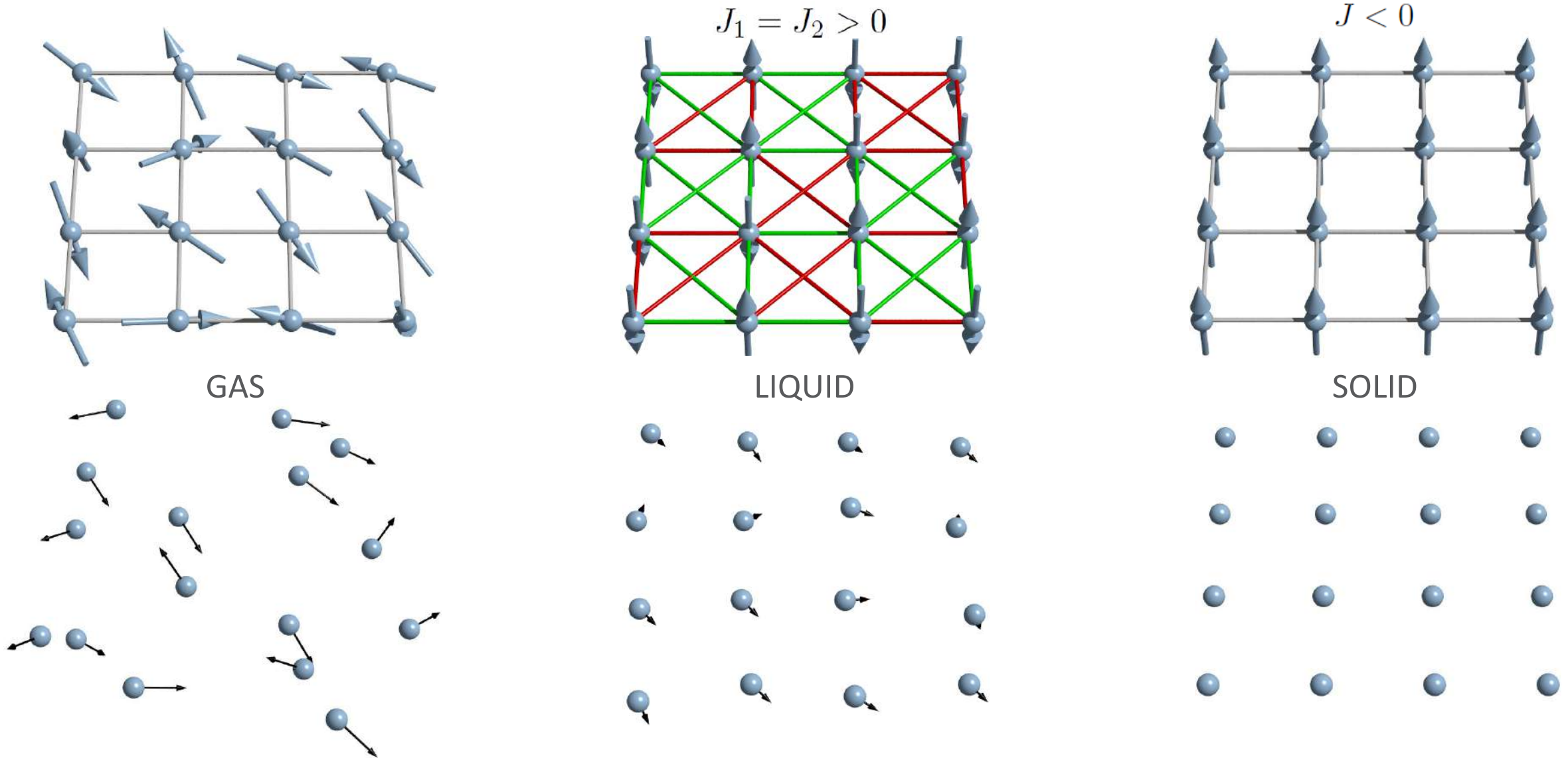
Analogy with States of Matter



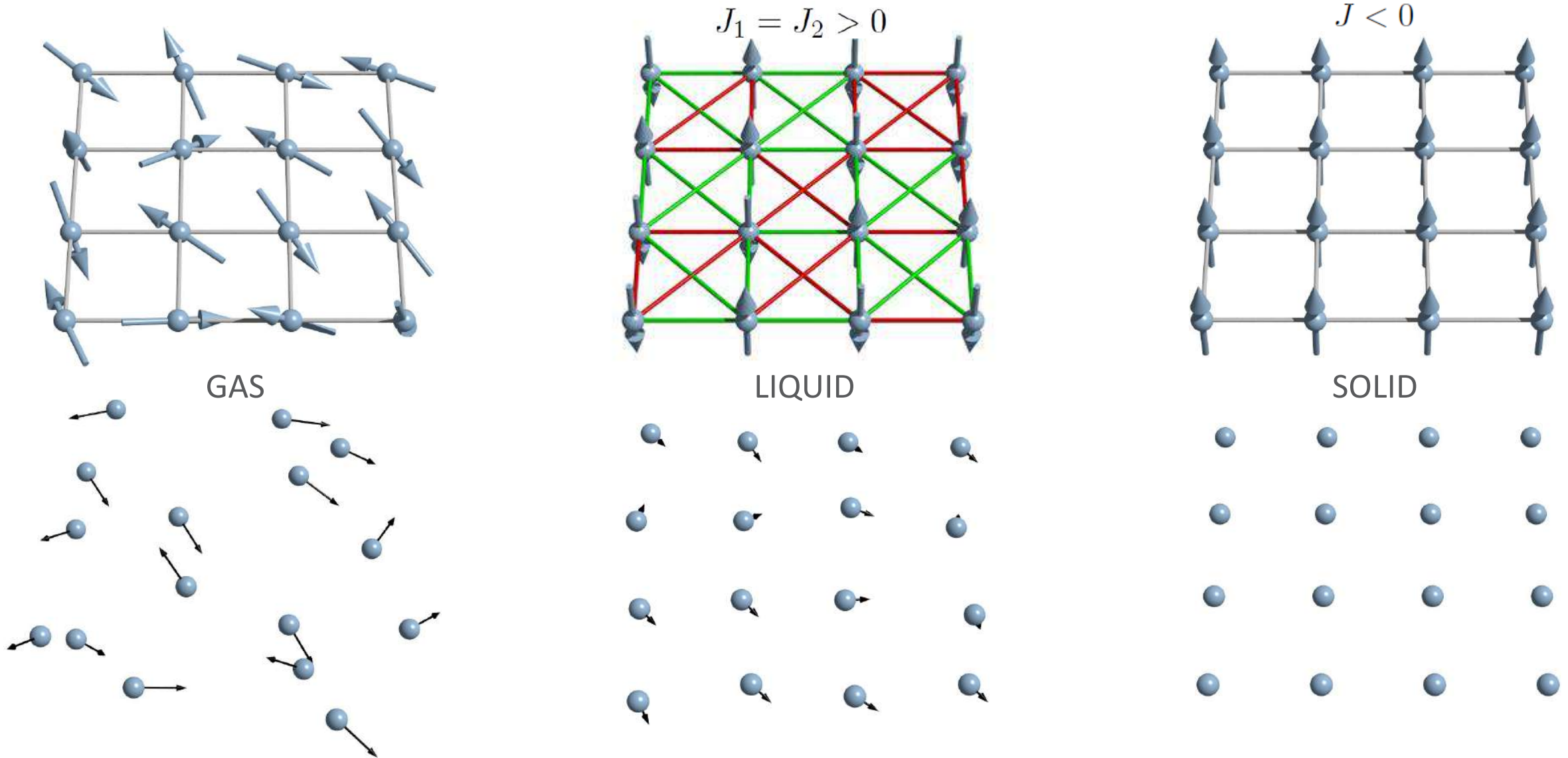
Analogy with States of Matter



Analogy with States of Matter

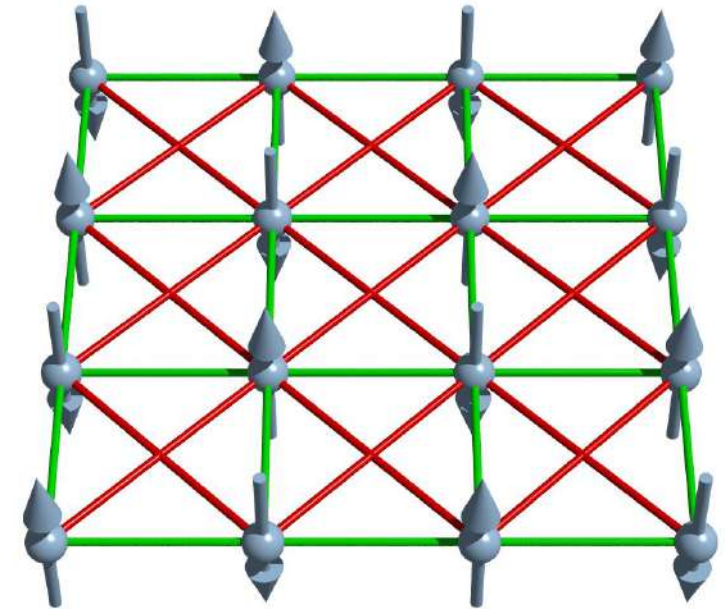


Analogy with States of Matter



Frustration in Magnetism

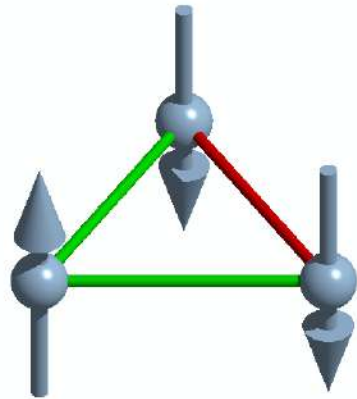
- Geometrical frustration: an inability to simultaneously minimize all local interactions as a consequence of the frustration of the forces or geometry.



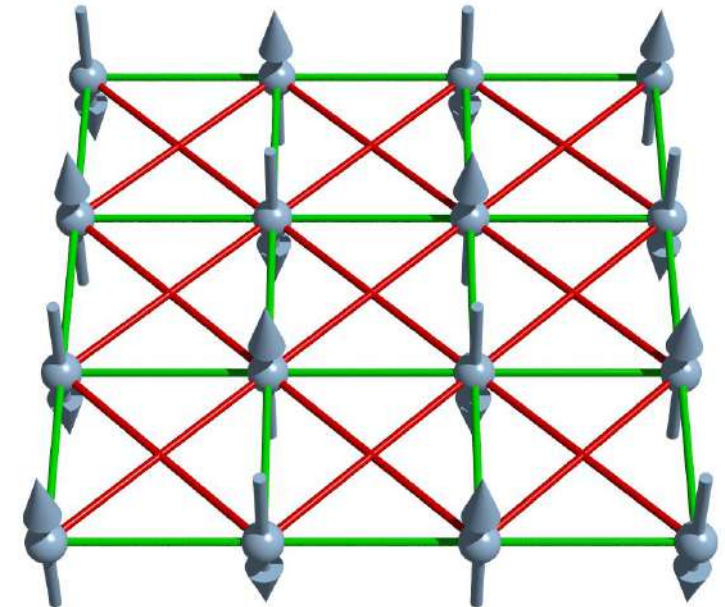
$$\mathcal{H} = \sum_{(i,j)} J_{ij} \vec{S}_i \cdot \vec{S}_j$$

Frustration in Magnetism

- Geometrical frustration: an inability to simultaneously minimize all local interactions as a consequence of the frustration of the forces or geometry.
- Generic example: Ising AFM triangle



$$\mathcal{H} = J \sum_{\Delta} S_i^z S_j^z$$

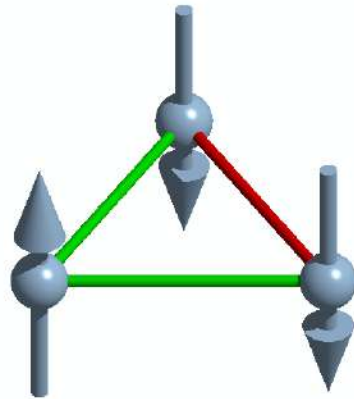


$$\mathcal{H} = \sum_{(i,j)} J_{ij} \vec{S}_i \cdot \vec{S}_j$$

Frustration in Magnetism

□ Geometrical frustration: an inability to simultaneously minimize all local interactions as a consequence of the frustration of the forces or geometry.

□ Generic example: Ising AFM triangle



$$\mathcal{H} = J \sum_{\Delta} S_i^z S_j^z$$

□ Macroscopic degeneracy: disordered state

Antiferromagnetism. The Triangular Ising Net

G. H. WANNIER

Bell Telephone Laboratories, Murray Hill, New Jersey

(Received February 11, 1950)

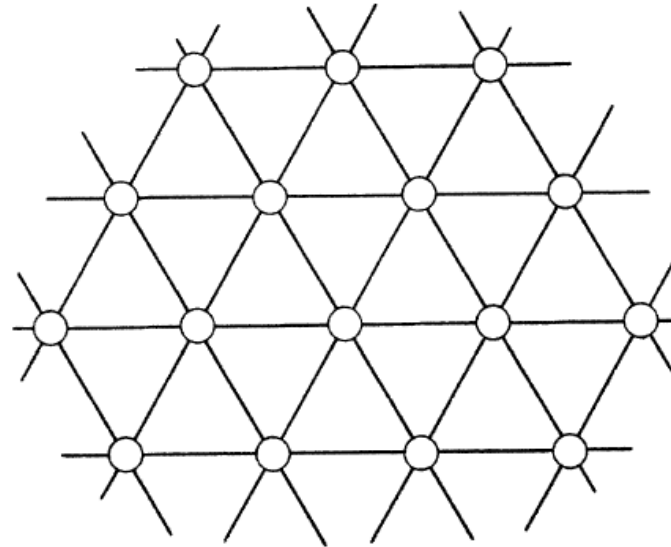


FIG. 2. Triangular Ising net. No perfectly regular antiferromagnetic arrangement can be fitted into this structure.



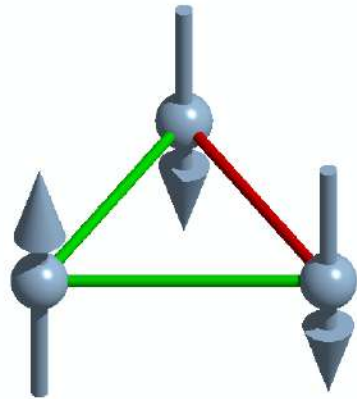
Wannier, *Phys. Rev.*
79, 357 (1950)



Frustration in Magnetism

□ Geometrical frustration: an inability to simultaneously minimize all local interactions as a consequence of the frustration of the forces or geometry.

□ Generic example: Ising AFM triangle



$$\mathcal{H} = J \sum_{\Delta} \vec{S}_i \cdot \vec{S}_j$$

□ Many-body entanglement: novel excitations

RESONATING VALENCE BONDS: A NEW KIND OF INSULATOR?*

P. W. Anderson
 Bell Laboratories, Murray Hill, New Jersey 07974
 and
 Cavendish Laboratory, Cambridge, England

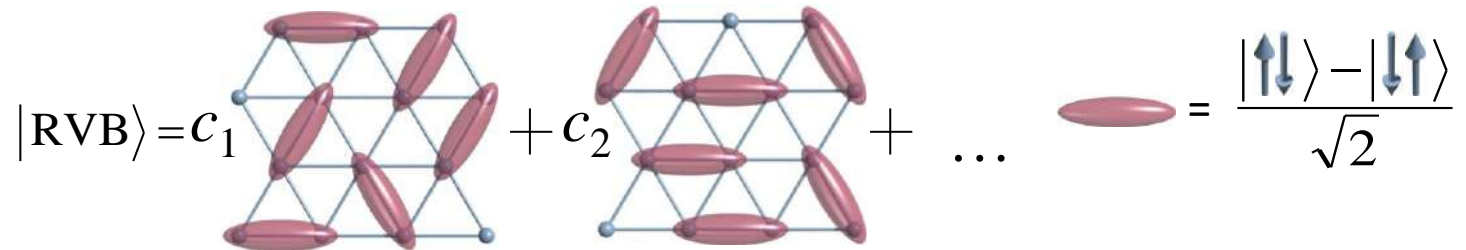
(Received December 5, 1972; Invited**)

ABSTRACT

The possibility of a new kind of electronic state is pointed out, corresponding roughly to Pauling's idea of "resonating valence bonds" in metals. As observed by Pauling, a pure state of this type would be insulating; it would represent an alternative state to the Néel antiferromagnetic state for S = 1/2. An estimate of its energy is made in one case.

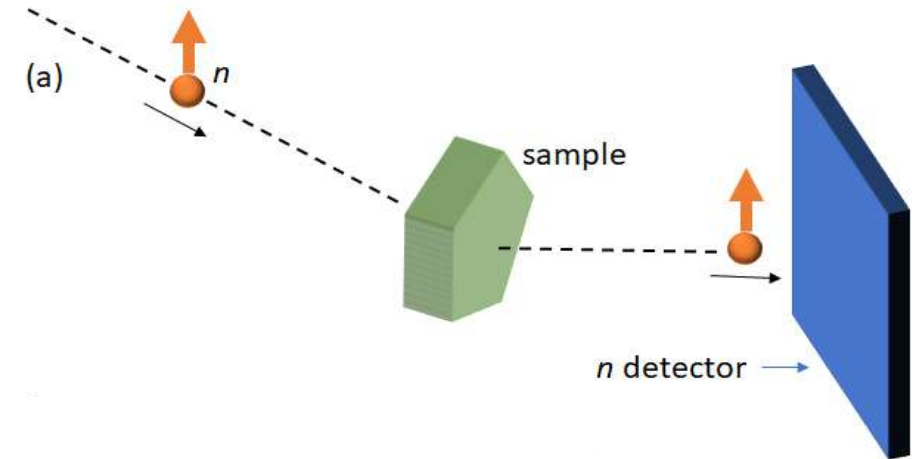


Anderson, Mat. Res. Bull. 8, 153 (1973)



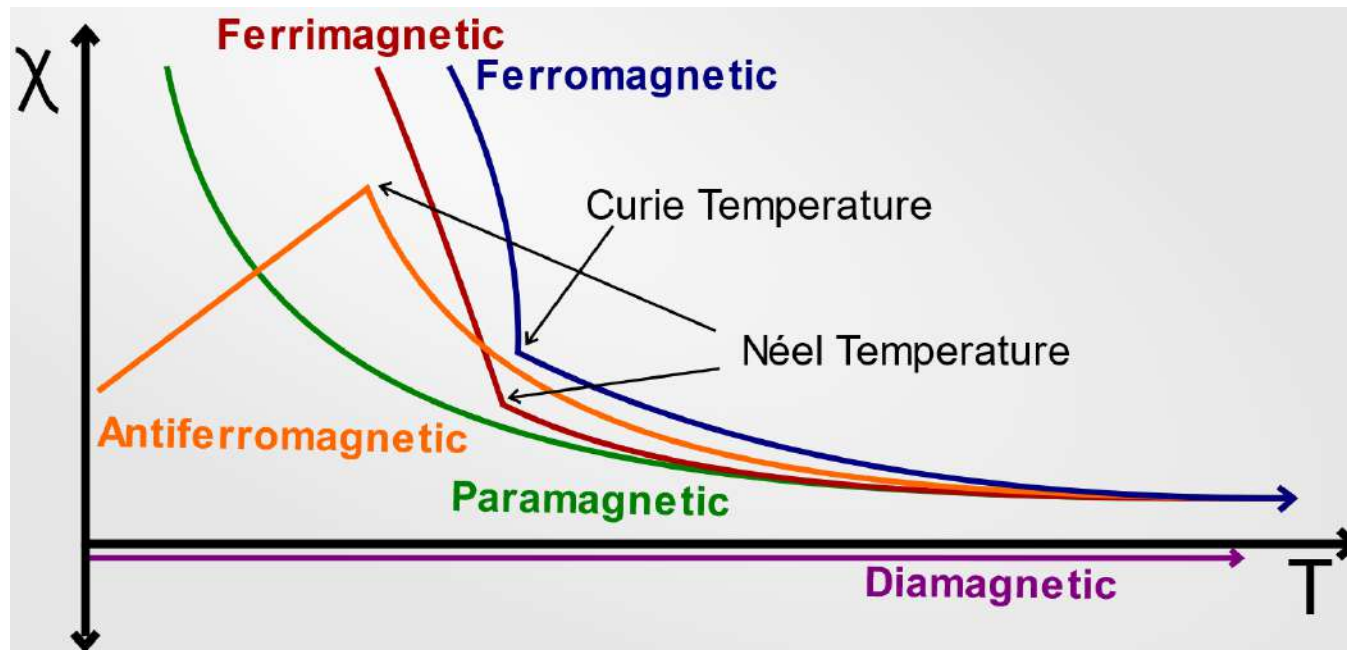
Outline

- Introduction to magnetism
- Probing magnetism: conventional bulk and scattering techniques
- Local probes of magnetism
- Electron spin resonance (ESR)
- Nuclear magnetic resonance (NMR)
- Muon spectroscopy (μ SR)
- Summary: the complementarity of local probes



Bulk Magnetization/Susceptibility

□ Detecting phase transitions:



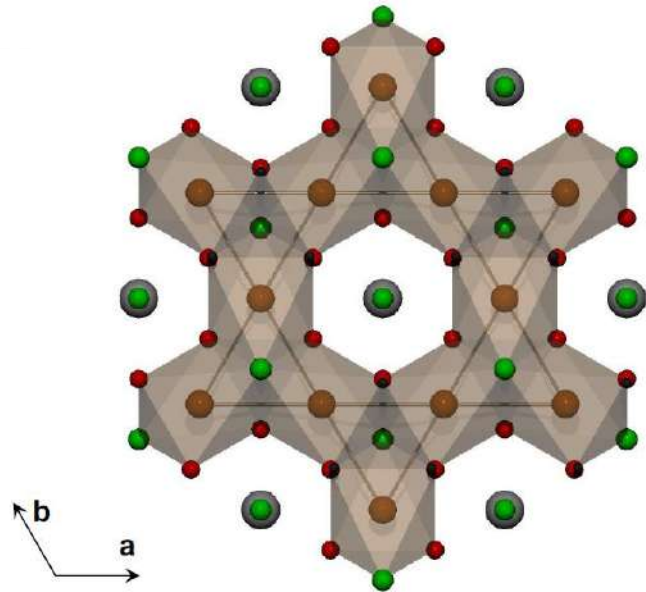
<https://mstudent.com>



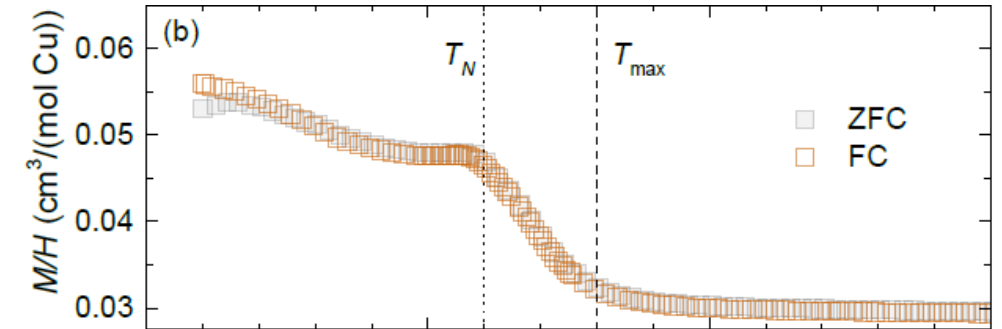
Bulk Magnetization/Susceptibility

- Averaging over the sample (constant B):
uniform response

$$\chi(q=0, \omega)$$



$\text{YCu}_3(\text{OH})_6\text{Cl}_3$: kagome AFM



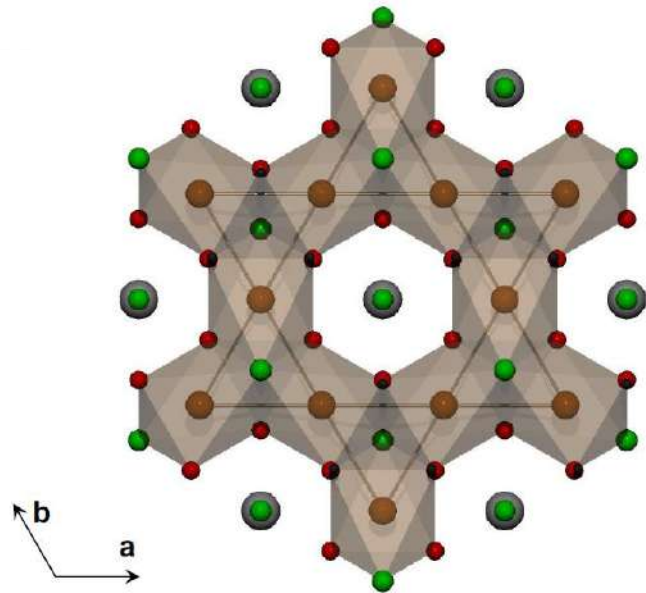
Arh *et al.*, Phys. Rev. Lett. **125**, 027203 (2020)



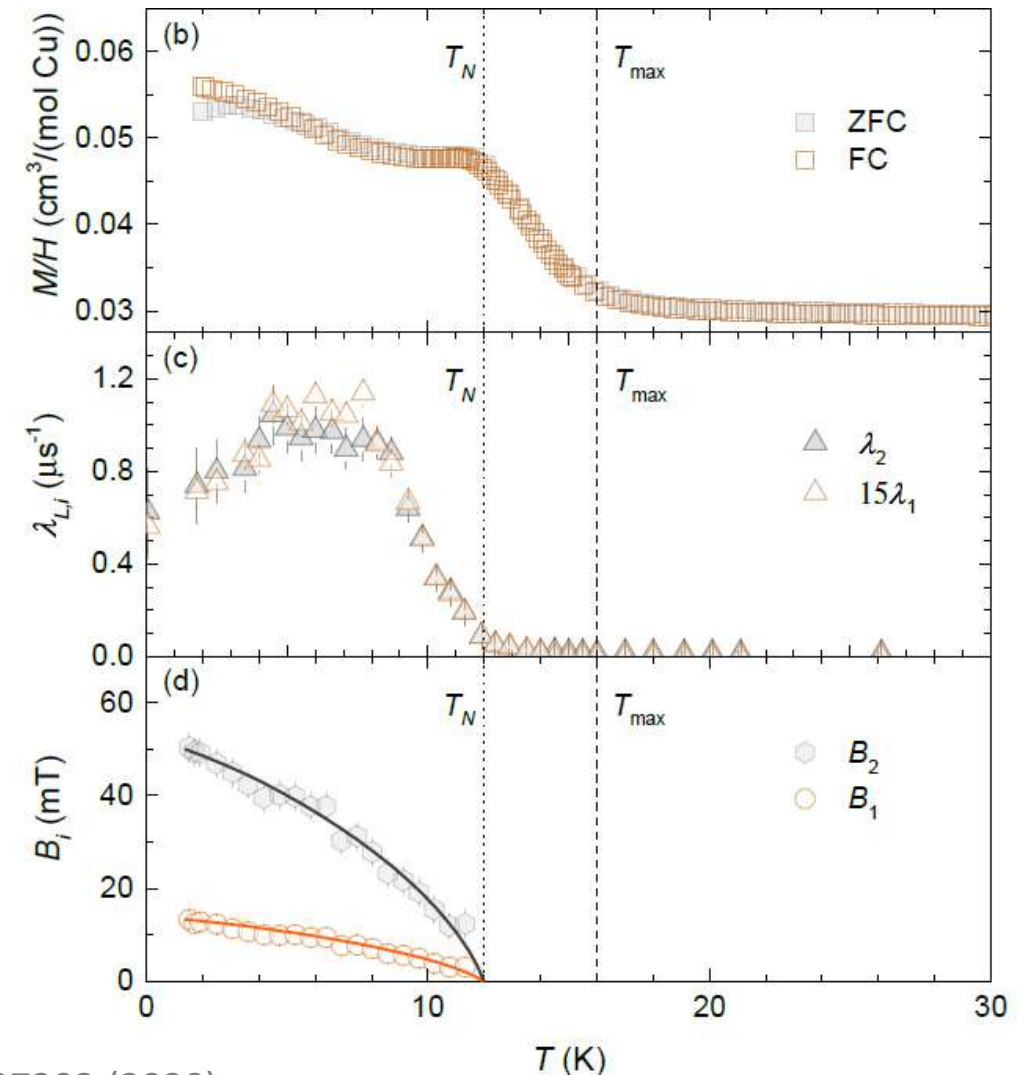
Bulk Magnetization/Susceptibility

- Averaging over the sample (constant B):
uniform response

$$\chi(q=0, \omega)$$



$\text{YCu}_3(\text{OH})_6\text{Cl}_3$: kagome AFM

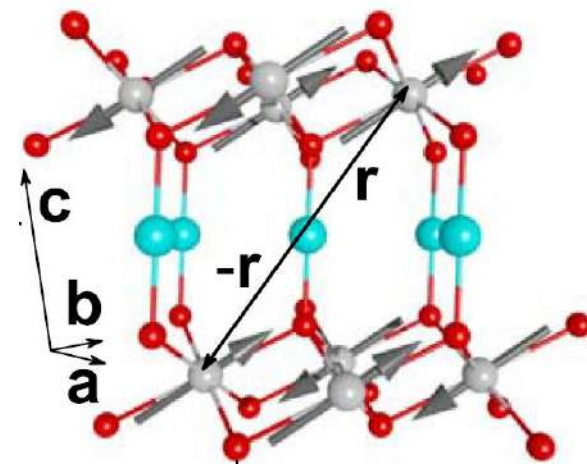
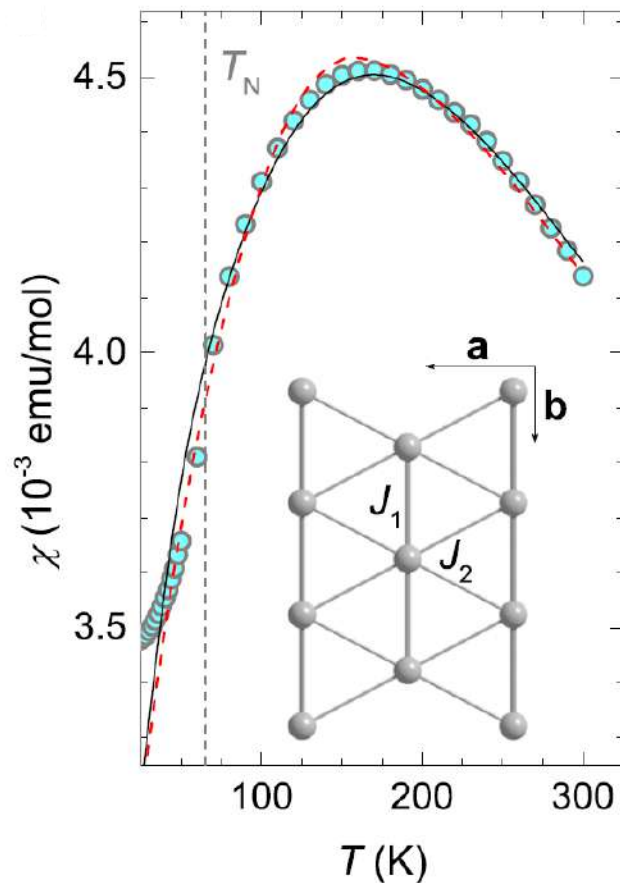


Arh *et al.*, Phys. Rev. Lett. **125**, 027203 (2020)

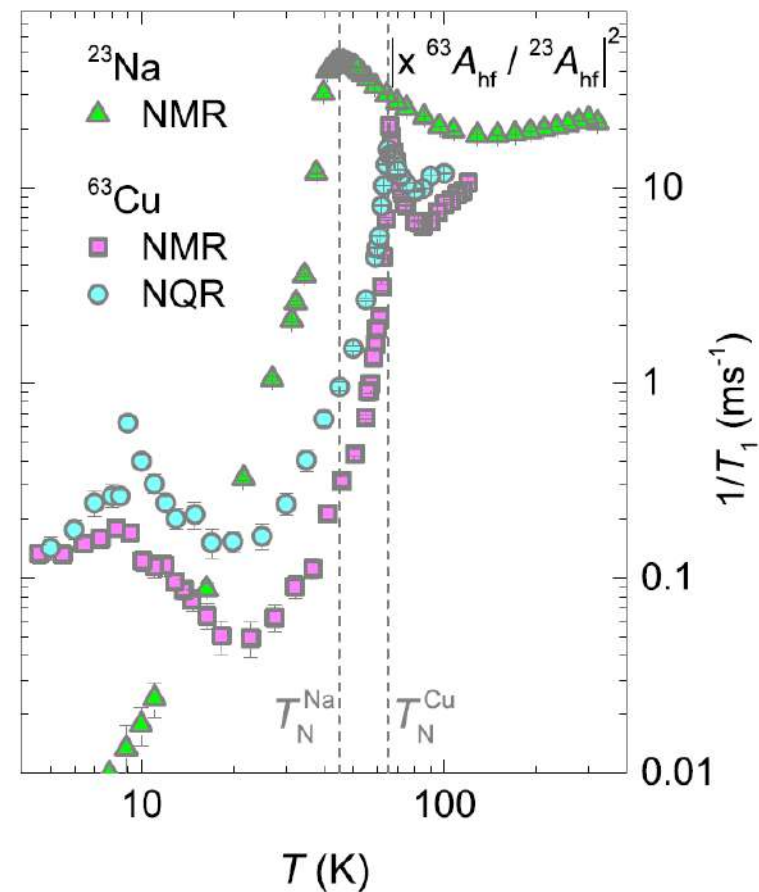


Bulk Magnetization/Susceptibility

□ Small bulk response at T_N :



NaMnO₂ & CuMnO₂:
triangular AFM



Zorko *et al.*, *Sci. Rep.* **5**, 9272 (2015)



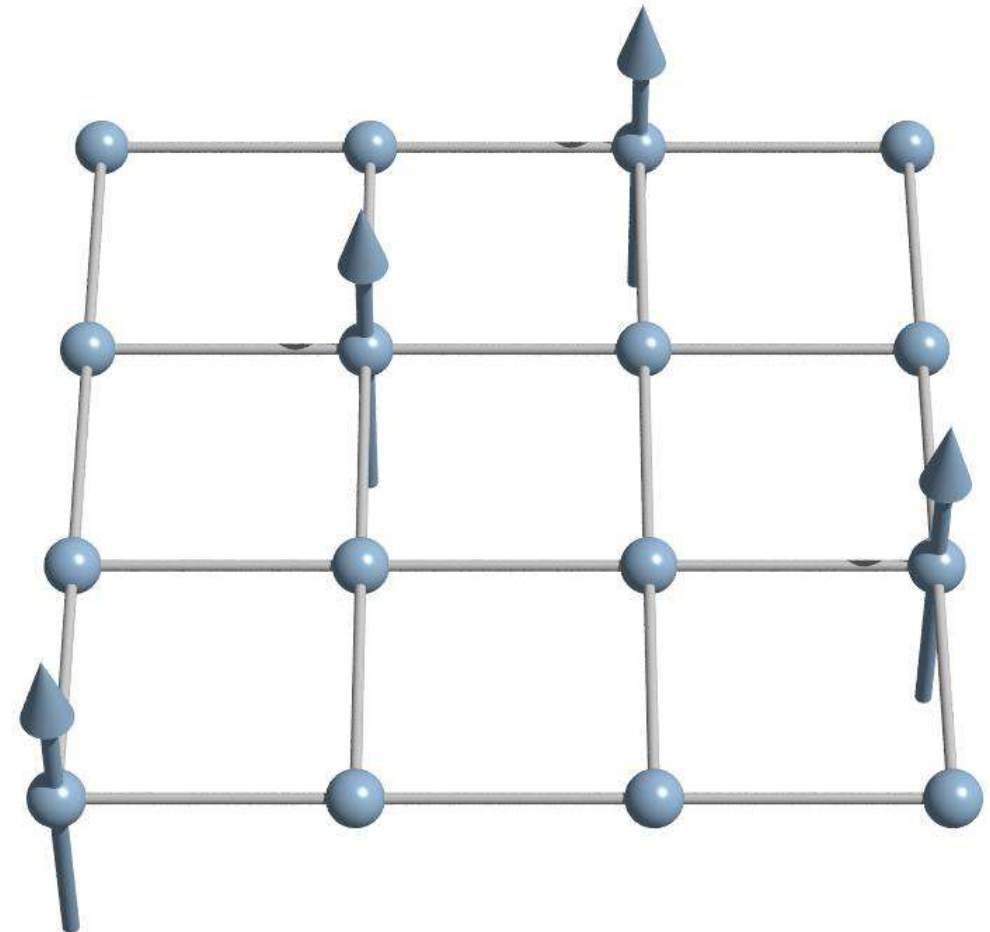
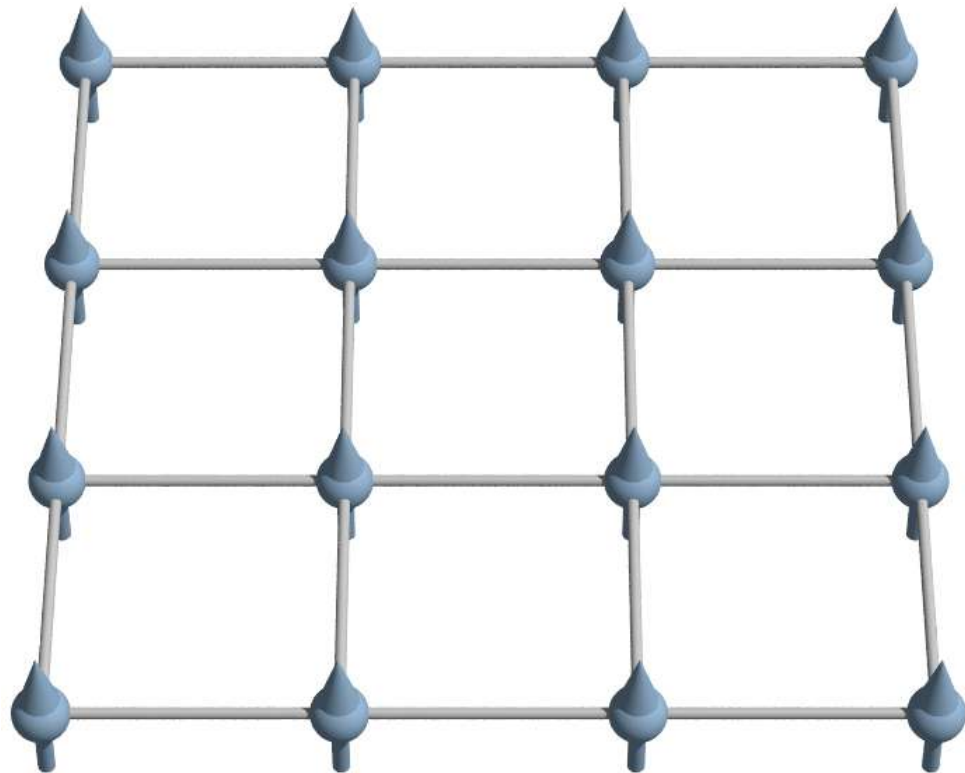
Bulk Magnetization/Susceptibility



Small ordered moments

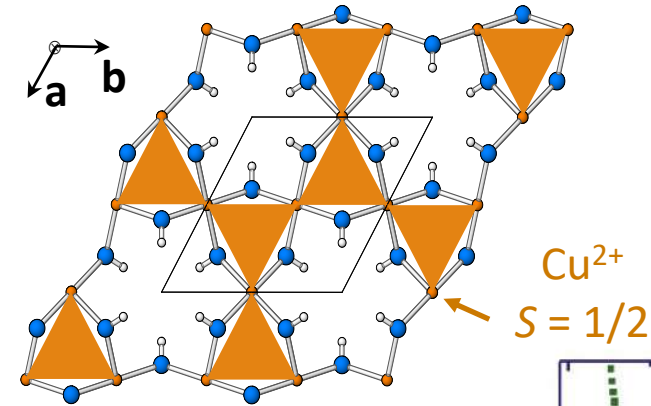
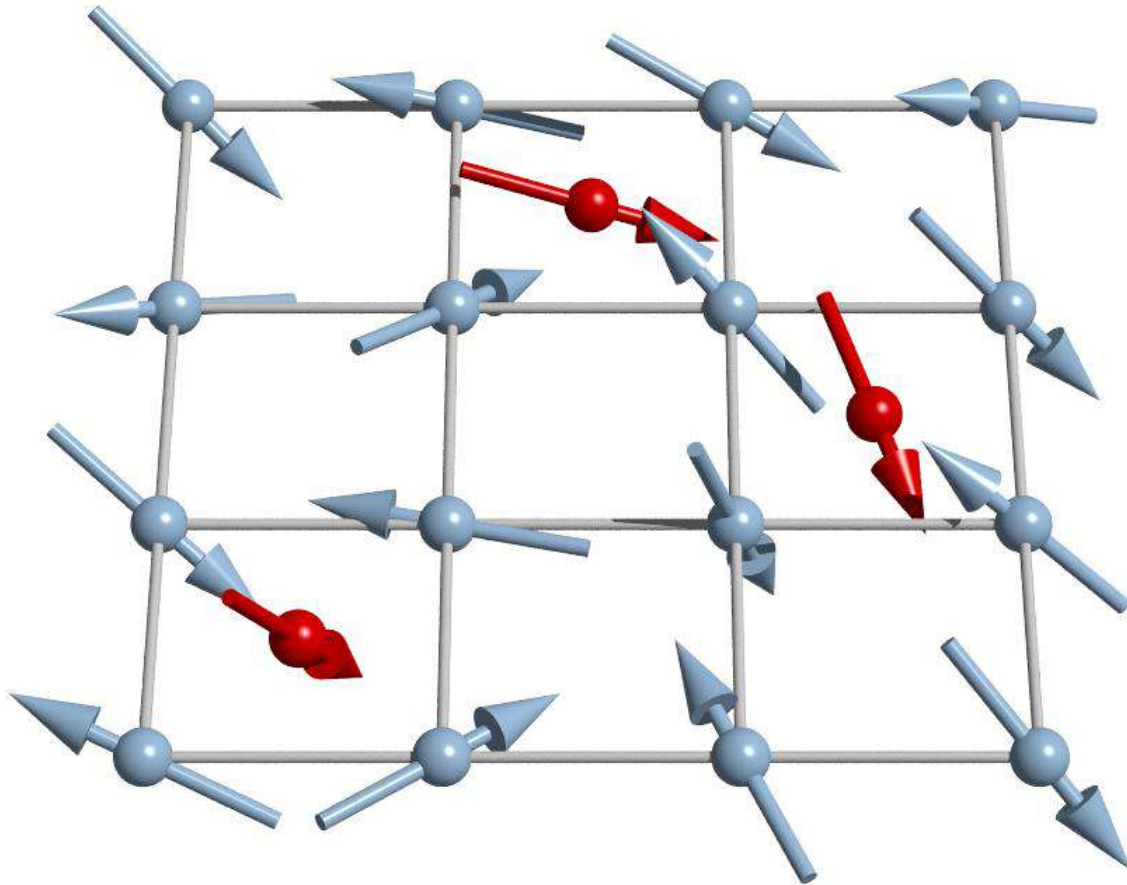
vs.

diluted moments:

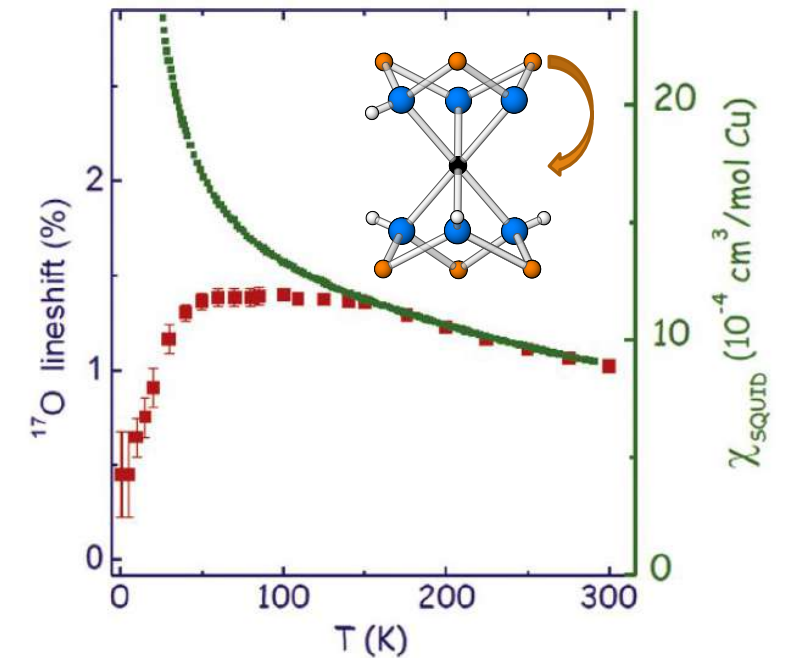


Bulk Magnetization/Susceptibility

□ Averaging over different contributions:



ZnCu₃(OH)₆Cl₂:
kagome AFM

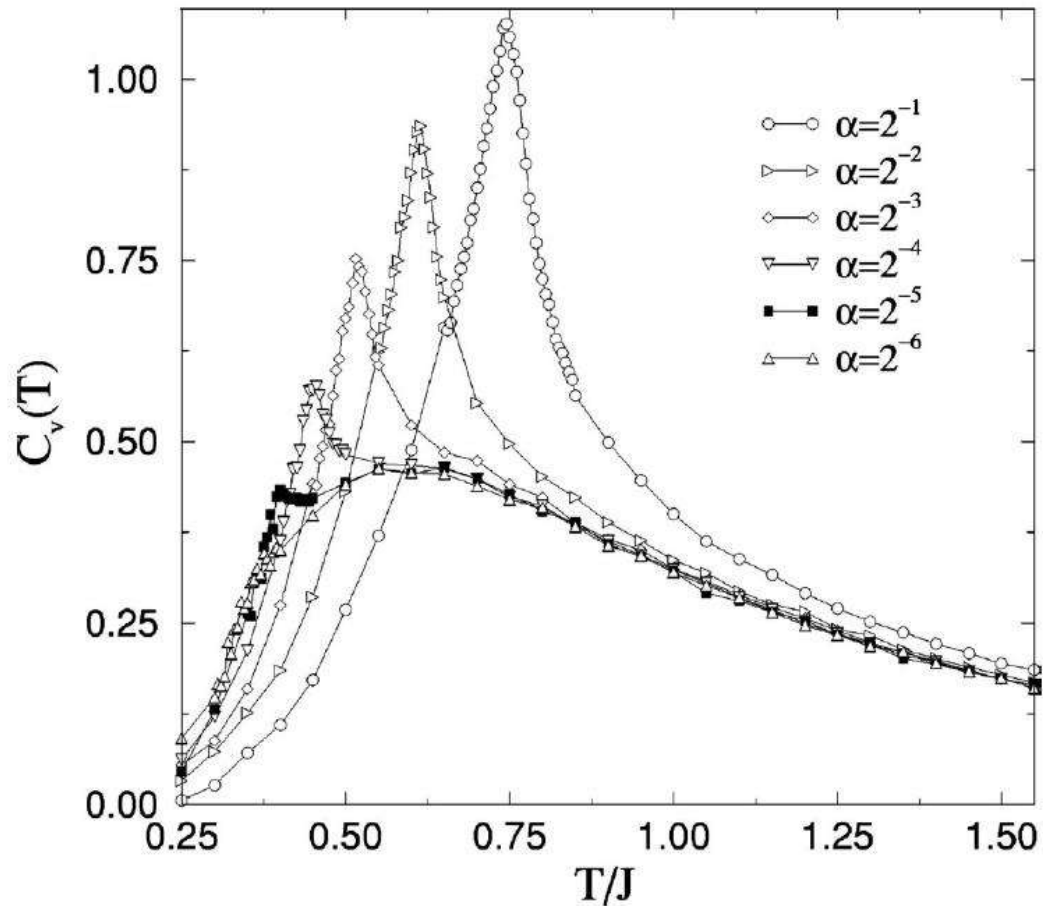


Olariu *et al.*, Phys. Rev. Lett. **100**, 087202 (2008)



Bulk Heat Capacity

□ Detecting phase transitions:



Sengupta *et al.*, Phys. Rev. B **68**, 094423 (2003)

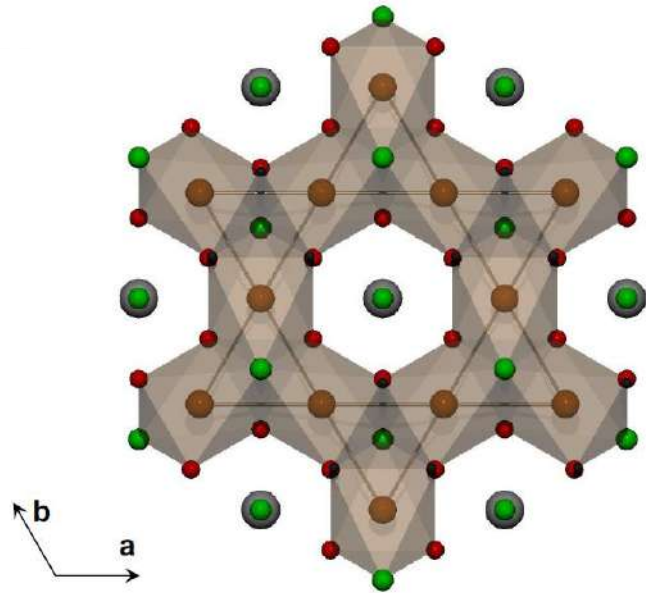


low-D magnets:
correlations far above T_N

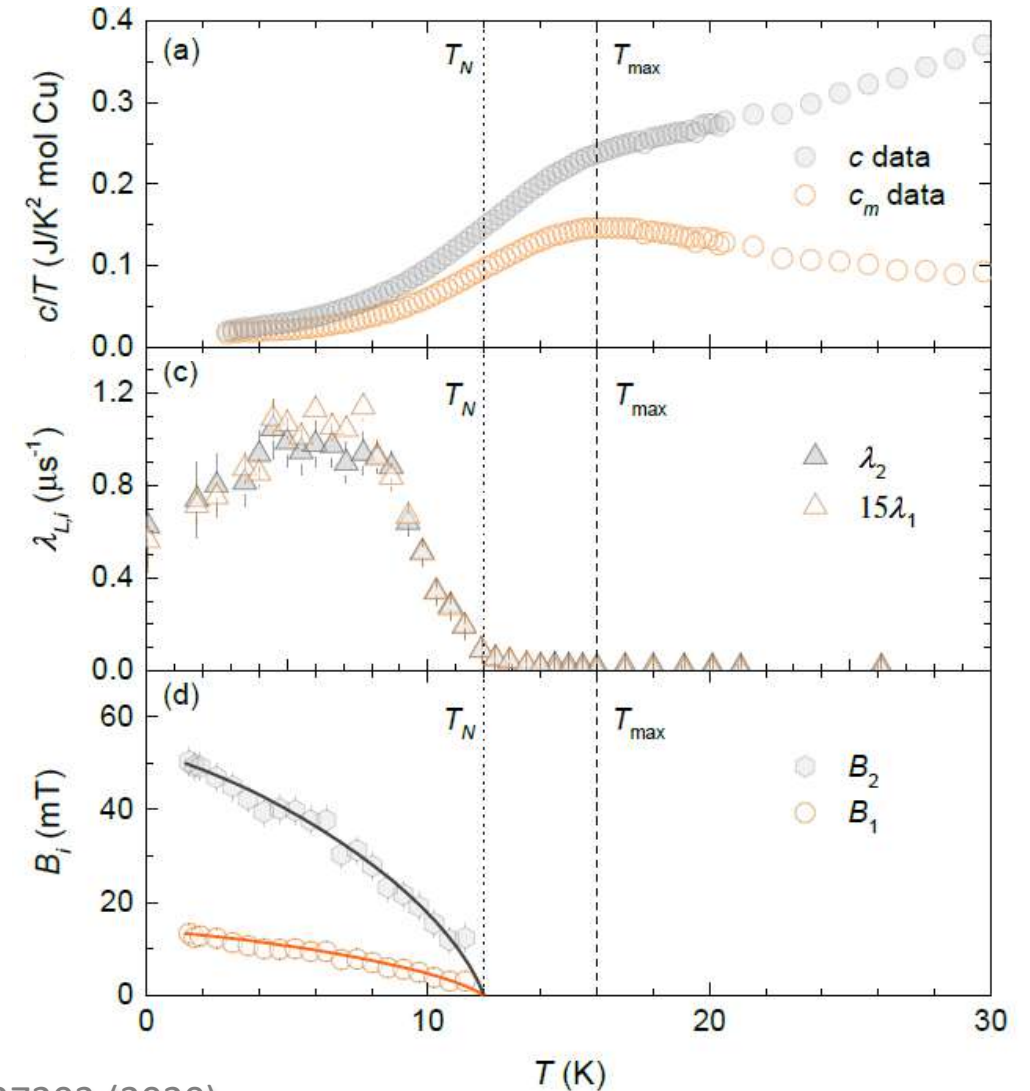


Bulk Heat Capacity

□ Small entropy release at T_N :



$\text{YCu}_3(\text{OH})_6\text{Cl}_3$: kagome AFM

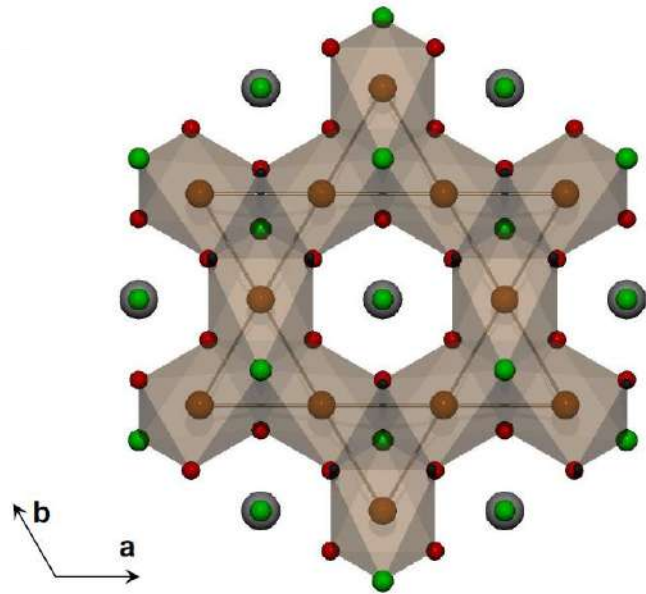


Arh *et al.*, Phys. Rev. Lett. **125**, 027203 (2020)

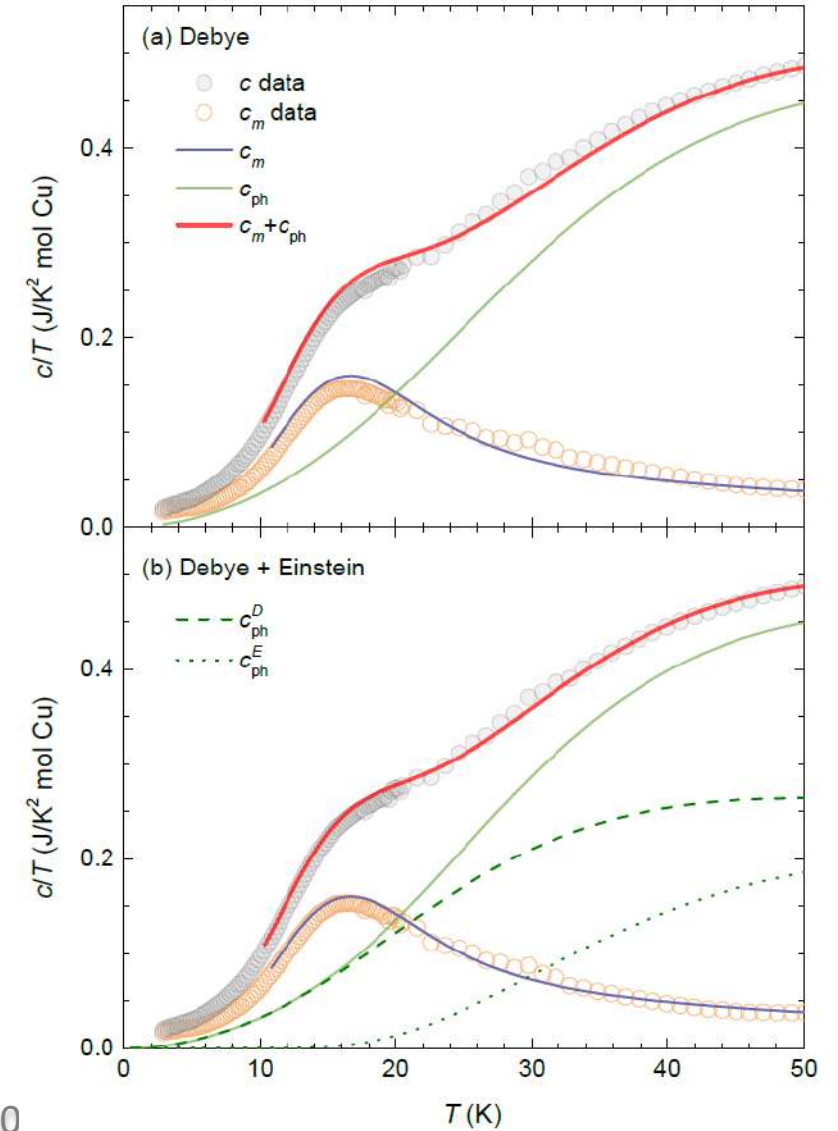


Bulk Heat Capacity

□ Magnetic c_p hard to extract:



$\text{YCu}_3(\text{OH})_6\text{Cl}_3$: kagome AFM



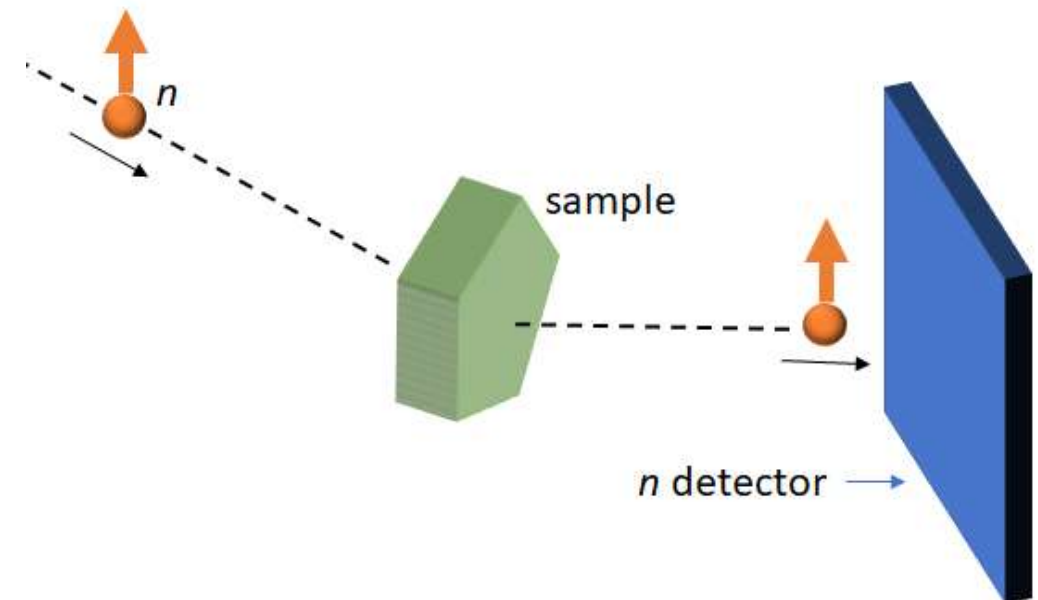
Arh *et al.*, Phys. Rev. Lett. **125**, 027203 (2020)



Magnetic Neutron Scattering

□ Properties of a neutron:

- zero electric charge: weak interaction with matter
- magnetic moment: magnetic interaction
$$\mu = -1.913\mu_N = -9.663 \times 10^{-27} \text{ Am}^2$$
- wavelengths comparable to interatomic distances: 0.3 – 15 Å
- energies comparable to structural and magnetic excitations: 1 – 1000 meV

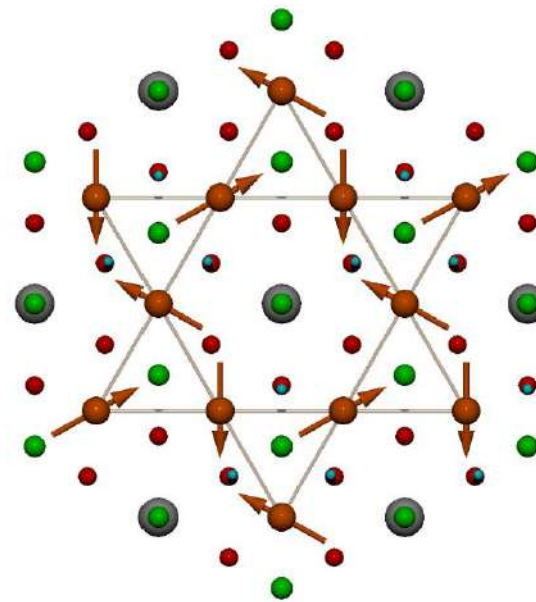


Magnetic Neutron Scattering

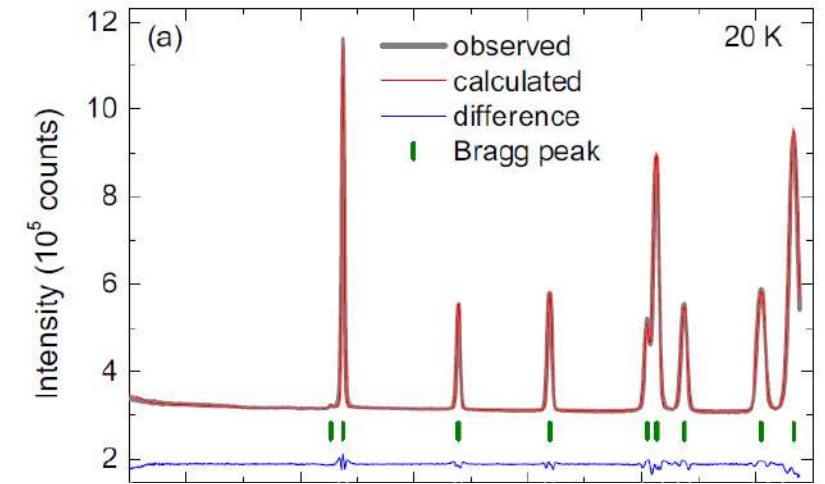
□ Magnetic long-range order: momentum-resolved insight



DMC, PSI, Switzerland



$\text{YCu}_3(\text{OH})_6\text{Cl}_3$: kagome AFM



Zorko *et al.*, Phys. Rev. B **100**, 144420 (2019)

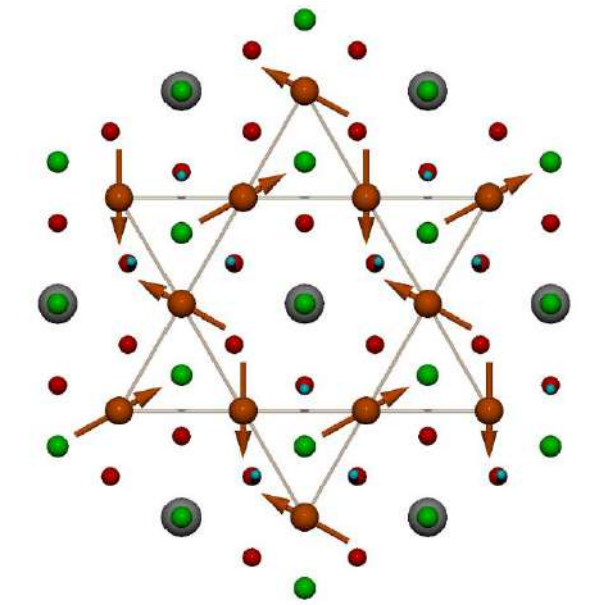


Magnetic Neutron Scattering

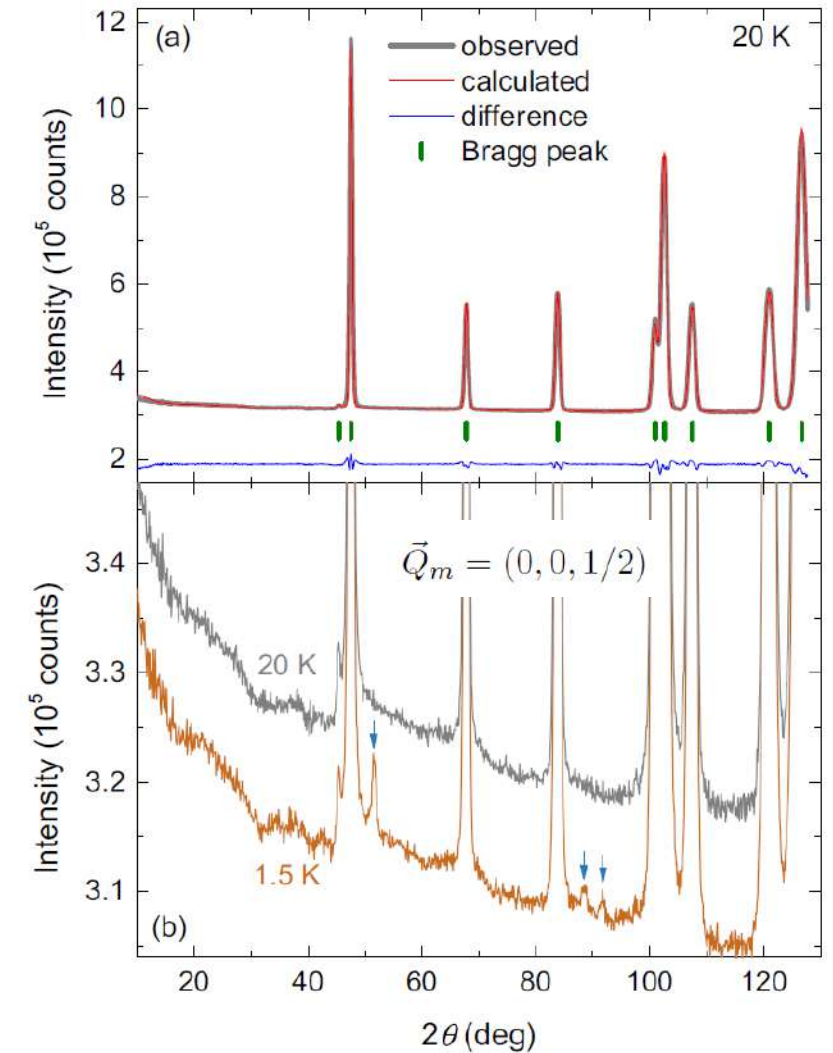
□ Magnetic long-range order: momentum-resolved insight



DMC, PSI, Switzerland



$\text{YCu}_3(\text{OH})_6\text{Cl}_3$: kagome AFM

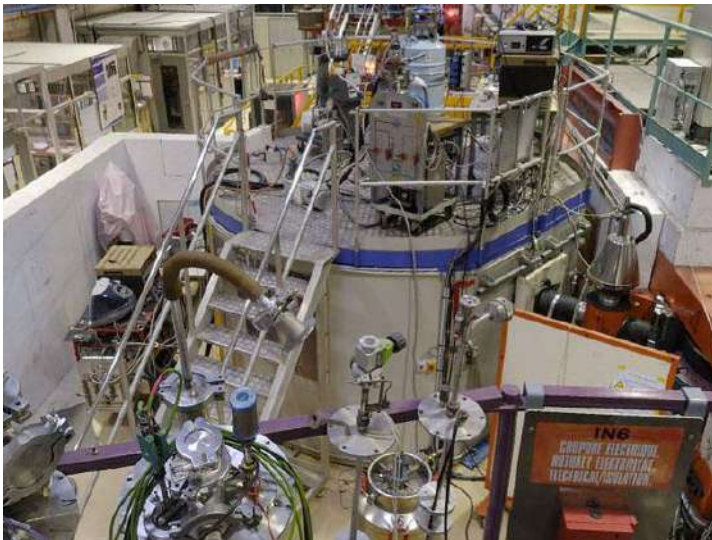


Zorko *et al.*, Phys. Rev. B **100**, 144420 (2019)

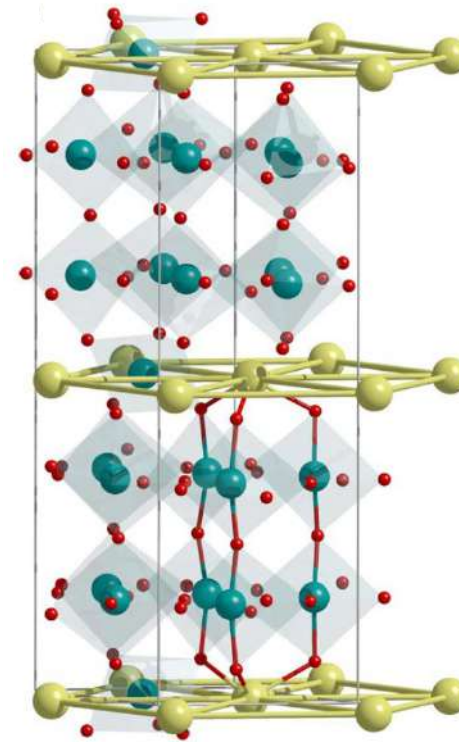


Magnetic Neutron Scattering

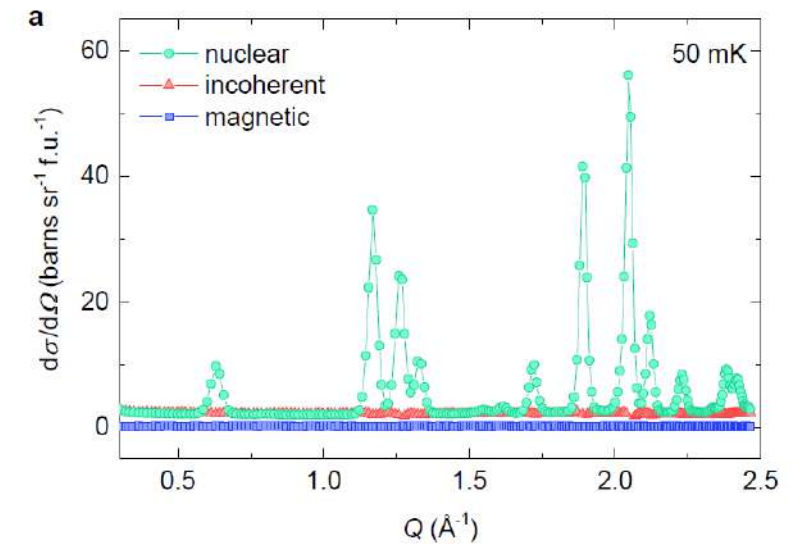
□ Polarized neutrons:



D7, ILL, France



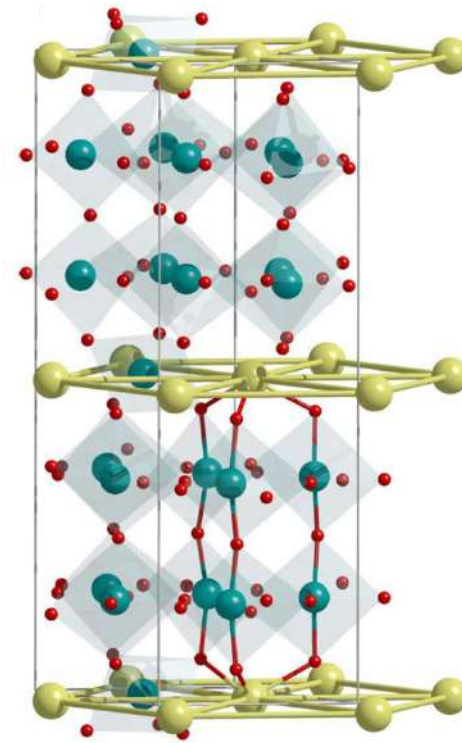
$\text{NdTa}_7\text{O}_{19}$:
triangular AFM



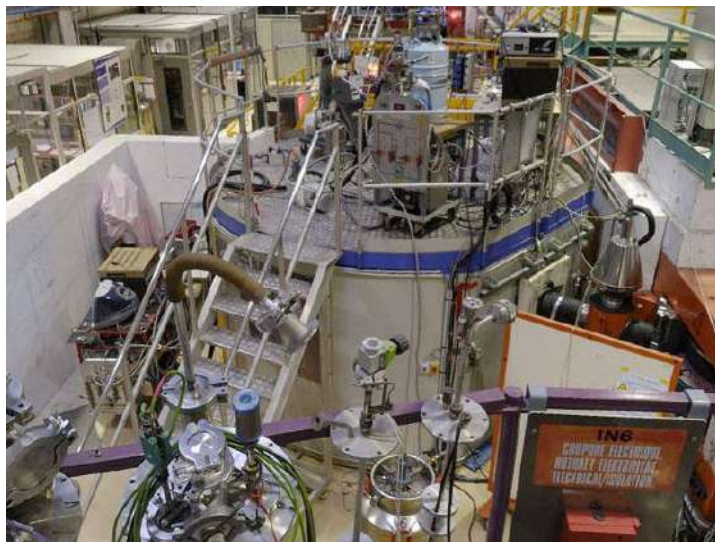
Arh *et al.*, Nat. Mater. **21**, 416 (2022).

Magnetic Neutron Scattering

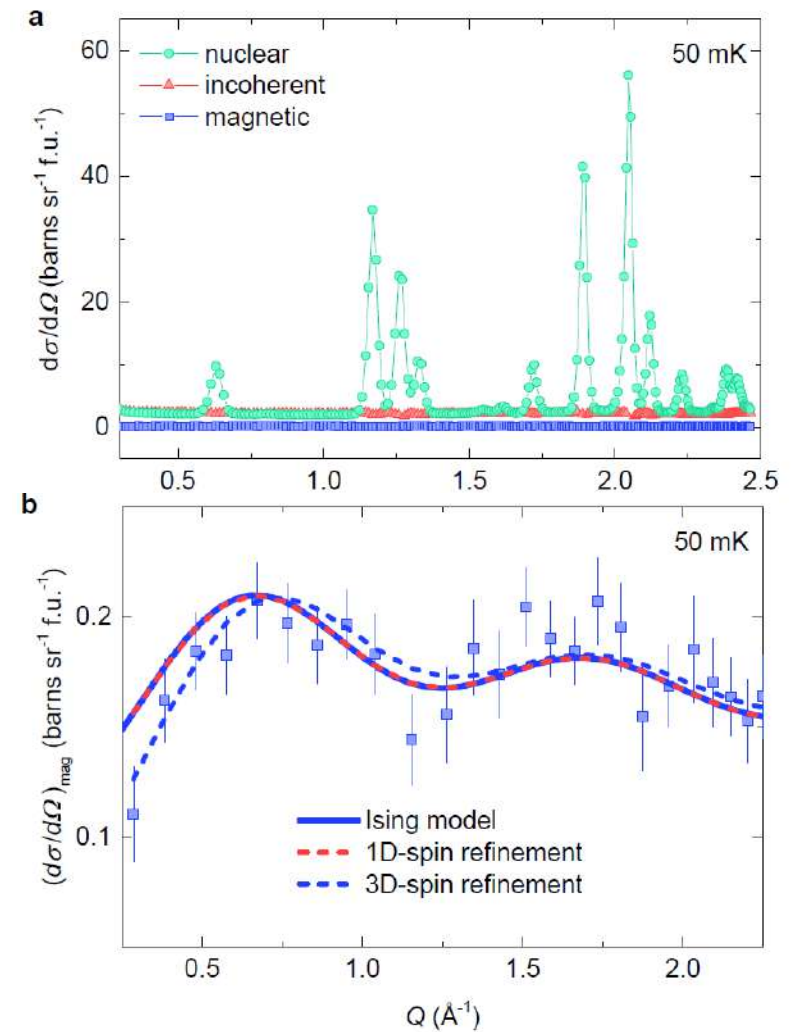
□ Polarized neutrons:



NdTa₇O₁₉:
triangular AFM



D7, ILL, France



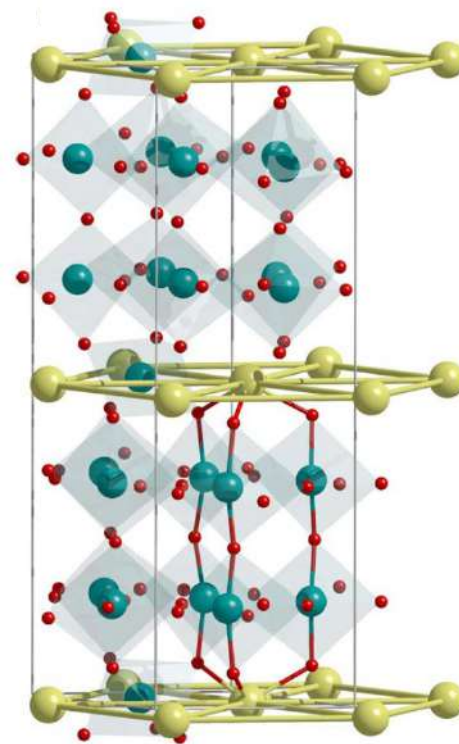
Arh *et al.*, Nat. Mater. **21**, 416 (2022).

Magnetic Neutron Scattering

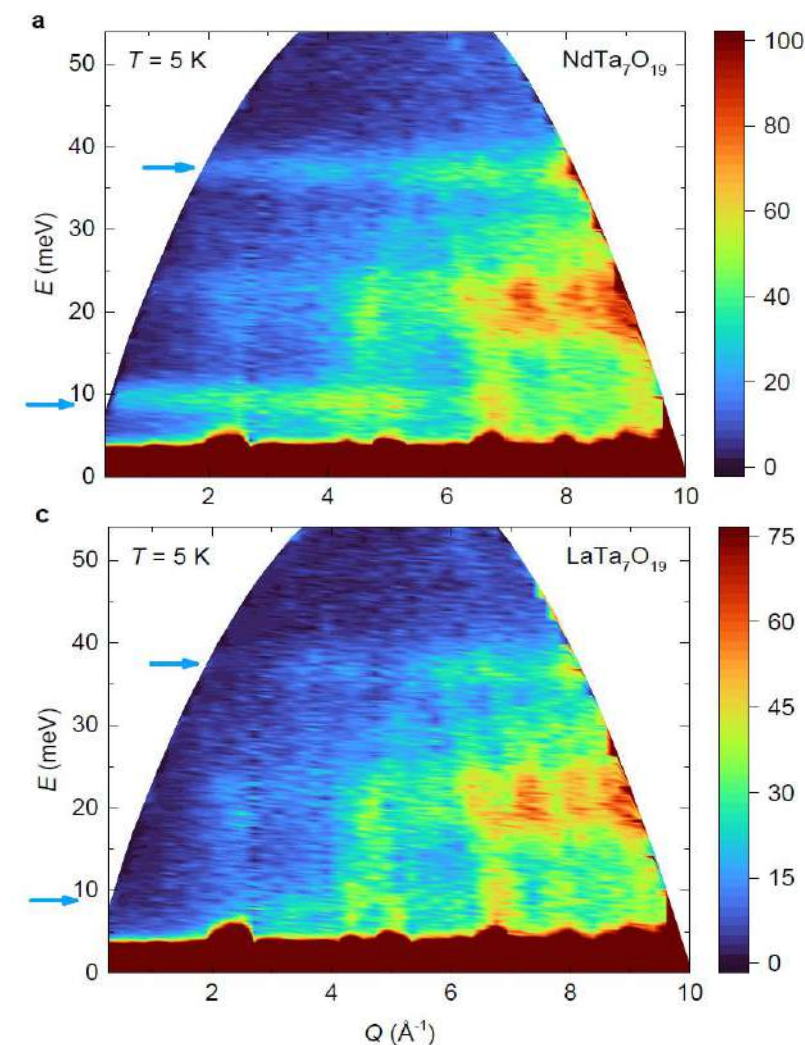
□ Energy-resolved insight:



MARI, ISIS, UK



$\text{NdTa}_7\text{O}_{19}$:
triangular AFM

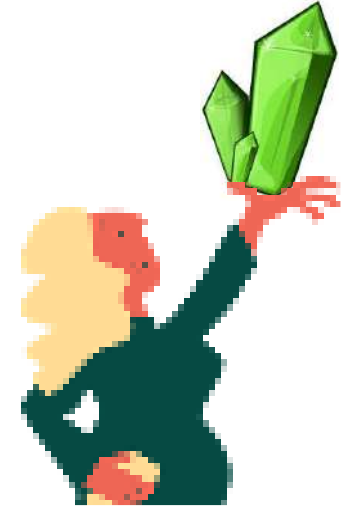


Arh *et al.*, Nat. Mater. **21**, 416 (2022).

Magnetic Neutron Scattering

□ Gives direct Q -space information but requires:

- large samples (magnetic scattering and INS are weak)
- large enough ordered moments (magnetic scattering and INS are weak)
- no strong incoherent scattering (H)
- no strong neutron absorption (Cd, Ir, B, ...)
- long counting times



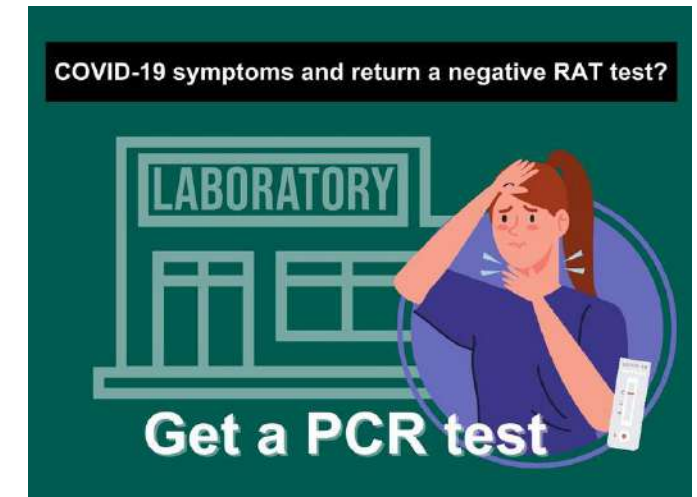
Bulk Techniques

❑ Provide necessary preliminary characterisation but have drawbacks:

➤ sensitivity

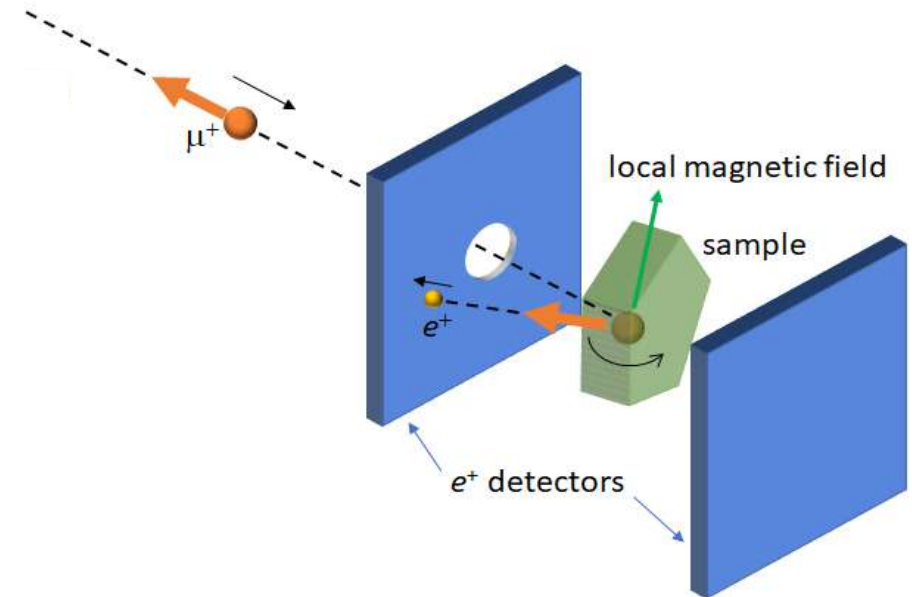
➤ average response

➤ no insight on the microscopic scale



Outline

- Introduction to magnetism
- Probing magnetism: conventional bulk and scattering techniques
- Local probes of magnetism
- Electron spin resonance (ESR)
- Nuclear magnetic resonance (NMR)
- Muon spectroscopy (μ SR)
- Summary: strengths, limitations and complementarity of local probes



Local Probes of Magnetism

□ Local probes: **intrinsic** (direct or indirect)

Probe	Charge	Spin	Mass	$\gamma/2\pi$ (MHz T ⁻¹)	Lifetime (μ s)	Method
e	$-e_0$	$\frac{1}{2}$	m_e	28.03×10^3	∞	ESR
p	e_0	$\frac{1}{2}$	$1836m_e$	42.58	∞	NMR

Local Probes of Magnetism

□ Local probes: **intrinsic** (direct or indirect) or **extrinsic**

Probe	Charge	Spin	Mass	$\gamma/2\pi$ (MHz T ⁻¹)	Lifetime (μ s)	Method
e	$-e_0$	$\frac{1}{2}$	m_e	28.03×10^3	∞	ESR
μ^+	e_0	$\frac{1}{2}$	$207m_e$	135.5	2.197	μ SR
p	e_0	$\frac{1}{2}$	$1836m_e$	42.58	∞	NMR

□ Measuring principles: **induction** (in cavity or coil) or **particle counting**

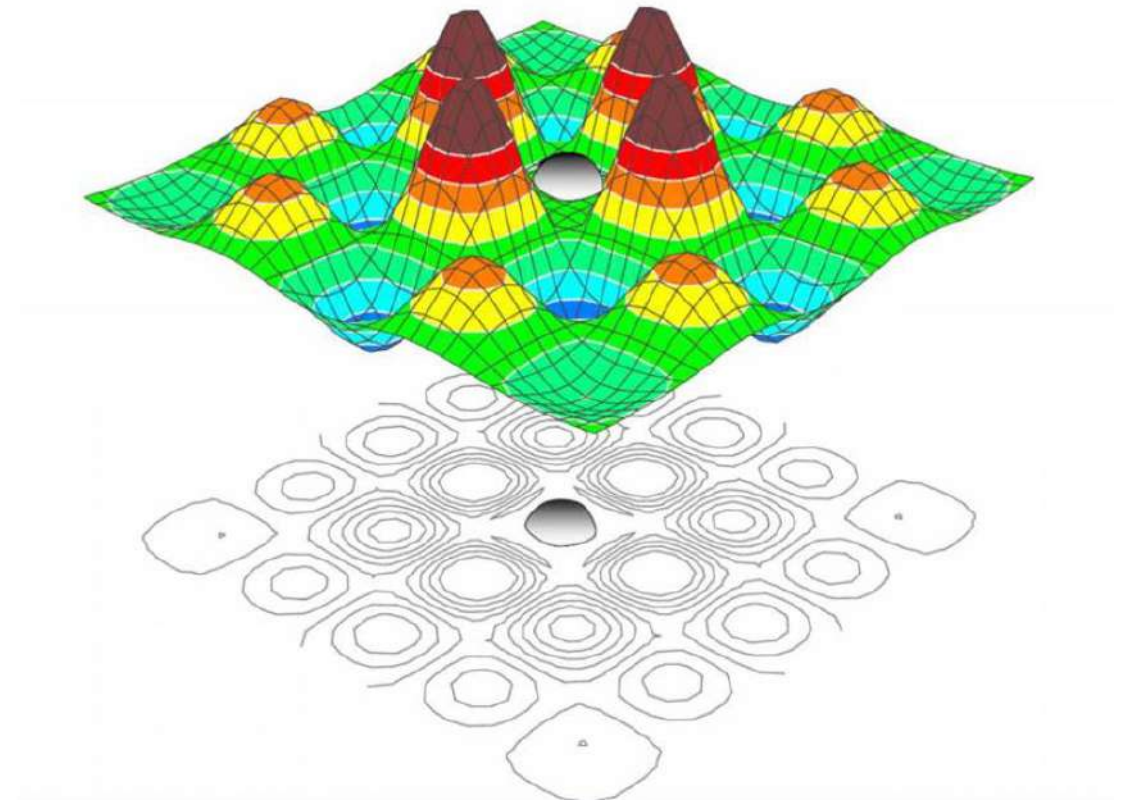


Local Probes of Magnetism

□ Local field:
$$\vec{B}(t) = \sum_j A_j \vec{S}_j(t) = \sum_{j, \vec{q}} A_j e^{i\vec{q} \cdot \vec{r}_j} S_{\vec{q}}$$

- q -integrated response
- selective (no extrinsic contributions)
- measurements of sublattice magnetization (AFM)
- measurements of phase separation/segregation

□ Detection of static and fluctuating local fields to study spin polarization



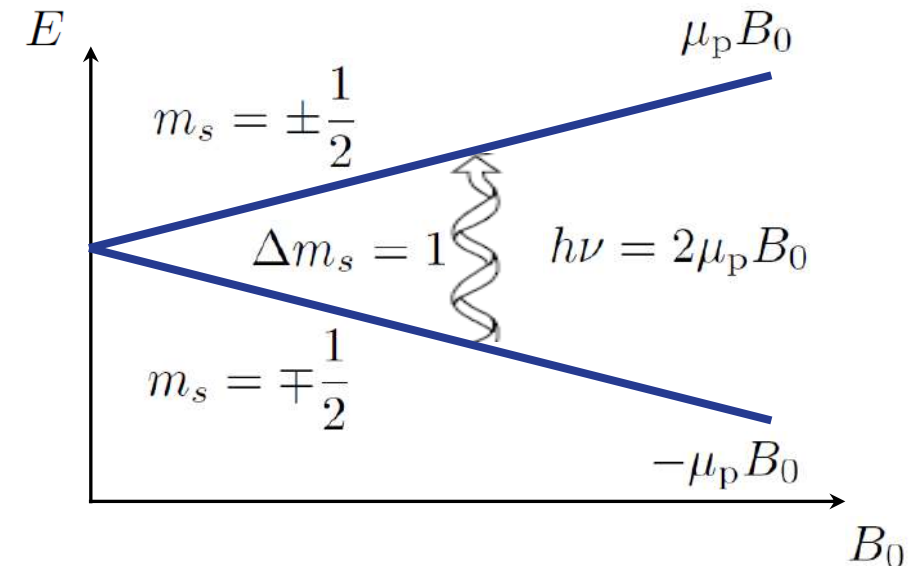
Alloul *et al.*, Rev. Mod. Phys. **81**, 45 (2009)

Local Probes of Magnetism

□ Hamiltonian:

$$\mathcal{H} = \mathcal{H}_Z + \mathcal{H}_{pe} + \mathcal{H}_{pn}$$

- Zeeman interaction: $\mathcal{H}_Z = -\vec{\mu}_p \cdot \vec{B}_0$
- probe – electronic-spins interaction
- probe – nuclear-spins interaction



Outline

- Introduction to magnetism
- Probing magnetism: conventional bulk and scattering techniques
- Local probes of magnetism
- Electron spin resonance (ESR)
- Nuclear magnetic resonance (NMR)
- Muon spectroscopy (μ SR)
- Summary: strengths, limitations and complementarity of local probes



Confusion with the name...

□ How many different techniques are there?

- EPR: Electron Paramagnetic Resonance
- ESR: Electron Spin Resonance
- EMR: Electron Magnetic Resonance

- AFMR/FMR: AntiFerroMagnetic Resonance/FerroMagnetic Resonance
- CESR: Conduction Electron Spin Resonance



Motivation for ESR Measurements

- Direct detection of the electron spins:

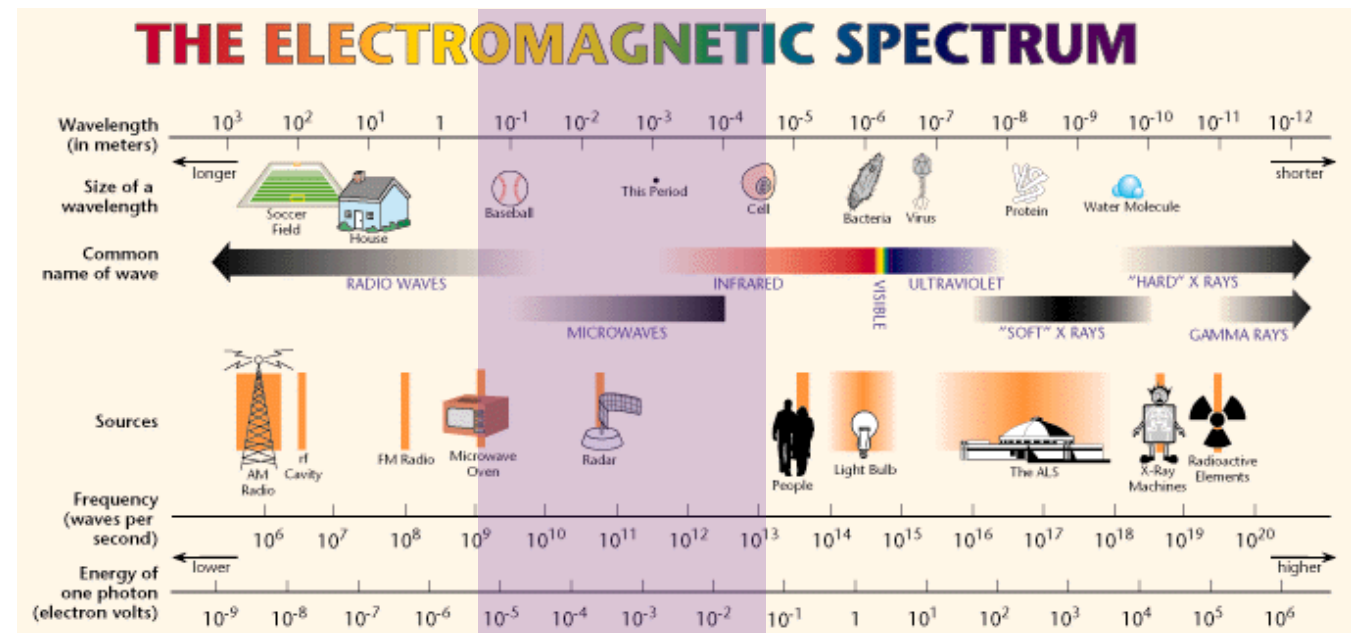
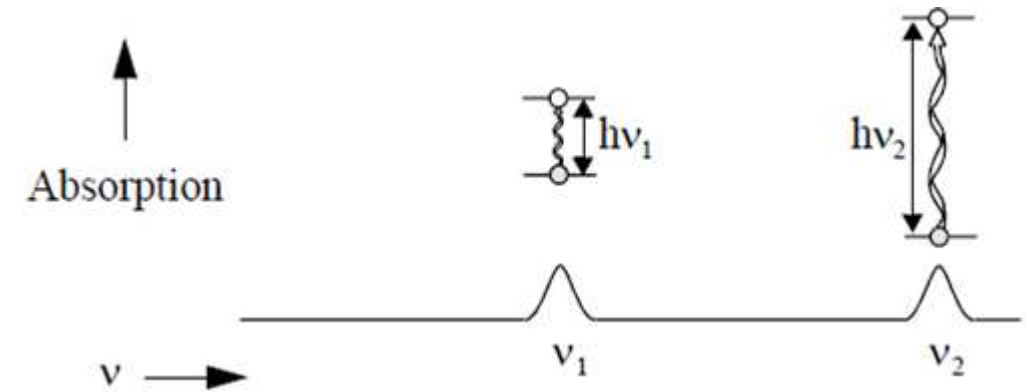
$$I(\omega) = \frac{1}{2} \omega H_0^2 \chi''(\mathbf{q} = 0, \omega)$$

- High sensitivity: $10^9 - 10^{15}$ spins
(a few mg of sample)

- High spectral resolution: $10^{-4} - 10^{-5}$

- Broad range of available frequencies:
 $10^9 - 10^{13}$ Hz

- CW and pulsed techniques



Motivation for ESR Measurements



□ Broad range of applications:

- kinetics of radical reactions
- oxidation and reduction processes
- catalytic reactions
- petroleum research
- ...

CHEMISTRY

- spin labeling
- free radicals in living tissues and fluids
- drug detection, metabolism, and toxicity
- spin trapping
- ...

BIOLOGY/
MEDICINE

- magnetic properties of TM and RE
- conduction electrons in conductors and semiconductors
- defects in crystals
- excited states of molecules
- crystal fields in crystalline solids
- ...

PHYSICS/
MATERIALS
RESEARCH



Motivation for ESR Measurements



□ Broad range of applications:

- kinetics of radical reactions
- oxidation and reduction processes
- catalytic reactions
- petroleum research
- ...

CHEMISTRY

- spin labeling
- free radicals in living tissues and fluids
- drug detection, metabolism, and toxicity
- spin trapping
- ...

BIOLOGY/
MEDICINE

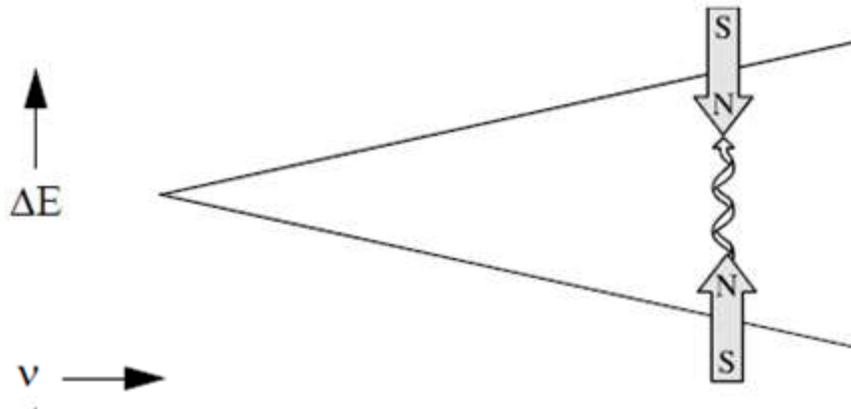
- magnetic properties of TM and RE
- conduction electrons in conductors and semiconductors
- defects in crystals
- excited states of molecules
- crystal fields in crystalline solids
- ...

PHYSICS/
MATERIALS
RESEARCH



A Brief History of ESR

- 1896: discovery of the Zeeman effect



$$\mathcal{H}_Z = -\vec{\mu}_p \cdot \vec{B}_0$$

The Nobel Prize in Physics 1902



Photo from the Nobel
Foundation archive.
**Hendrik Antoon
Lorentz**
Prize share: 1/2



Photo from the Nobel
Foundation archive.
Pieter Zeeman
Prize share: 1/2

The Nobel Prize in Physics 1902 was awarded jointly to Hendrik Antoon Lorentz and Pieter Zeeman "in recognition of the extraordinary service they rendered by their researches into the influence of magnetism upon radiation phenomena."

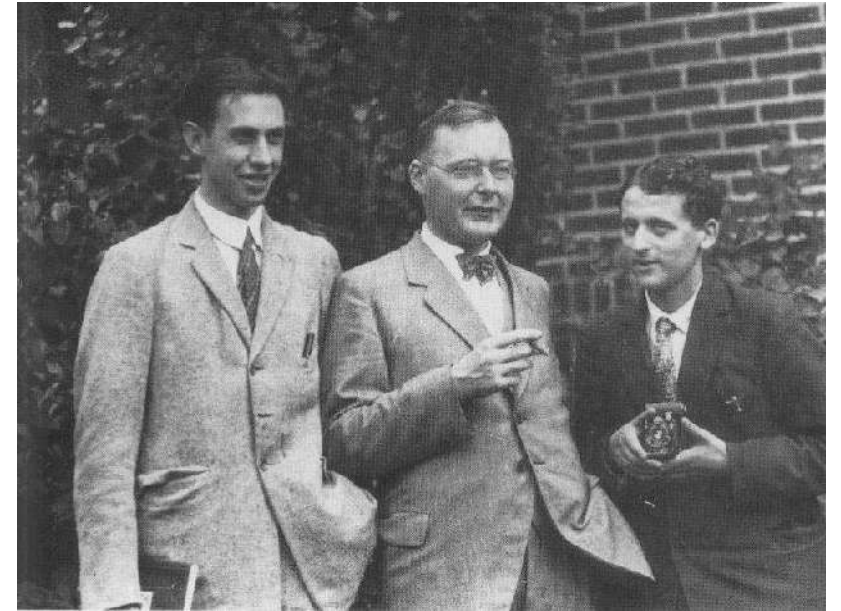
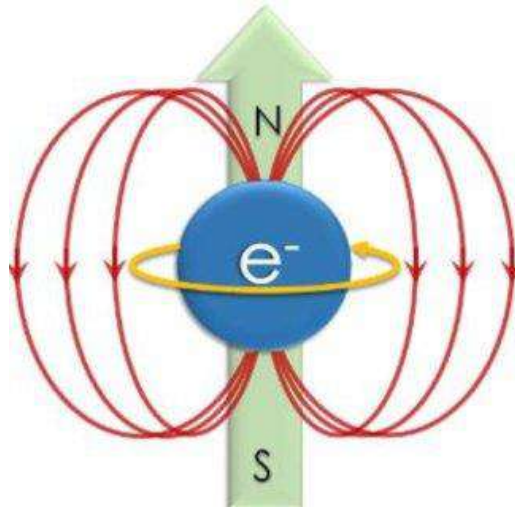
<https://www.nobelprize.org>



A Brief History of ESR

- 1925: discovery of the electron spin

$$\vec{\mu} = -g_J \mu_B \vec{J}$$

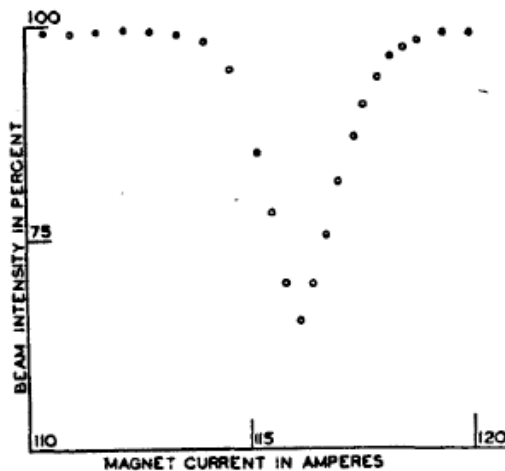
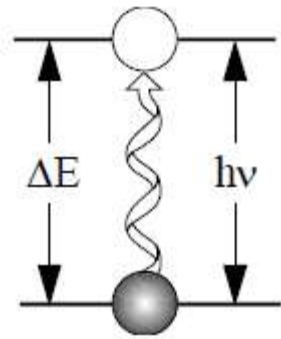


G. E. Uhlenbeck

S. Goudsmit

A Brief History of ESR

- 1938: interactions of LiCl molecular beams with EM waves in a static magnetic field



The Nobel Prize in Physics 1944



Photo from the Nobel
Foundation archive.

Isidor Isaac Rabi

Prize share: 1/1

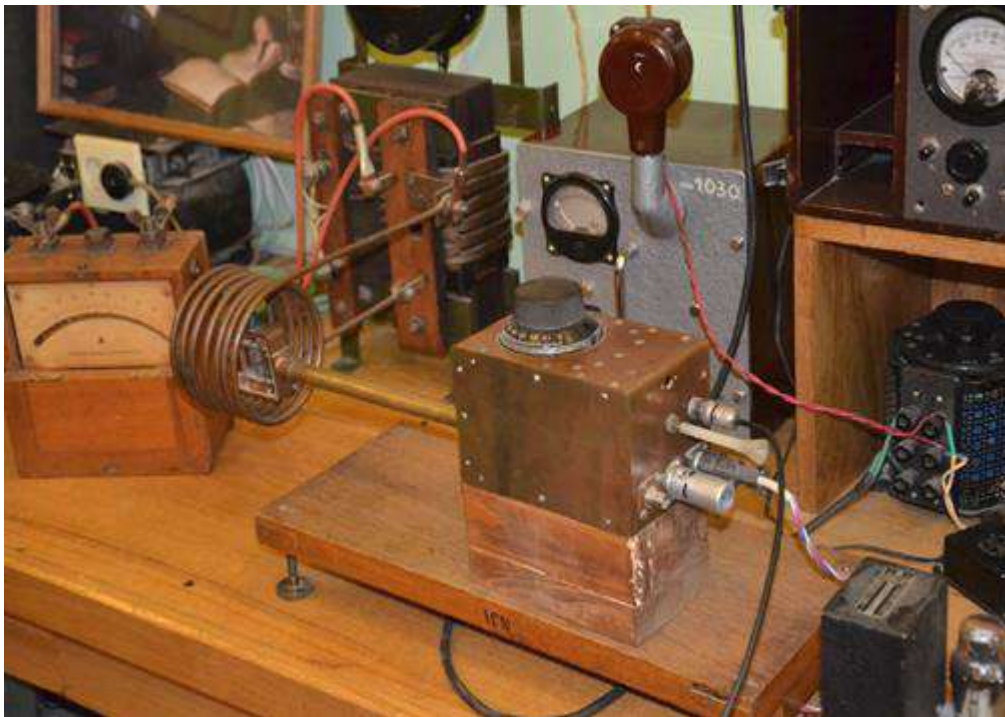
The Nobel Prize in Physics 1944 was awarded to Isidor Isaac Rabi "for his resonance method for recording the magnetic properties of atomic nuclei."

<https://www.nobelprize.org>

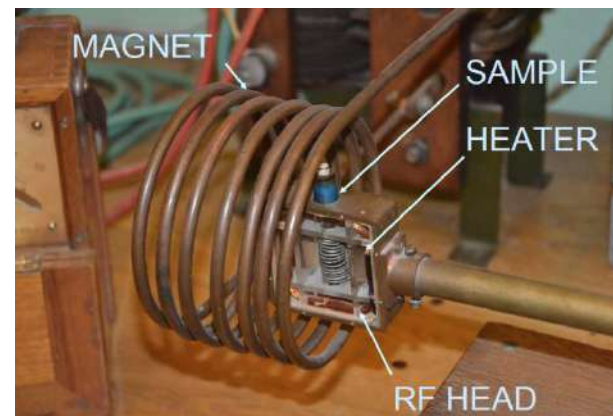


A Brief History of ESR

- 1944: discovery of ESR (first ESR spectrometer at the Kazan University, USSR)



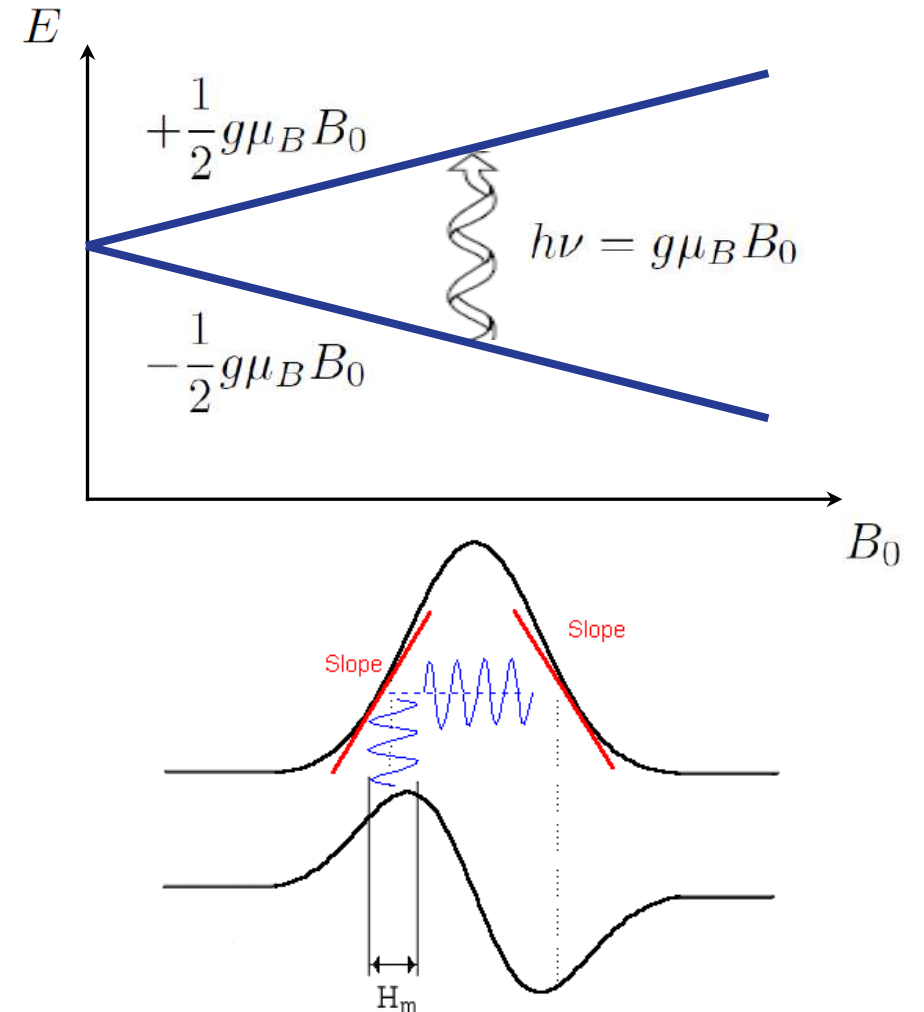
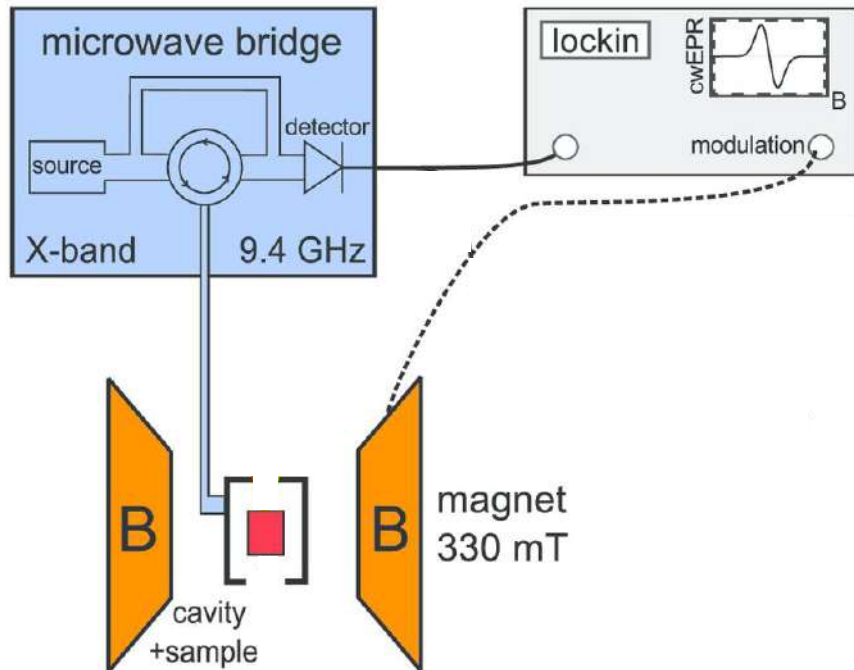
Cu-based salts
20 MHz (7.5 Oe)



Yevgeny Zavoisky

ESR Apparatus

- ❑ magnet (static + modulation)
- ❑ MW source
- ❑ detector

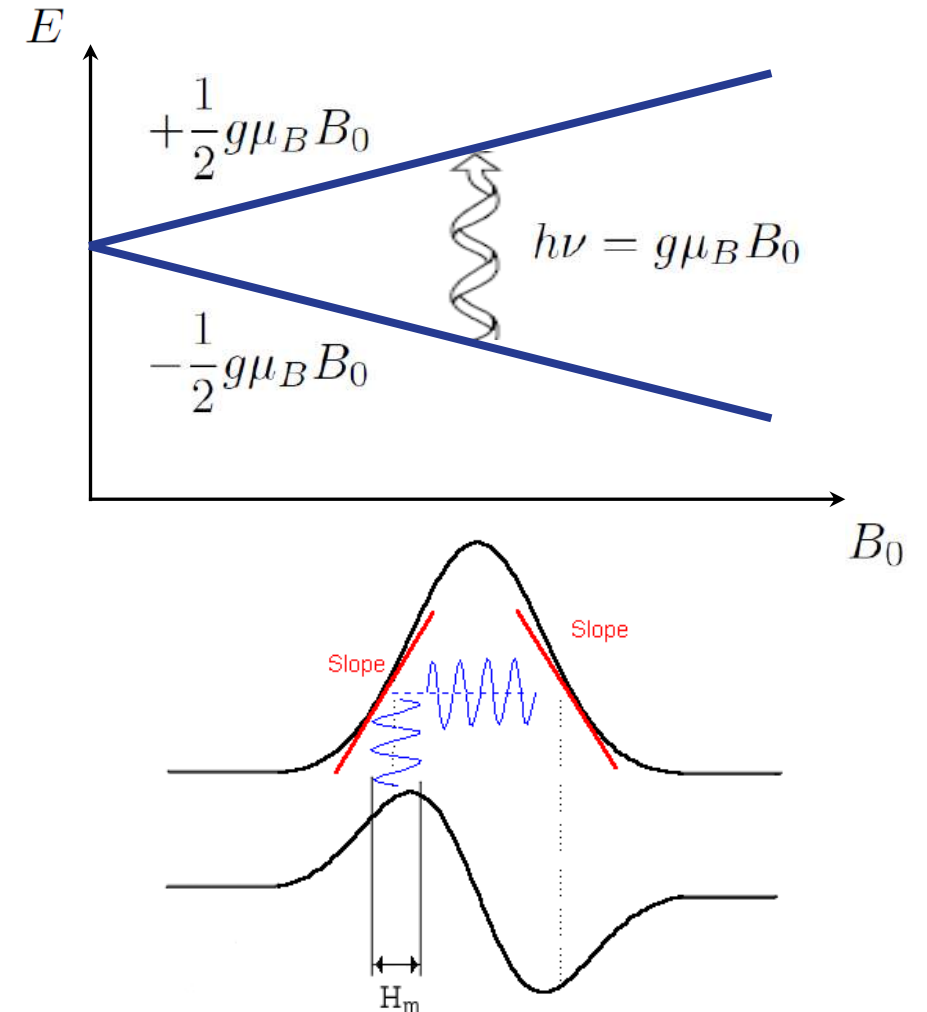


ESR Apparatus

- magnet (static + modulation)
- MW source
- detector



Bruker Elexsys E580 CW/FT EPR spectrometer



ESR Spectrum

□ ESR absorption:

$$I(\omega) = \frac{1}{2} \omega H_0^2 \chi''(\mathbf{q} = 0, \omega)$$

$$\chi''(\omega) = \frac{\omega V}{2k_B T} \int_{-\infty}^{\infty} \langle M^+(t) M^-(0) \rangle e^{-i\omega t} dt$$

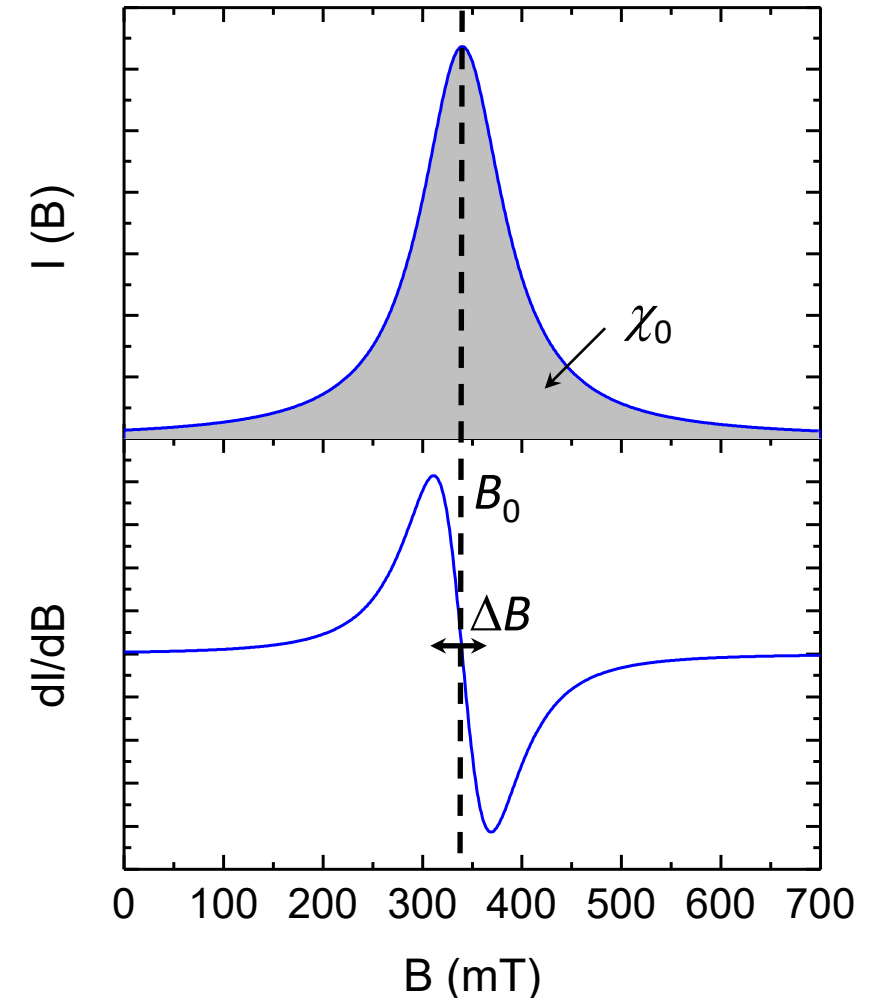
□ ESR parameters:

➤ ESR intensity: local static susceptibility

➤ ESR resonance field: interaction with CF

$$\Delta g = g - 2.0023$$

➤ ESR linewidth: magnetic anisotropy, inhomogeneities, interaction with phonons



Spin Hamiltonian

$$\chi''(\omega) = \frac{\omega V}{2k_B T} \int_{-\infty}^{\infty} \langle M^+(t) M^-(0) \rangle e^{-i\omega t} dt$$

$$\frac{d}{dt} M^\pm(t) = \frac{i}{\hbar} [\mathcal{H}, M^\pm(t)]$$

□ The effective spin Hamiltonian:

$$\mathcal{H} = \mathcal{H}_{eZ} + \mathcal{H}_{cf} + \mathcal{H}_{hf} + \mathcal{H}_{ee} + \mathcal{H}_{nZ}$$

electron Zeeman interaction
zero-field splitting in crystal field
hyperfine coupling
electron-electron interaction
nuclear Zeeman interaction

□ Magnetic systems: $\mathcal{H} = \mathcal{H}_{eZ} + \mathcal{H}_{ex} + \mathcal{H}'$

exchange interaction
magnetic anisotropy

$\mathcal{H}_{ex} = \sum_{(i,j)} J_{ij} \vec{S}_i \cdot \vec{S}_j$

complicated 4-spin correlation function
!

□ 2-spin coupling: $\vec{S}_i \cdot \underline{J}_{ij} \cdot \vec{S}_j$

$$\underline{J}_{ij} = J_{ij} \begin{bmatrix} 1 & 0 & 0 \\ 0 & 1 & 0 \\ 0 & 0 & 1 \end{bmatrix} + \begin{bmatrix} E & 0 & 0 \\ 0 & -E & 0 \\ 0 & 0 & D \end{bmatrix} + \begin{bmatrix} 0 & d_z & -d_y \\ -d_z & 0 & d_x \\ d_y & -d_x & 0 \end{bmatrix}$$

isotropic exchange
symmetric anisotropy
Dzyaloshinskii-Moriya

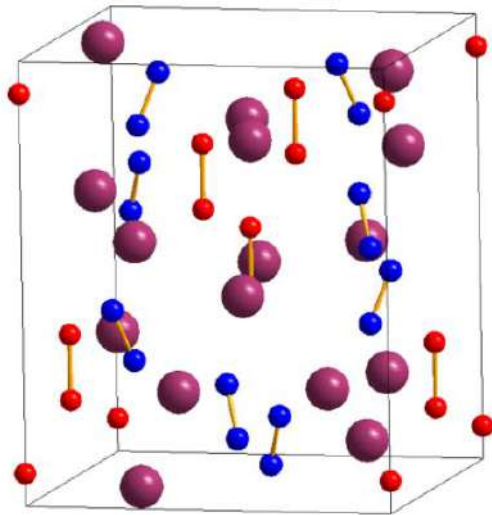


ESR Intensity

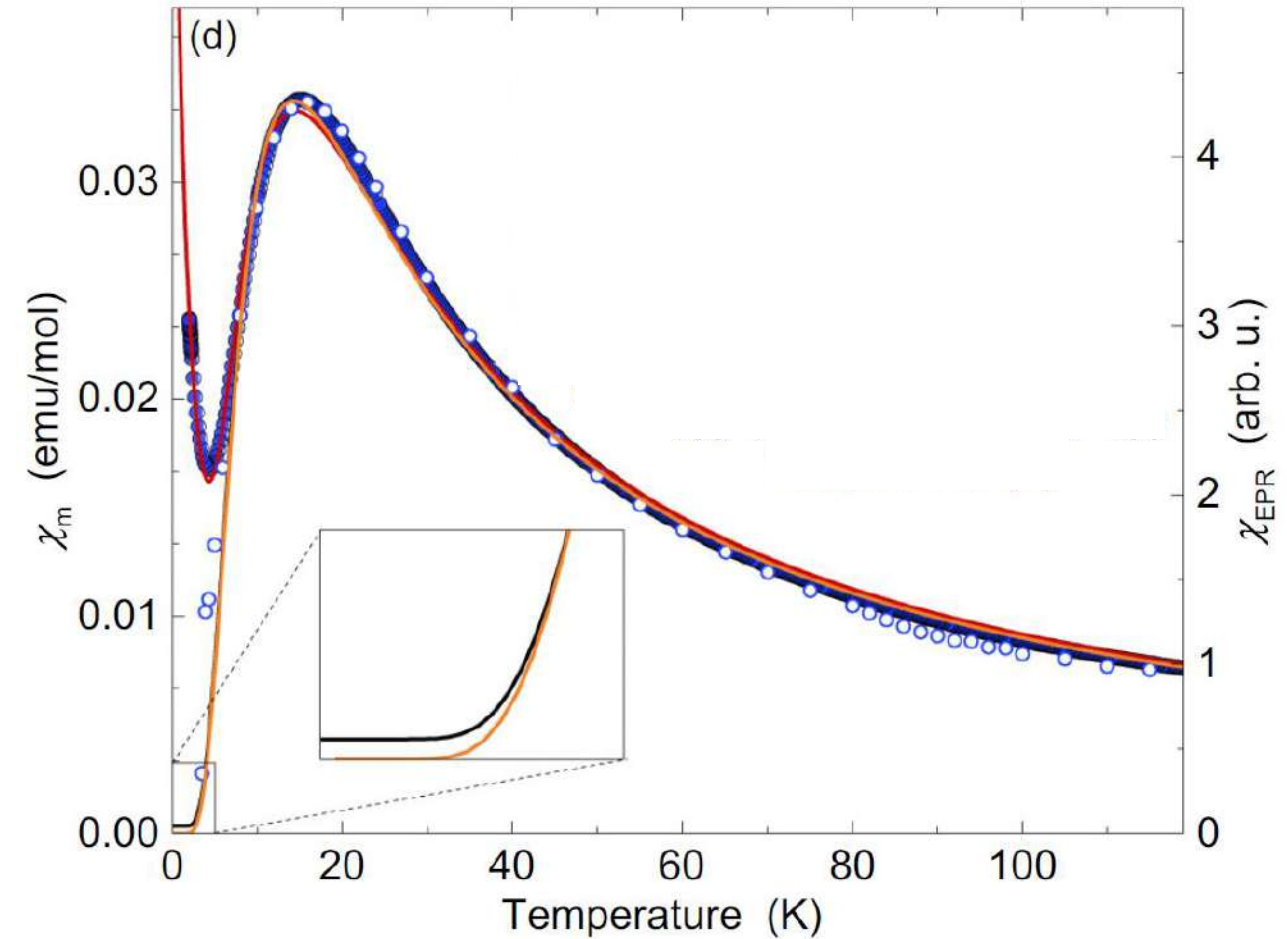
□ Kramers-Kronig relations:

$$\chi'(\omega = 0) = \frac{1}{\pi} \int_{-\infty}^{\infty} \frac{\chi''(\omega')}{\omega'} d\omega'$$

$$I(\omega) = \frac{1}{2} \omega H_0^2 \chi''(\mathbf{q} = 0, \omega) \xrightarrow{\Delta B \ll B_0} \int_{-\infty}^{\infty} I(\omega) d\omega \propto \chi_0$$



□ Dimerization of molecular O₂⁻ anions : mixed-valence compound Rb₄O₆



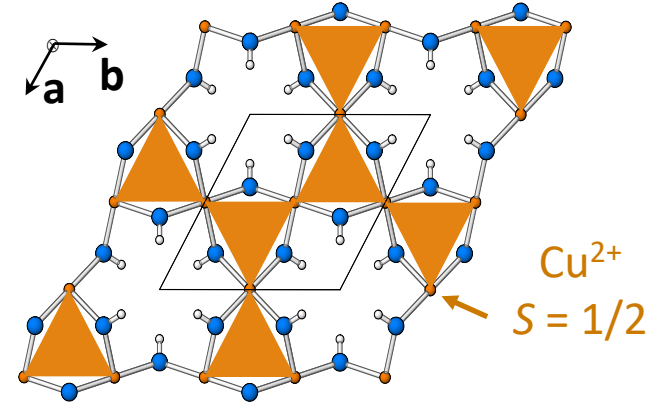
Knaflič *et al.*, Phys. Rev. B **101**, 024419 (2020)

ESR Intensity

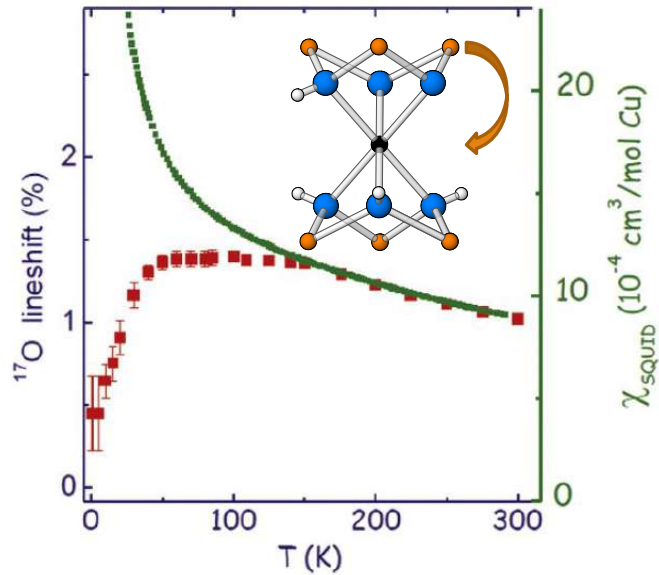
□ Kramers-Kronig relations:

$$\chi'(\omega = 0) = \frac{1}{\pi} \int_{-\infty}^{\infty} \frac{\chi''(\omega')}{\omega'} d\omega'$$

$$I(\omega) = \frac{1}{2} \omega H_0^2 \chi''(\mathbf{q} = 0, \omega) \xrightarrow{\Delta B \ll B_0} \int_{-\infty}^{\infty} I(\omega) d\omega \propto \chi_0$$

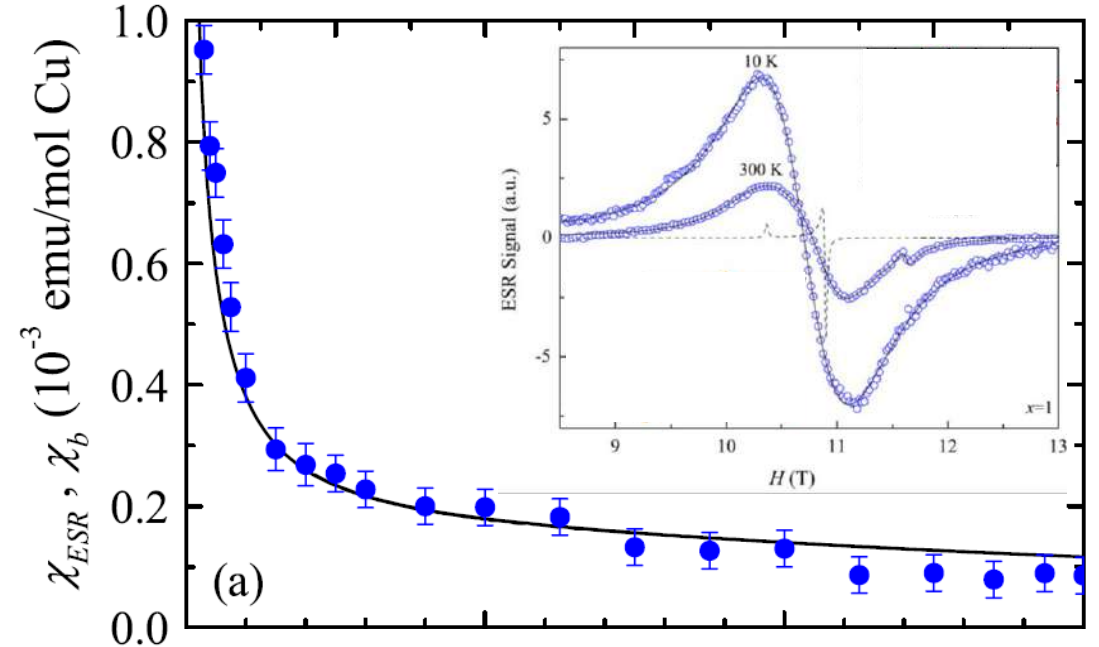


$\text{ZnCu}_3(\text{OH})_6\text{Cl}_2$:
kagome AFM



coupling
between
impurity and
intrinsic spins

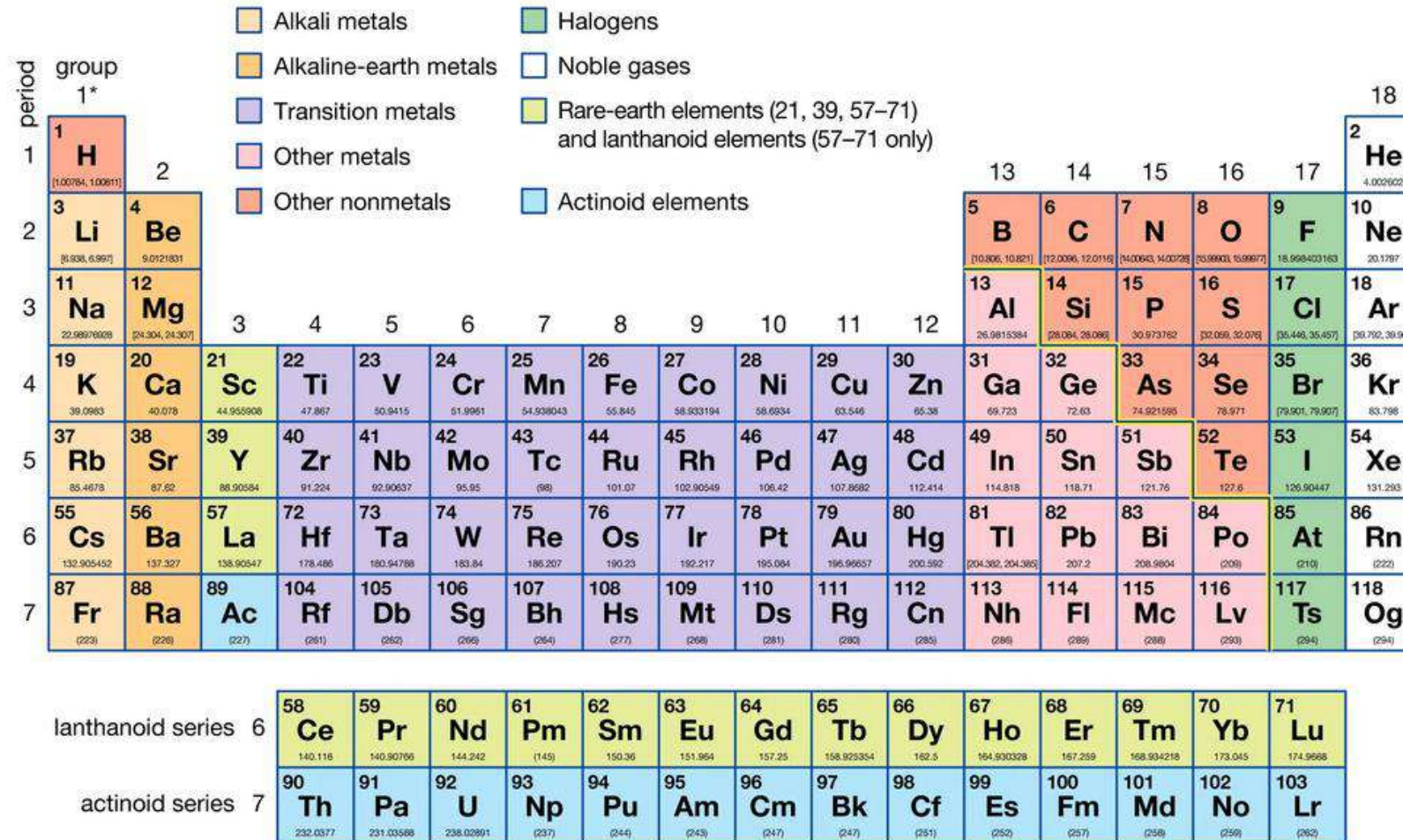
Olariu *et al.*, Phys. Rev. Lett.
100, 087202 (2008)



Zorko *et al.*, Phys. Rev. Lett. **101**, 024419 (2008)



ESR Resonance Field



ESR Resonance Field

□ Rare-earths: $\mathcal{H}_{cf} \ll \mathcal{H}_{LS} = \lambda \vec{L} \cdot \vec{S}$ \longrightarrow $\vec{J} = \vec{L} + \vec{S}$

group	1*	2	3	4	5	6	7	8	9	10	11	12	13	14	15	16	17	18
1	1 H [1.00784, 1.00811]																	2 He 4.002602
2	3 Li [6.938, 6.997]	4 Be 9.0121831											5 B [10.806, 10.821]	6 C [12.0096, 12.0116]	7 N [14.00643, 14.00728]	8 O [15.99903, 15.99977]	9 F 18.998403163	10 Ne 20.1797
3	11 Na 22.98976928	12 Mg [24.304, 24.307]											13 Al 26.9815384	14 Si [28.086, 28.086]	15 P [30.973762]	16 S [32.059, 32.076]	17 Cl [35.448, 35.457]	18 Ar [39.702, 39.963]
4	19 K 39.0983	20 Ca 40.078	21 Sc 44.955908	22 Ti 47.867	23 V 50.9415	24 Cr 51.9961	25 Mn 54.938043	26 Fe 55.845	27 Co 58.933194	28 Ni 58.6934	29 Cu 63.546	30 Zn 65.38	31 Ga 69.723	32 Ge 72.63	33 As 74.921595	34 Se 78.971	35 Br [79.901, 79.907]	36 Kr 83.798
5	37 Rb 85.4678	38 Sr 87.62	39 Y 88.90584	40 Zr 91.224	41 Nb 92.90637	42 Mo 95.95	43 Tc (98)	44 Ru 101.07	45 Rh 102.90549	46 Pd 106.42	47 Ag 107.8682	48 Cd 112.414	49 In 114.818	50 Sn 118.71	51 Sb 121.76	52 Te 127.6	53 I 126.90447	54 Xe 131.293
6	55 Cs 132.905452	56 Ba 137.327	57 La 138.90547	72 Hf 178.486	73 Ta 180.94788	74 W 183.84	75 Re 186.207	76 Os 190.23	77 Ir 192.217	78 Pt 195.084	79 Au 196.96657	80 Hg 200.592	81 Tl [204.382, 204.385]	82 Pb 207.2	83 Bi 208.9804	84 Po (209)	85 At (210)	86 Rn (222)
7	87 Fr (223)	88 Ra (226)	89 Ac (227)	104 Rf (261)	105 Db (262)	106 Sg (266)	107 Bh (264)	108 Hs (271)	109 Mt (268)	110 Ds (281)	111 Rg (283)	112 Cn (285)	113 Nh (286)	114 Fl (286)	115 Mc (288)	116 Lv (293)	117 Ts (294)	118 Og (294)

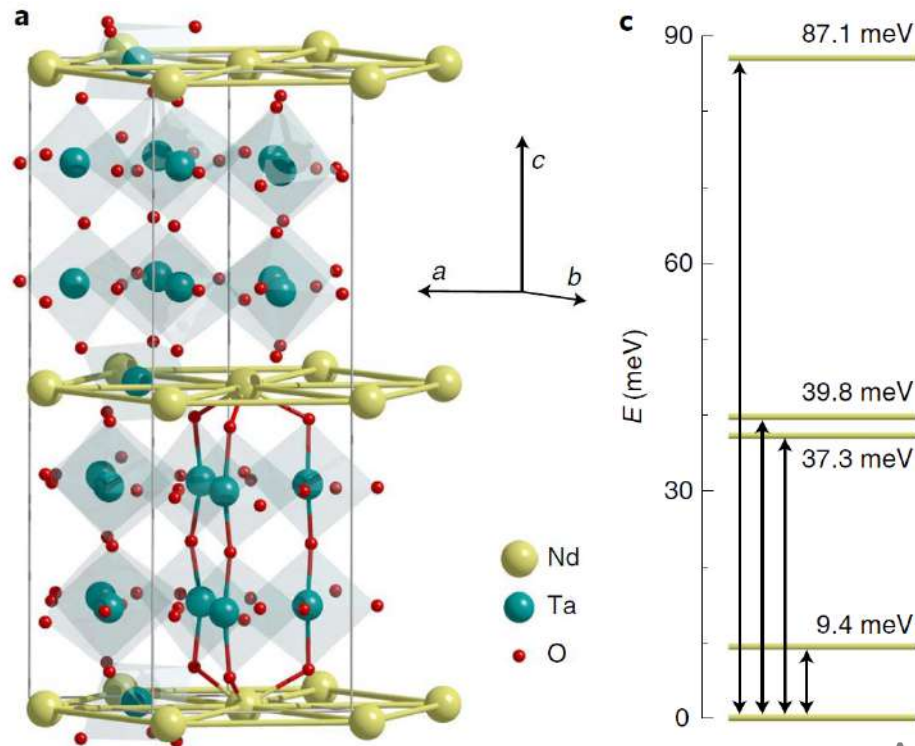
lanthanoid series 6	58 Ce 140.116	59 Pr 140.90766	60 Nd 144.242	61 Pm (145)	62 Sm 150.36	63 Eu 151.964	64 Gd 157.25	65 Tb 158.925354	66 Dy 162.5	67 Ho 164.930328	68 Er 167.259	69 Tm 168.934218	70 Yb 173.045	71 Lu 174.9668
actinoid series 7	90 Th 232.0377	91 Pa 231.03688	92 U 238.02891	93 Np (237)	94 Pu (244)	95 Am (243)	96 Cm (247)	97 Bk (247)	98 Cf (251)	99 Es (252)	100 Fm (257)	101 Md (258)	102 No (259)	103 Lr (262)



ESR Resonance Field

□ Rare-earths: $\mathcal{H}_{cf} \ll \mathcal{H}_{LS} = \lambda \vec{L} \cdot \vec{S}$ \longrightarrow $\vec{J} = \vec{L} + \vec{S}$

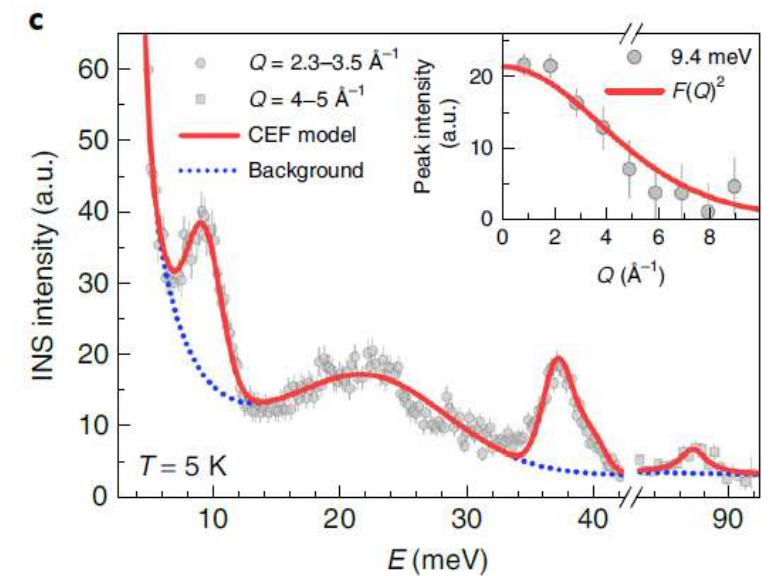
□ CF splitting: $\text{NdTa}_7\text{O}_{19}$
(triangular AFM with $J = 9/2$)



GS doublet:

$ \pm m_J\rangle$	$\pm\omega_0$
$ \pm 9/2\rangle$	0
$ \pm 7/2\rangle$	0
$ \pm 5/2\rangle$	0.933
$ \pm 3/2\rangle$	0
$ \pm 1/2\rangle$	0
$ \mp 1/2\rangle$	∓ 0.244
$ \mp 3/2\rangle$	0
$ \mp 5/2\rangle$	0
$ \mp 7/2\rangle$	0.263
$ \mp 9/2\rangle$	0
$E(\text{meV})$	0

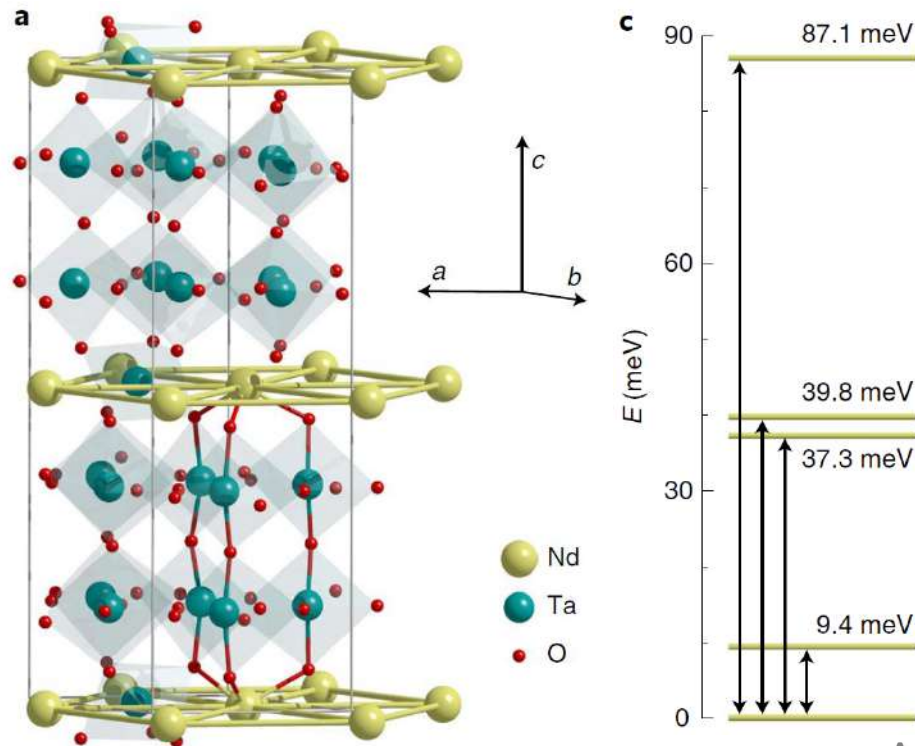
Arh *et al.*, Nat. Mater. **21**, 416 (2022).



ESR Resonance Field

□ Rare-earths: $\mathcal{H}_{cf} \ll \mathcal{H}_{LS} = \lambda \vec{L} \cdot \vec{S}$ \longrightarrow $\vec{J} = \vec{L} + \vec{S}$

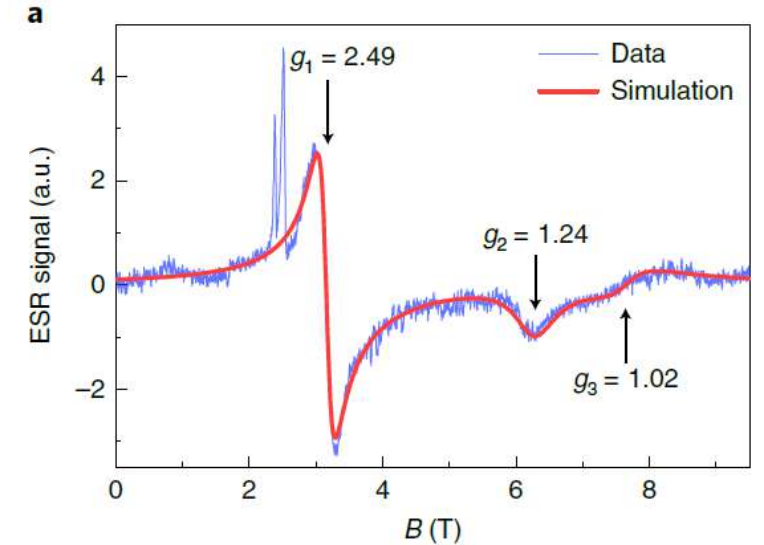
□ CF splitting: $\text{NdTa}_7\text{O}_{19}$
(triangular AFM with $J = 9/2$)



GS doublet:

$ \pm m_J\rangle$	$\pm\omega_0$
$ \pm 9/2\rangle$	0
$ \pm 7/2\rangle$	0
$ \pm 5/2\rangle$	0.933
$ \pm 3/2\rangle$	0
$ \pm 1/2\rangle$	0
$ \mp 1/2\rangle$	∓ 0.244
$ \mp 3/2\rangle$	0
$ \mp 5/2\rangle$	0
$ \mp 7/2\rangle$	0.263
$ \mp 9/2\rangle$	0
$E(\text{meV})$	0

Arh *et al.*, Nat. Mater. **21**, 416 (2022).



$$\mathcal{H}_{\text{ex}} = \sum_{\langle i,j \rangle} \mathcal{J}_z S_i^z S_j^z + \mathcal{J}_{xy} (S_i^x S_j^x + S_i^y S_j^y)$$

$$\mathcal{J}_\alpha = \mathcal{J}_0 g_\alpha^2 (g_J - 1)^2 / g_J^2$$

$$\mathcal{J}_z = 0.90(2) \text{ K}$$

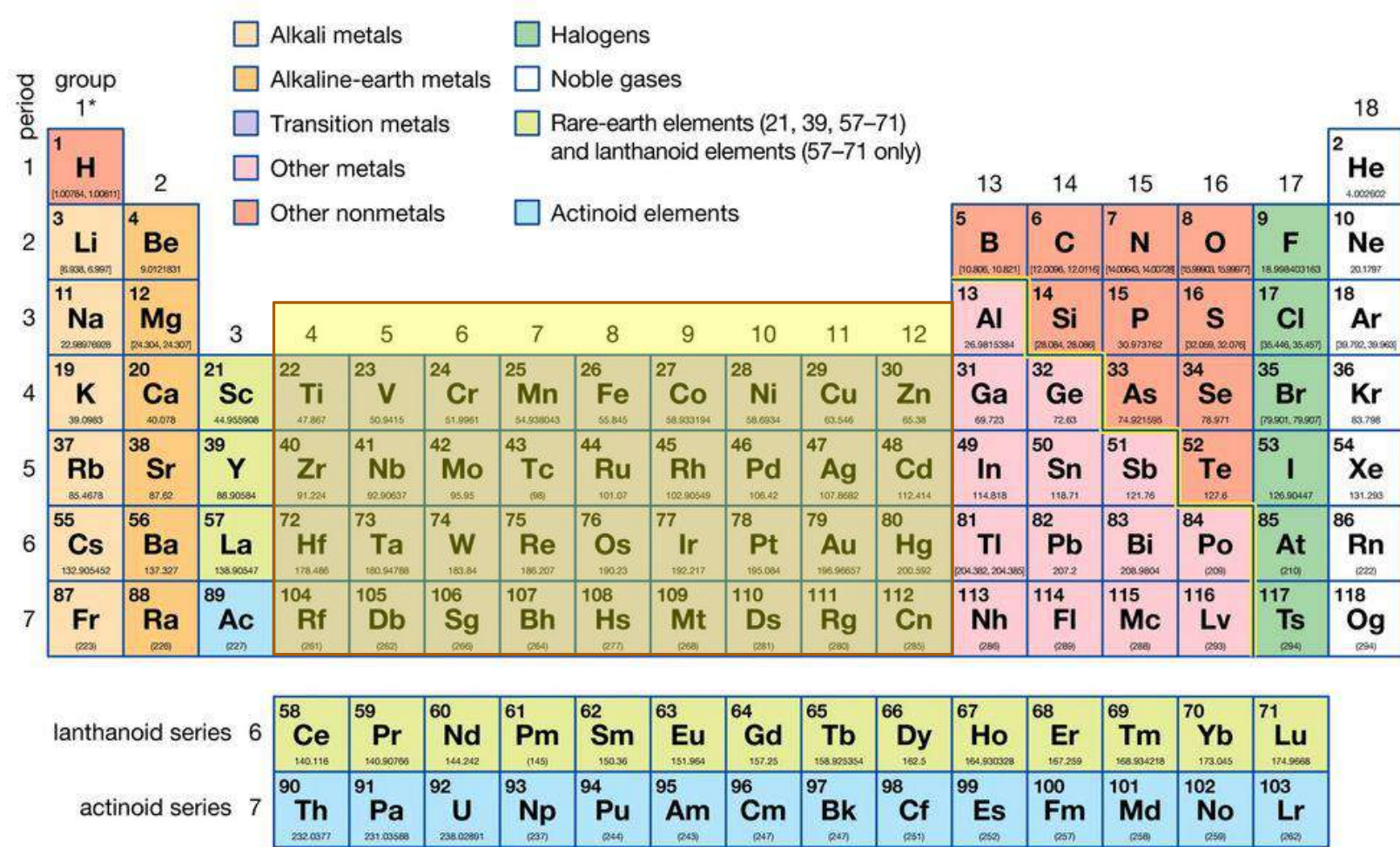
$$\mathcal{J}_{xy} = 0.16(2) \text{ K}$$

Ising TAFM



ESR Resonance Field

□ Transition metals:



ESR Resonance Field

Transition metals: $\mathcal{H}_{cf} \gg \mathcal{H}_{LS} = \lambda \vec{L} \cdot \vec{S}$ \longrightarrow $\langle \hat{L} \rangle = 0$ (quenching of the orbital momentum)

CF levels mixing: $\mathcal{H}_{LS} = \lambda \mathbf{L} \cdot \mathbf{S}$

$$\Lambda_{\mu,\nu} = \frac{\langle 0 | L_{\mu} | n \rangle \langle n | L_{\nu} | 0 \rangle}{E_n - E_0}$$

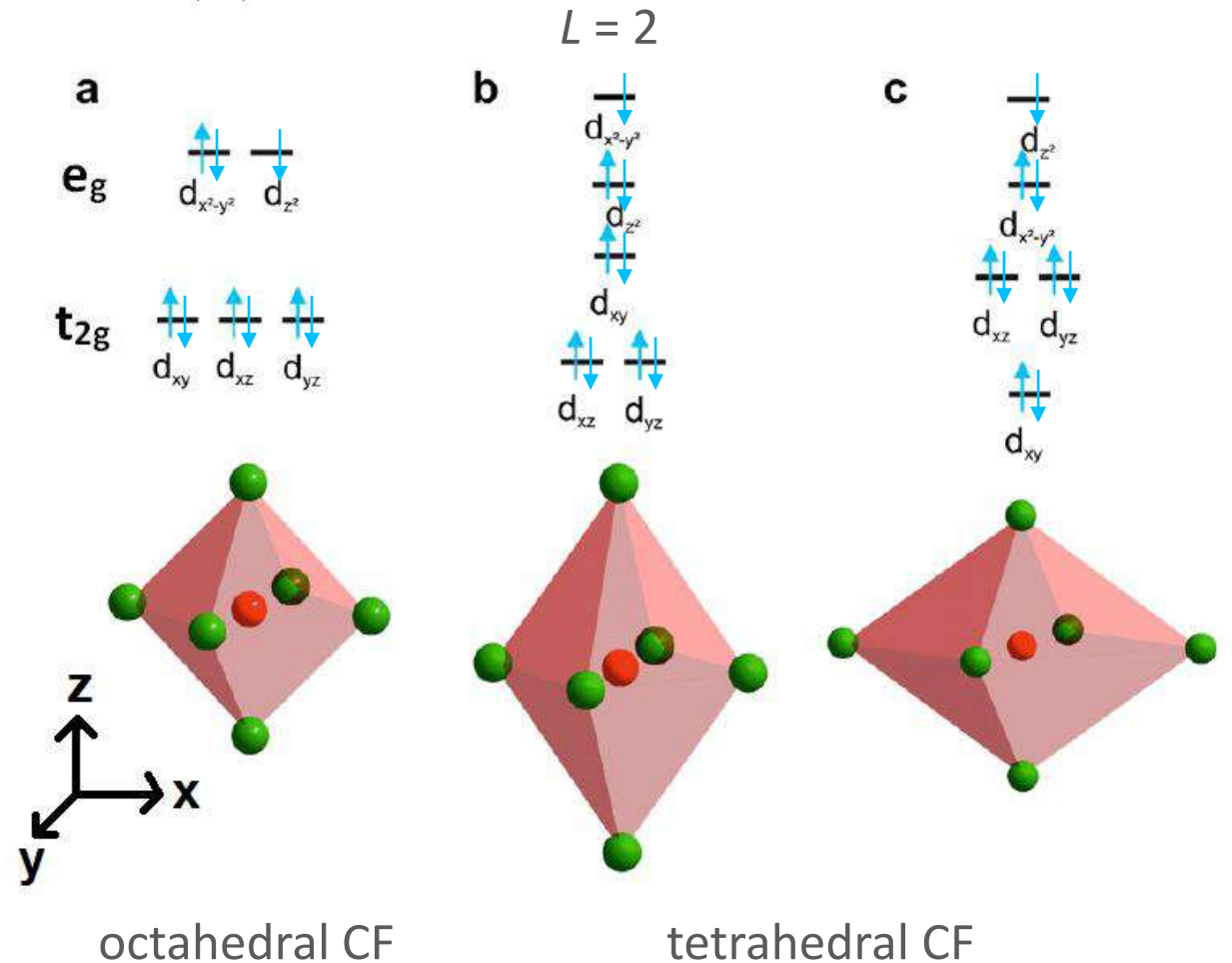
Zeeman term:

$$\mathcal{H}_{eZ} = \mu_B \mathbf{B} \cdot \underline{\mathbf{g}} \cdot \mathbf{S}$$

$$\underline{\mathbf{g}} = g_0 (\underline{\mathbf{g}} - \lambda \underline{\mathbf{\Lambda}})$$

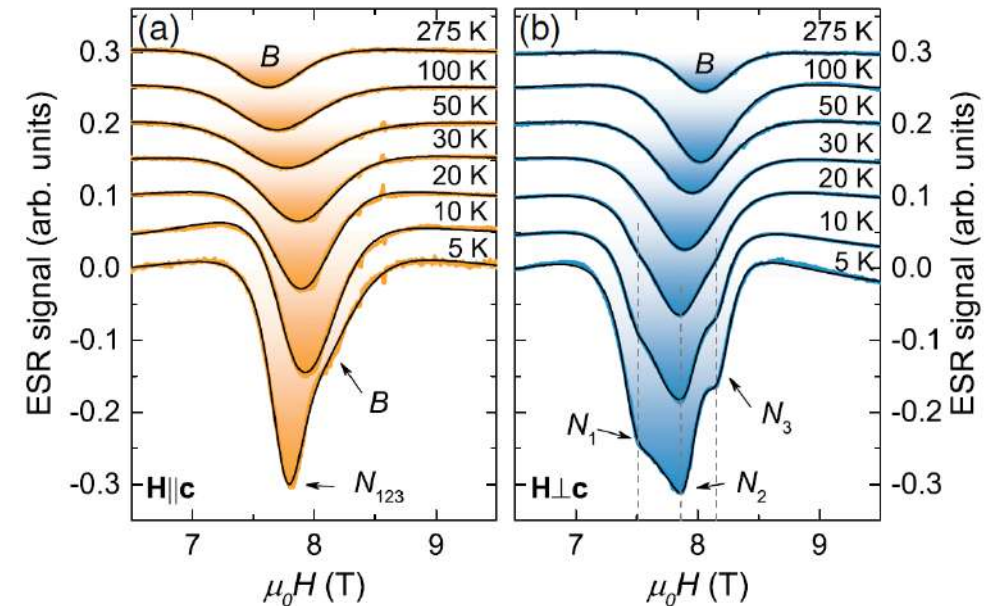
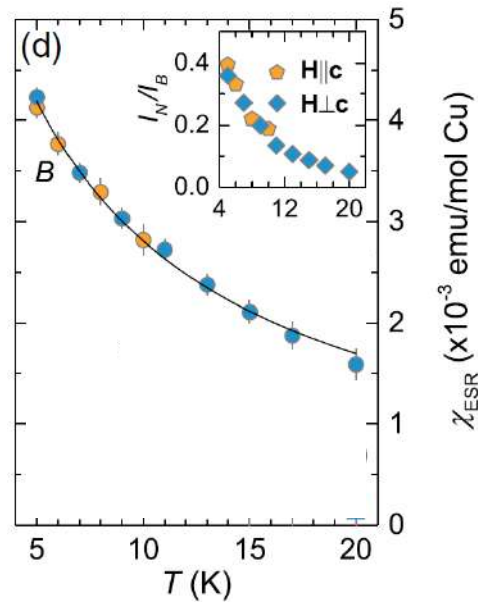
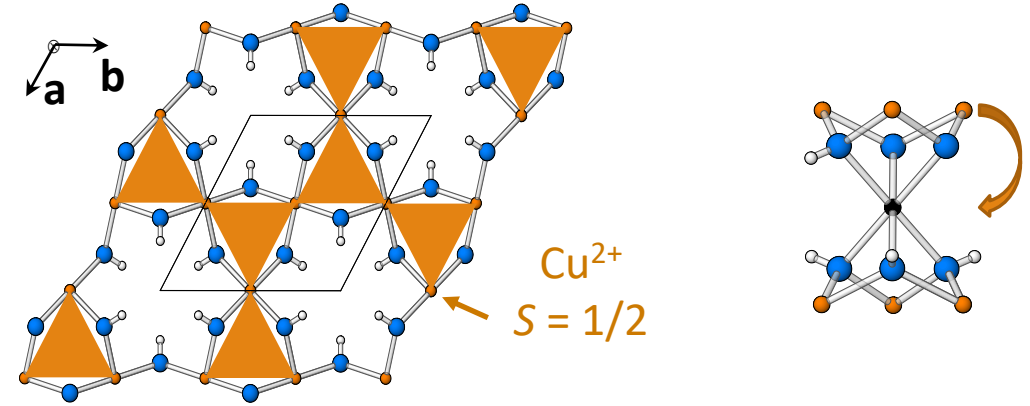
CF term:

$$\begin{aligned} \mathcal{H}_{cf} &= -\lambda^2 \mathbf{S} \cdot \underline{\mathbf{\Lambda}} \cdot \mathbf{S} = \\ &= D \left(S_z^2 - \frac{1}{3} S(S+1) \right) + E (S_x^2 - S_y^2) \end{aligned}$$



ESR Resonance Field

□ Defects in herbertsmithite:



Zorko *et al.*, Phys. Rev. Lett. **118**, 017202 (2017)



ESR Resonance Field

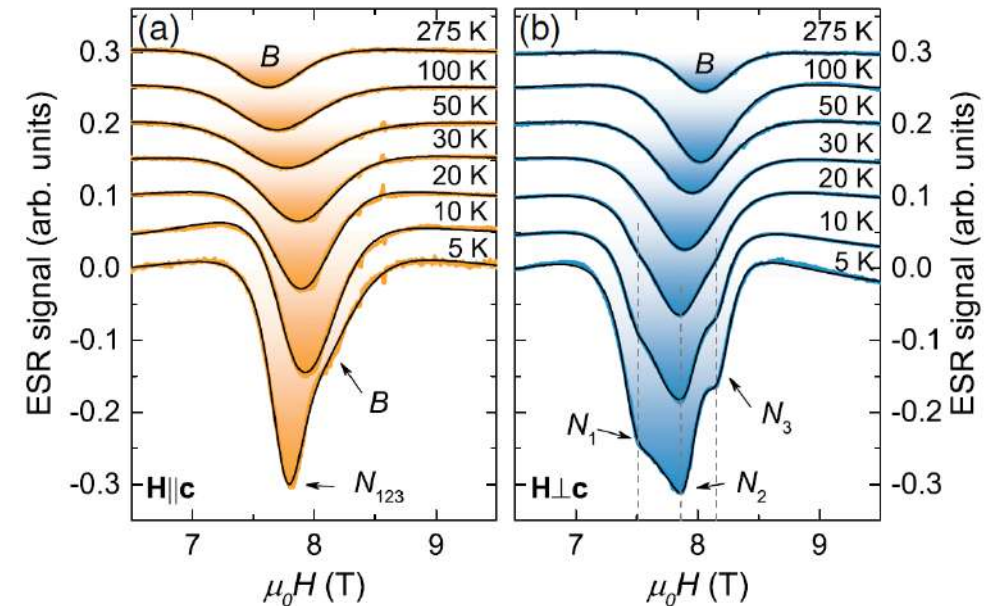
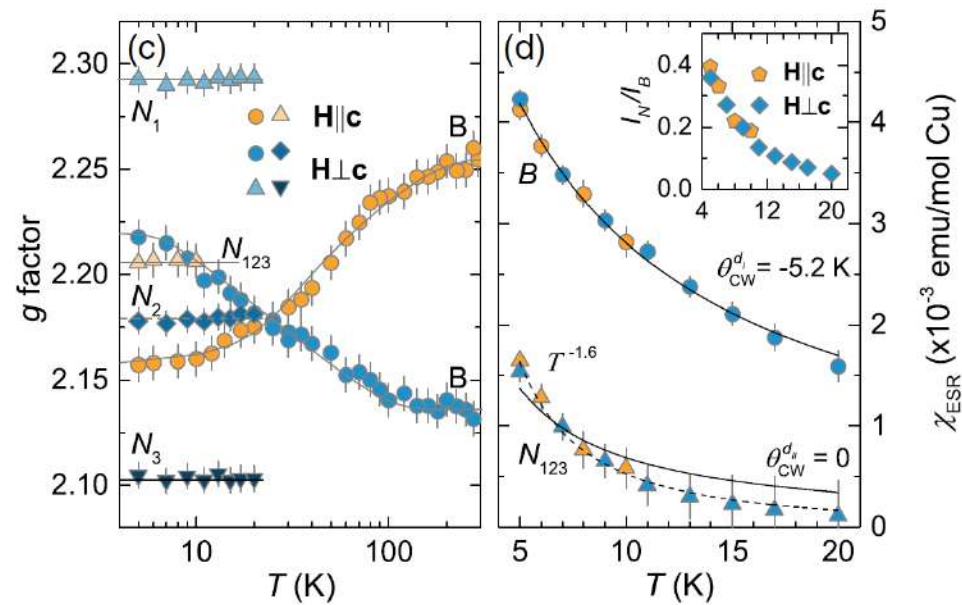
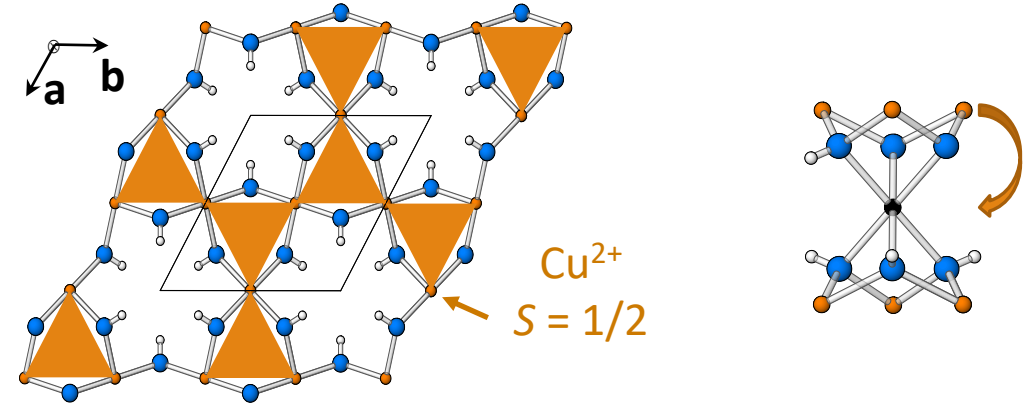
Defects in herbertsmithite:

- defect site 1: broad lines

$$J^{d_I} > J_H = \Delta g \mu_B \mu_0 H / k_B \approx 2 \text{ K}$$

- defect site 2: narrow lines

$$|J^{d_{II}}| \ll J_H$$



Zorko *et al.*, Phys. Rev. Lett. **118**, 017202 (2017)



ESR Resonance Field

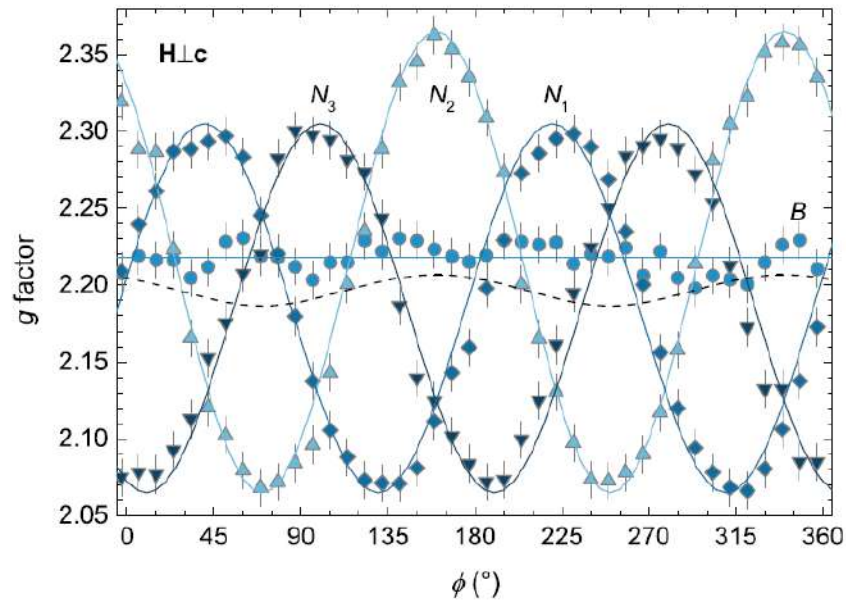
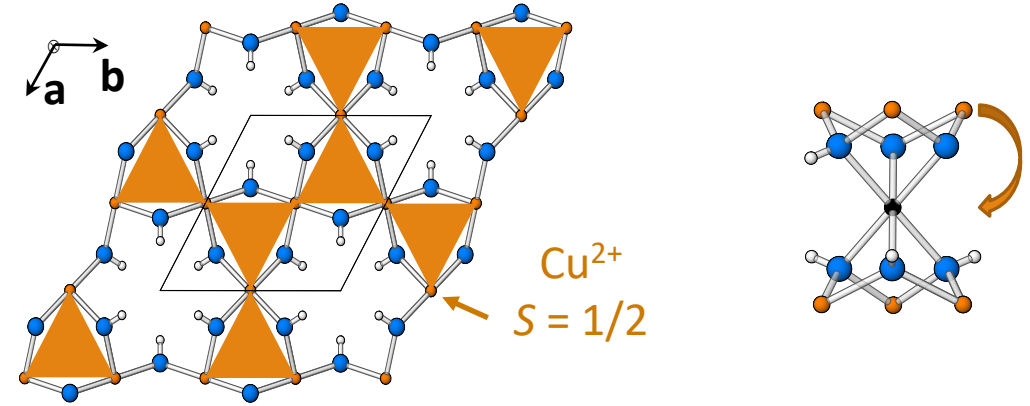
□ Defects in herbertsmithite:

➤ defect site 1: broad lines

$$J^{d_I} > J_H = \Delta g \mu_B \mu_0 H / k_B \approx 2 \text{ K}$$

➤ defect site 2: narrow lines

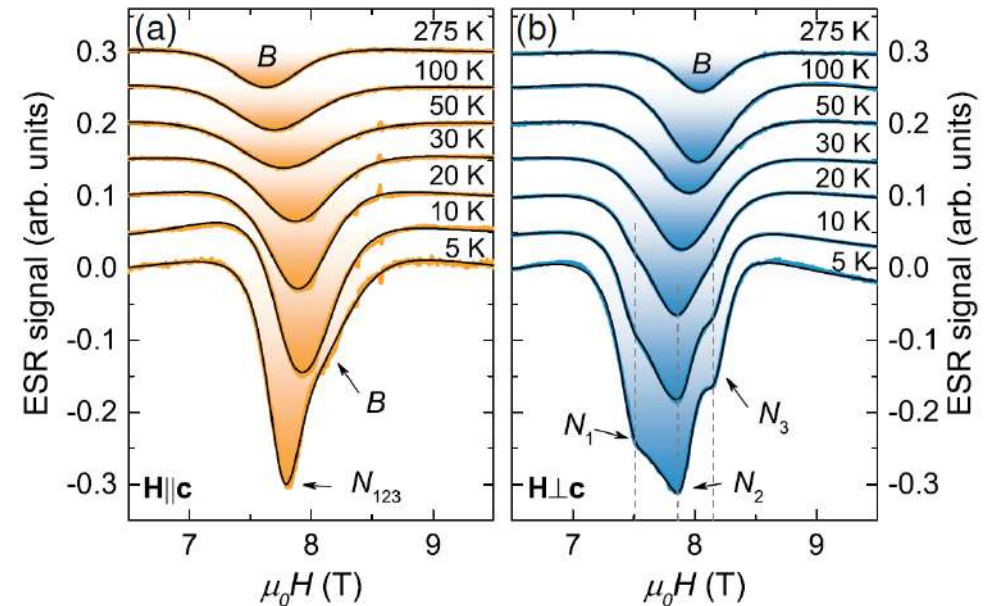
$$|J^{d_{II}}| \ll J_H$$



broken axial
symmetry:

$$\Delta g_{ab}^{d_{II}} = 0.02$$

$$|\Delta g_{ab}^{d_I}| \sim 0.003(1)$$



Zorko *et al.*, Phys. Rev. Lett. **118**, 017202 (2017)



ESR Resonance Field

□ Temperature dependent line shift: $\mathcal{H}' \ll \mathcal{H}_{ex}, \mathcal{H}_Z$

$$\delta B = \frac{1}{g\mu_B} \left(\frac{M_1}{M_0} - B_0 \right) = \frac{\langle [S^-, [S^+, \mathcal{H}']] \rangle}{2g\mu_B \langle S^z \rangle}$$

$$\mathcal{H}' = \frac{1}{2} \sum_{i,j \neq i} \mathbf{S}_i \cdot \underline{K}_{ij} \cdot \mathbf{S}_j$$

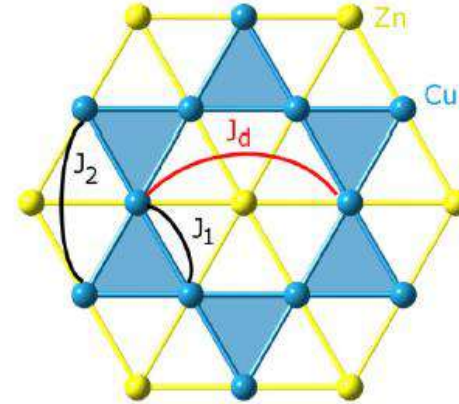
$$\underline{K}_{ij} = \underline{\delta}_{ij} + \underline{D}_{ij}$$

dipolar interaction symmetric AE

$$\Delta g^z(T) = \frac{\langle S^z \rangle}{2\mu_B B_0} \sum_{j \neq i} \left(2K_{ij}^{zz} - K_{ij}^{xx} - K_{ij}^{yy} \right)$$

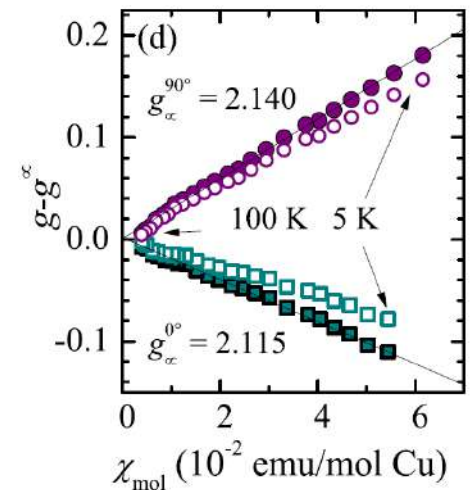
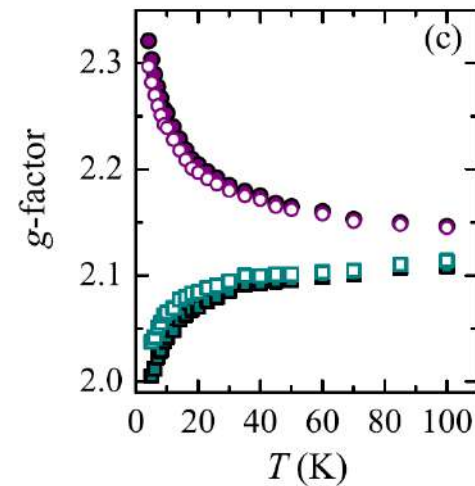
$$\langle S^z \rangle = \sum_i \langle S_i^z \rangle = \frac{\chi_{mol}(T) B_0}{N_A g \mu_0 \mu_B}$$

Nagata *et al.*, JPSJ **32**, 337 (1972)



ZnCu₃(OH)₆Cl₂
kapellasite:
27%-depleted
kagome AFM

$$|D'^{cc} / J_1| = 3\%$$



Kermarrec *et al.*, Phys. Rev. B **90**, 205103 (2014)



ESR Linewidth

□ Relaxation Function (Kubo-Tomita approach): $\mathcal{H}' \ll \mathcal{H}_0 = \mathcal{H}_Z + \mathcal{H}_{ex}$

$$\varphi(t) = \langle \tilde{S}^+(t) S^-(0) \rangle / \langle S^+(0) S^-(0) \rangle \quad \longrightarrow \quad I(\omega) \propto \int_{-\infty}^{\infty} \varphi(t) e^{i(\omega - \omega_0)t} dt$$

$$\omega_0 = g\mu_B B_0 / \hbar$$

➤ slow spin fluctuations:

$$\omega_0 \tau_c \gg 1 \quad (\tau_c \approx \hbar / J)$$



$$\varphi(t) = \exp\left(-\frac{1}{2} \frac{M_2}{\hbar^2} t^2\right)$$



Gaussian line shape

➤ fast spin fluctuations:

$$\omega_0 \tau_c \ll 1 \quad (\tau_c \approx \hbar / J)$$



$$\varphi(t) = \exp\left(-\sqrt{\frac{\pi}{2}} \frac{M_2}{\hbar^2} \tau_c t\right)$$



Lorentzian line shape

$$\Delta B = C \frac{k_B}{g\mu_B} \sqrt{\frac{M_2^3}{M_4}} \propto \frac{M_2}{J}$$

$$M_2 = \frac{\langle [\mathcal{H}', S^+] [S^-, \mathcal{H}'] \rangle}{\langle S^+ S^- \rangle},$$

$$M_4 = \frac{\langle [\mathcal{H} - \mathcal{H}_Z, [\mathcal{H}', S^+]] [\mathcal{H} - \mathcal{H}_Z, [\mathcal{H}', S^-]] \rangle}{\langle S^+ S^- \rangle}$$

A. Zorko, Determination of Magnetic Anisotropy by EPR, in *Topics From EPR Research* (ed. Ahmed Maghraby), IntechOpen, 2018.



ESR Linewidth

□ Relaxation Function (Kubo-Tomita approach): $\mathcal{H}' \ll \mathcal{H}_0 = \mathcal{H}_Z + \mathcal{H}_{ex}$ $\omega_0 = g\mu_B B_0 / \hbar$

$$\varphi(t) = \langle \tilde{S}^+(t) S^-(0) \rangle / \langle S^+(0) S^-(0) \rangle \quad \longrightarrow \quad I(\omega) \propto \int_{-\infty}^{\infty} \varphi(t) e^{i(\omega - \omega_0)t} dt$$

➤ slow spin fluctuations:

$$\omega_0 \tau_c \gg 1 \quad (\tau_c \approx \hbar / J)$$



$$\varphi(t) = \exp\left(-\frac{1}{2} \frac{M_2}{\hbar^2} t^2\right)$$



Gaussian line shape

➤ fast spin fluctuations:

$$\omega_0 \tau_c \ll 1 \quad (\tau_c \approx \hbar / J)$$



$$\varphi(t) = \exp\left(-\sqrt{\frac{\pi}{2}} \frac{M_2}{\hbar^2} \tau_c t\right)$$



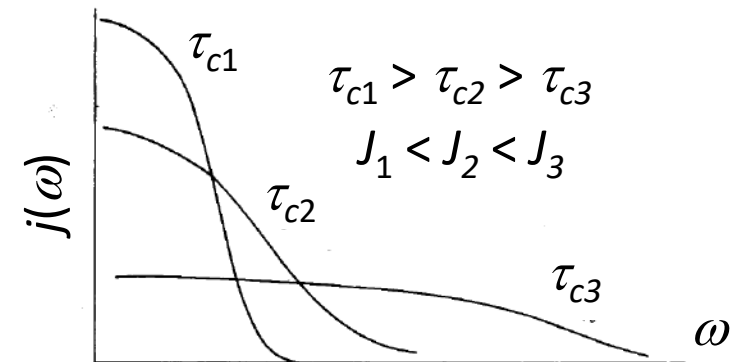
Lorentzian line shape

$$\Delta B = C \frac{k_B}{g\mu_B} \sqrt{\frac{M_2^3}{M_4}} \propto \frac{M_2}{J}$$



❖ exchange narrowing

❖ finite linewidth due to \mathcal{H}'



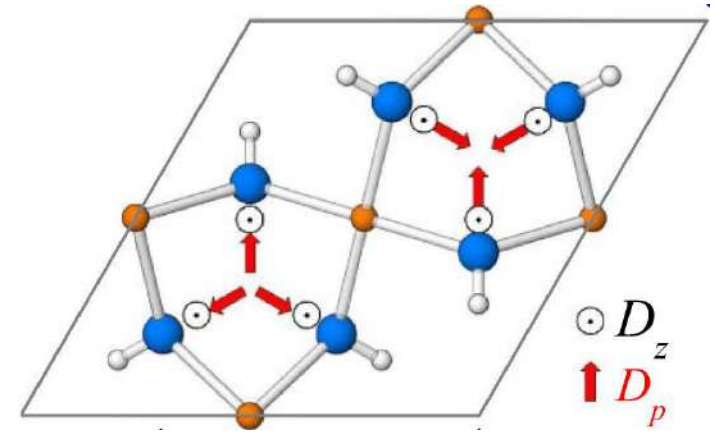
Zorko, Determination of Magnetic Anisotropy by EPR, in *Topics From EPR Research* (ed. Ahmed Maghraby), IntechOpen, 2018.



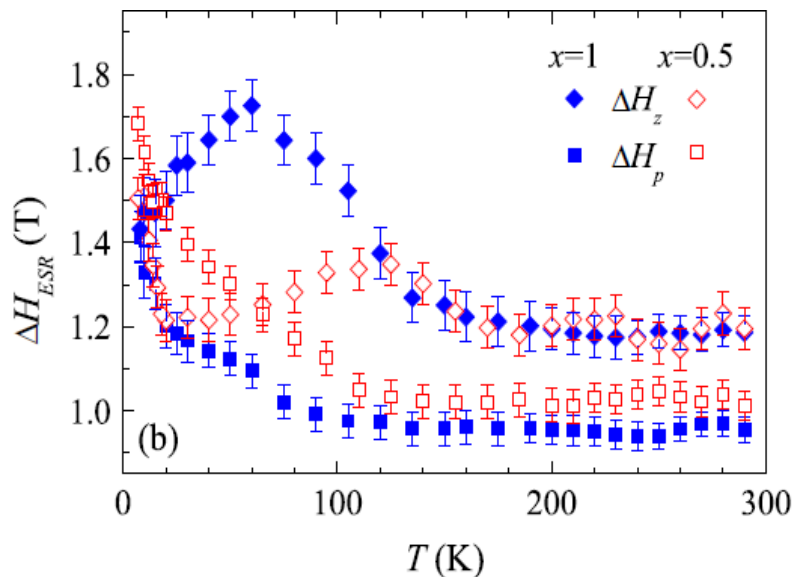
ESR Linewidth

□ ESR linewidth on the kagome lattice: $\mathcal{H}_{\text{DM}} = \vec{D} \cdot \sum_{(i,j)} \vec{S}_i \times \vec{S}_j$

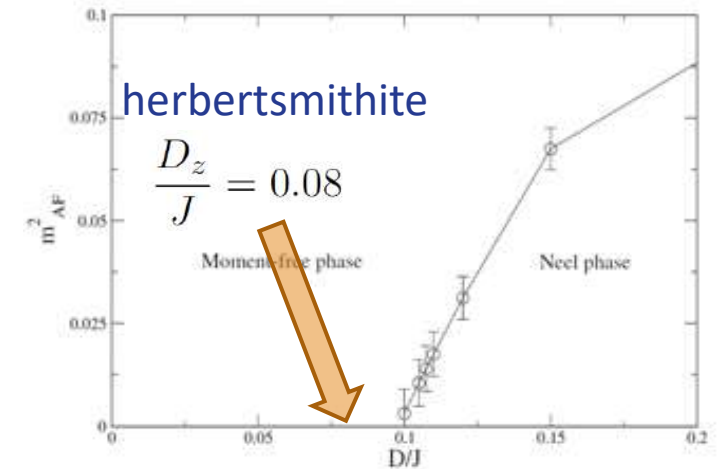
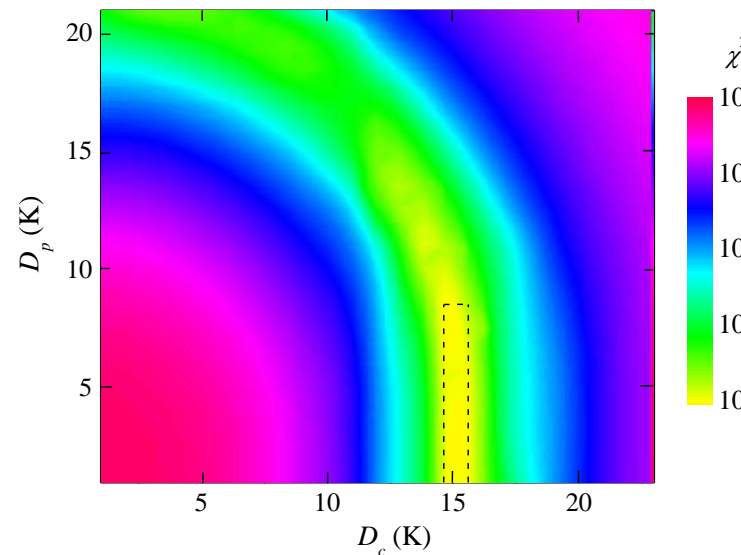
$$\Delta B(\theta) = \sqrt{2\pi} \frac{k_b}{2g(\theta)\mu_B J} \sqrt{\frac{(2d_z^2 + 3d_p^2 + (2d_z^2 - d_p^2) \cos^2 \theta)^3}{16d_z^2 + 78d_p^2 + (16d_z^2 - 26d_p^2) \cos^2 \theta}}$$



□ Herbertsmithite: kagome AFM



Zorko *et al.*, Phys. Rev. Lett. **101**, 026405 (2008)



Cepas *et al.*, Phys. Rev. B **78**, 140405(R) (2008)

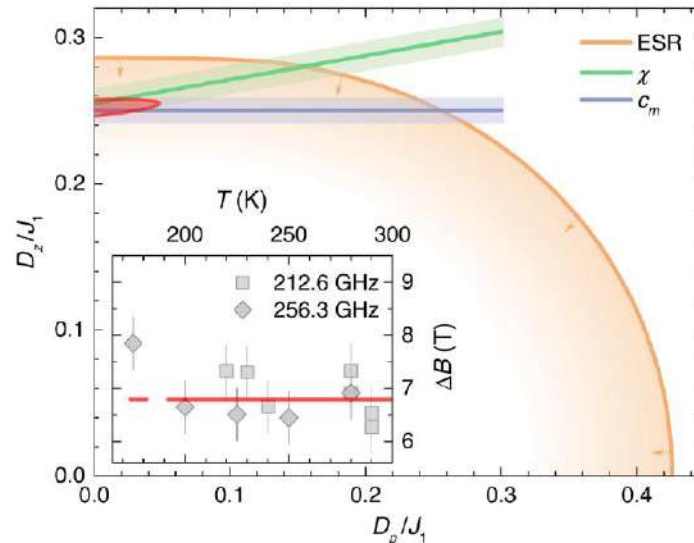
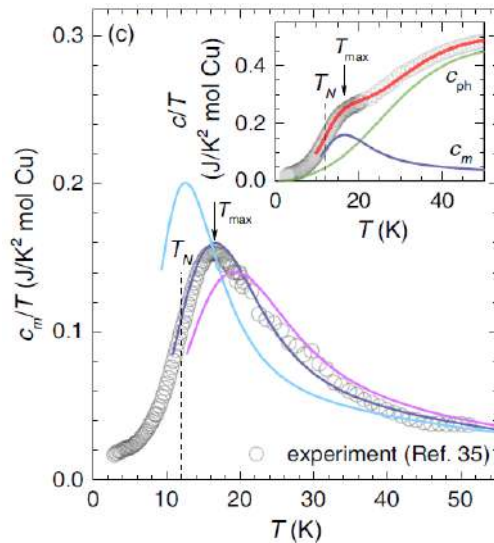
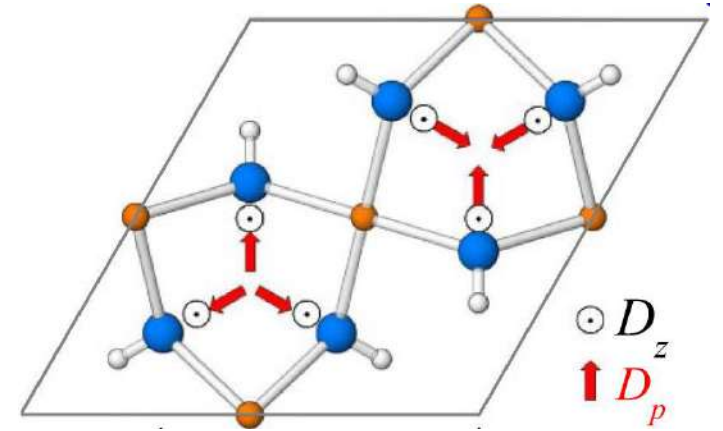


ESR Linewidth

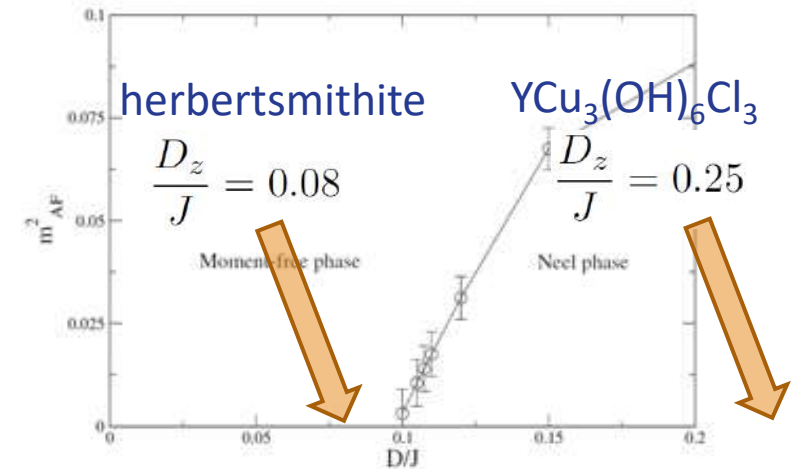
□ ESR linewidth on the kagome lattice: $\mathcal{H}_{\text{DM}} = \vec{D} \cdot \sum_{(i,j)} \vec{S}_i \times \vec{S}_j$

$$\Delta B(\theta) = \sqrt{2\pi} \frac{k_b}{2g(\theta)\mu_B J} \sqrt{\frac{(2d_z^2 + 3d_p^2 + (2d_z^2 - d_p^2) \cos^2 \theta)^3}{16d_z^2 + 78d_p^2 + (16d_z^2 - 26d_p^2) \cos^2 \theta}}$$

□ $\text{YCu}_3(\text{OH})_6\text{Cl}_3$: kagome AFM



Arh *et al.*, Phys. Rev. Lett. **125**, 027203 (2020)



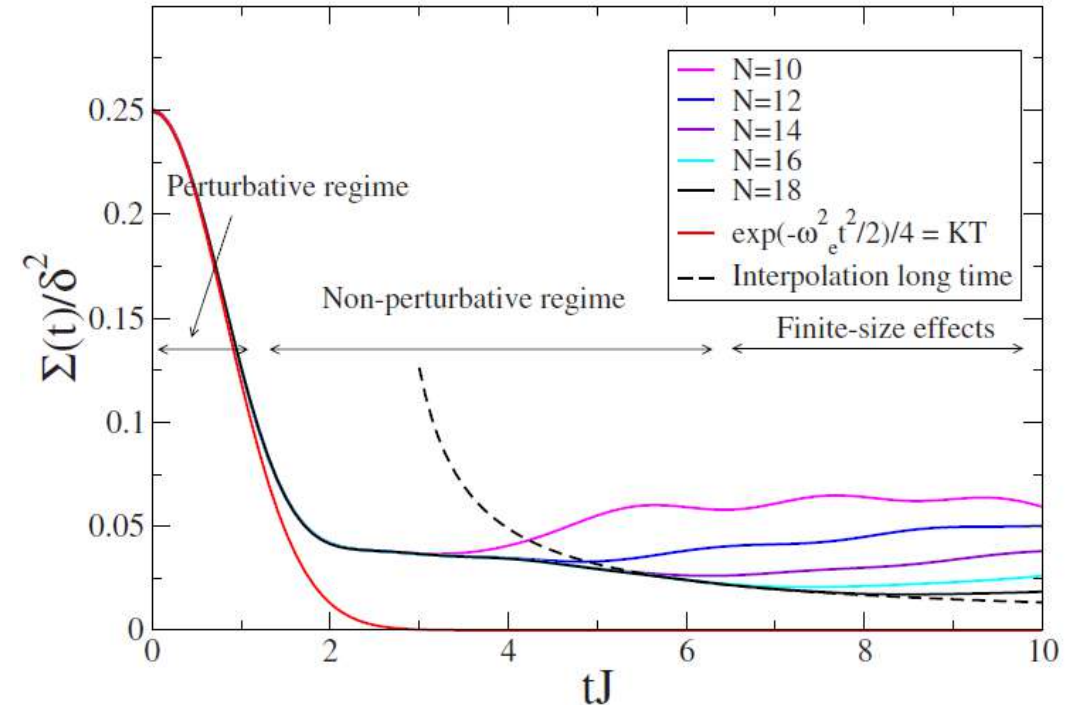
Cepas *et al.*, Phys. Rev. B **78**, 140405(R) (2008)



ESR Linewidth

□ Limitations of the Kubo-Tomita approach:

- high temperatures
- transformation of the DM term to higher-order terms due to hidden symmetry
 - ❖ staggered DM in spin chains
Choukroun *et al.*, Phys. Rev. Lett. **87**, 127207 (2001)
 - ❖ reducible DM components in 2D
Cheng *et al.*, Phys. Rev. B **75**, 144422 (2007)
- slower decay of spin correlations in low-D magnets
 - ➔ overestimation of magnetic anisotropy



El Shawish *et al.*, Phys. Rev. B **81**, 224421 (2010)



Outline

- Introduction to magnetism
- Probing magnetism: conventional bulk and scattering techniques
- Local probes of magnetism
- Electron spin resonance (ESR)
- Nuclear magnetic resonance (NMR)
- Muon spectroscopy (μ SR)
- Summary: strengths, limitations and complementarity of local probes



Motivation for NMR Measurements

□ Most common nuclei:

Isotope	Occurrence in nature (%)	Spin number I	Magnetic moment μ (μ_N)	Electric quadrupole moment ($e \times 10^{-24} \text{ cm}^2$)	Operating frequency at 7 T (MHz)	Relative sensitivity
^1H	99.984	$\frac{1}{2}$	2.79628	0	300.13	1
^2H	0.016	1	0.85739	0.0028	46.07	0.0964
^{10}B	18.8	3	1.8005	0.074	32.25	0.0199
^{11}B	81.2	$\frac{3}{2}$	2.6880	0.026	96.29	0.165
^{12}C	98.9	0	0	0	0	0
^{13}C	1.1	$\frac{1}{2}$	0.70220	0	75.47	0.0159
^{14}N	99.64	1	0.40358	0.071	21.68	0.00101
^{15}N	0.37	$\frac{1}{2}$	-0.28304	0	30.41	0.00104
^{16}O	99.76	0	0	0	0	0
^{17}O	0.0317	$\frac{5}{2}$	-1.8930	-0.0040	40.69	0.0291
^{19}F	100	$\frac{1}{2}$	2.6273	0	282.40	0.834
^{28}Si	92.28	0	0	0	0	0
^{29}Si	4.70	$\frac{1}{2}$	-0.5548	0	59.63	0.0785
^{31}P	100	$\frac{1}{2}$	1.1205	0	121.49	0.0664
^{35}Cl	75.4	$\frac{3}{2}$	0.92091	-0.079	29.41	0.0047
^{37}Cl	24.6	$\frac{3}{2}$	0.68330	-0.062	24.48	0.0027

<https://en.wikipedia.org>



Motivation for NMR Measurements



□ Broad range of applications:

- analysis of chemicals and chemical compositions
- molecular structure
- molecular physics/dynamics
- purity determination
- process control (pharmaceutical industry, polymer production, cosmetics, food manufacturing, study of batteries,...)
- ...

CHEMISTRY/
INDUSTRY

- biochemical studies of tissues
- magnetic resonance imaging (MRI)
- ...

BIOLOGY/
MEDICINE

- magnetic properties of materials
- structural properties of materials
- ...

PHYSICS/
MATERIALS
RESEARCH



Motivation for NMR Measurements



□ Broad range of applications:

- analysis of chemicals and chemical compositions
- molecular structure
- molecular physics/dynamics
- purity determination
- process control (pharmaceutical industry, polymer production, cosmetics, food manufacturing, study of batteries,...)
- ...

CHEMISTRY/
INDUSTRY

- biochemical studies of tissues
- magnetic resonance imaging (MRI)
- ...

BIOLOGY/
MEDICINE

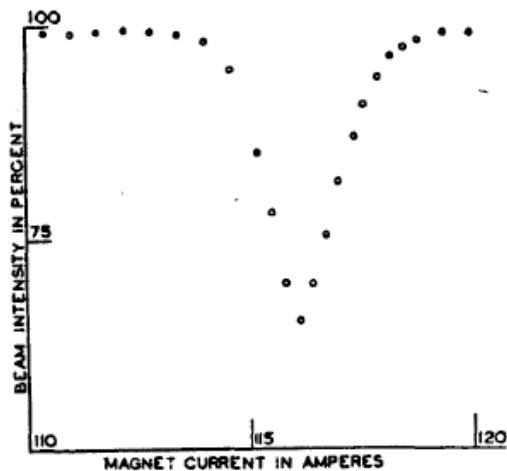
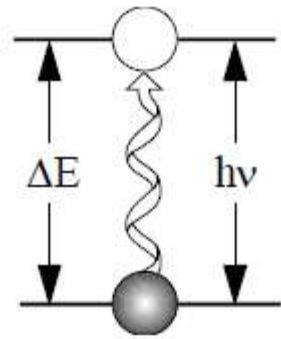
- magnetic properties of materials
- structural properties of materials
- ...

PHYSICS/
MATERIALS
RESEARCH



A Brief History of NMR

- 1938: interactions of LiCl molecular beams with EM waves in a static magnetic field



The Nobel Prize in Physics 1944



Photo from the Nobel
Foundation archive.

Isidor Isaac Rabi

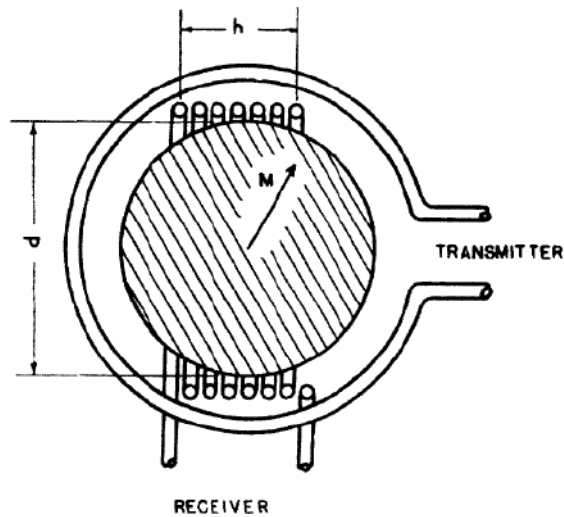
Prize share: 1/1

The Nobel Prize in Physics 1944 was awarded to Isidor Isaac Rabi "for his resonance method for recording the magnetic properties of atomic nuclei."

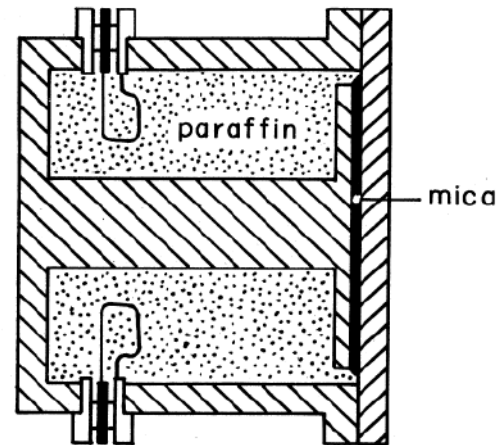
<https://www.nobelprize.org>

A Brief History of NMR

□ 1945: NMR in condensed matter



in water



in paraffin

The Nobel Prize in Physics 1952



Photo from the Nobel
Foundation archive.

Felix Bloch

Prize share: 1/2



Photo from the Nobel
Foundation archive.

Edward Mills Purcell

Prize share: 1/2

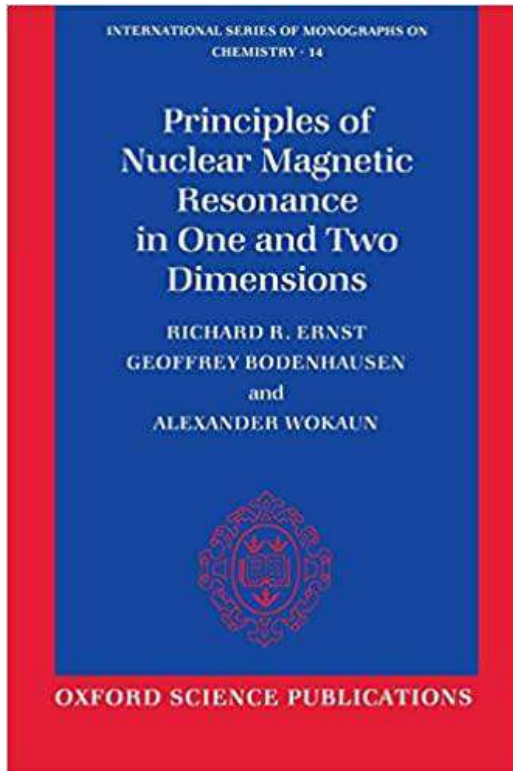
The Nobel Prize in Physics 1952 was awarded jointly to Felix Bloch and Edward Mills Purcell "for their development of new methods for nuclear magnetic precision measurements and discoveries in connection therewith."

<https://www.nobelprize.org>



A Brief History of NMR

- 1950's and 1960's: high resolution NMR (FT NMR, noise decoupling, novel pulse techniques, 2D NMR,...)



The Nobel Prize in Chemistry 1991



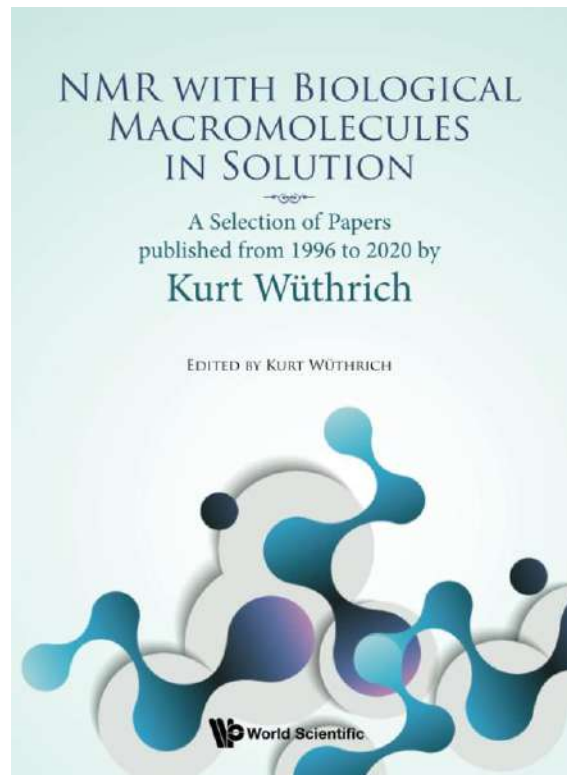
Photo from the Nobel
Foundation archive.
Richard R. Ernst
Prize share: 1/1

The Nobel Prize in Chemistry 1991 was awarded to Richard R. Ernst "for his contributions to the development of the methodology of high resolution nuclear magnetic resonance (NMR) spectroscopy."

<https://www.nobelprize.org>

A Brief History of NMR

- 1970's and 1980's: 3D structure of biological macromolecules in solution with NMR



The Nobel Prize in Chemistry 2002



Photo from the Nobel Foundation archive.
John B. Fenn
Prize share: 1/4



Photo from the Nobel Foundation archive.
Koichi Tanaka
Prize share: 1/4



Photo from the Nobel Foundation archive.
Kurt Wüthrich
Prize share: 1/2

The Nobel Prize in Chemistry 2002 was awarded "for the development of methods for identification and structure analyses of biological macromolecules" with one half jointly to John B. Fenn and Koichi Tanaka "for their development of soft desorption ionisation methods for mass spectrometric analyses of biological macromolecules" and the other half to Kurt Wüthrich "for his development of nuclear magnetic resonance spectroscopy for determining the three-dimensional structure of biological macromolecules in solution."

<https://www.nobelprize.org>



A Brief History of NMR

- 1970's: magnetic resonance imaging (MRI)



The Nobel Prize in Physiology or Medicine 2003



Photo from the Nobel
Foundation archive.
Paul C. Lauterbur
Prize share: 1/2



Photo from the Nobel
Foundation archive.
Sir Peter Mansfield
Prize share: 1/2

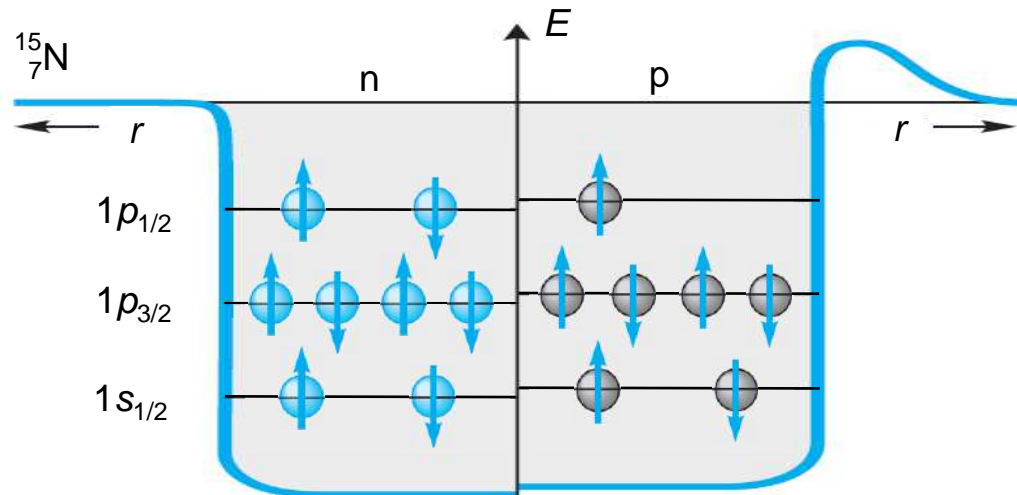
The Nobel Prize in Physiology or Medicine 2003 was awarded jointly to Paul C. Lauterbur and Sir Peter Mansfield "for their discoveries concerning magnetic resonance imaging."

<https://www.nobelprize.org>



Nuclear Magnetism

□ Shell model: nuclear spin I



□ Nuclear magnetic moment:

$$\vec{\mu} = g\mu_n\vec{I} = \hbar\gamma_n\vec{I}$$

$$\mu_n = \frac{e_0\hbar}{2m_p} = 5.05 \times 10^{-27} \text{ Am}^2$$

The Nobel Prize in Physics 1963



Photo from the Nobel Foundation archive.
Eugene Paul Wigner
Prize share: 1/2



Photo from the Nobel Foundation archive.
Maria Goeppert Mayer
Prize share: 1/4

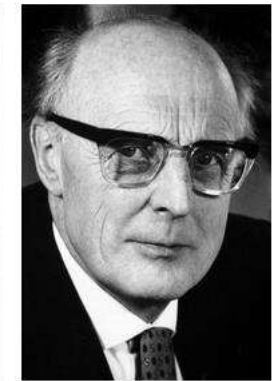


Photo from the Nobel Foundation archive.
J. Hans D. Jensen
Prize share: 1/4

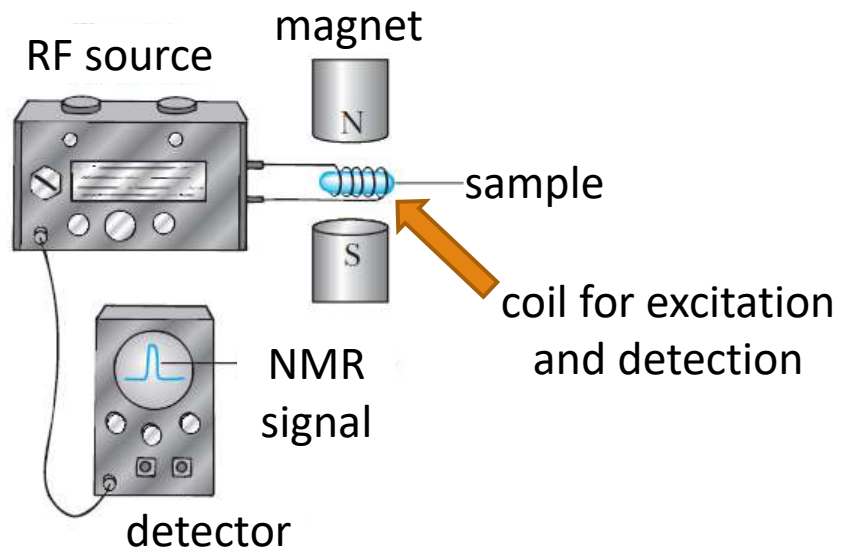
The Nobel Prize in Physics 1963 was divided, one half awarded to Eugene Paul Wigner "for his contributions to the theory of the atomic nucleus and the elementary particles, particularly through the discovery and application of fundamental symmetry principles", the other half jointly to Maria Goeppert Mayer and J. Hans D. Jensen "for their discoveries concerning nuclear shell structure."

<https://www.nobelprize.org>



NMR Apparatus

- magnet
- RF source
- detector

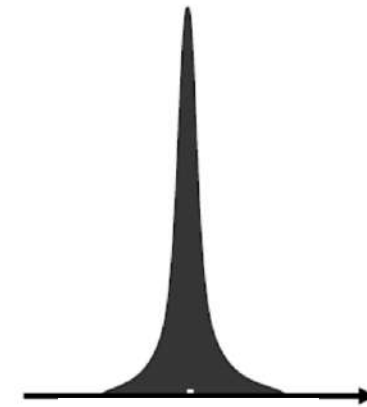
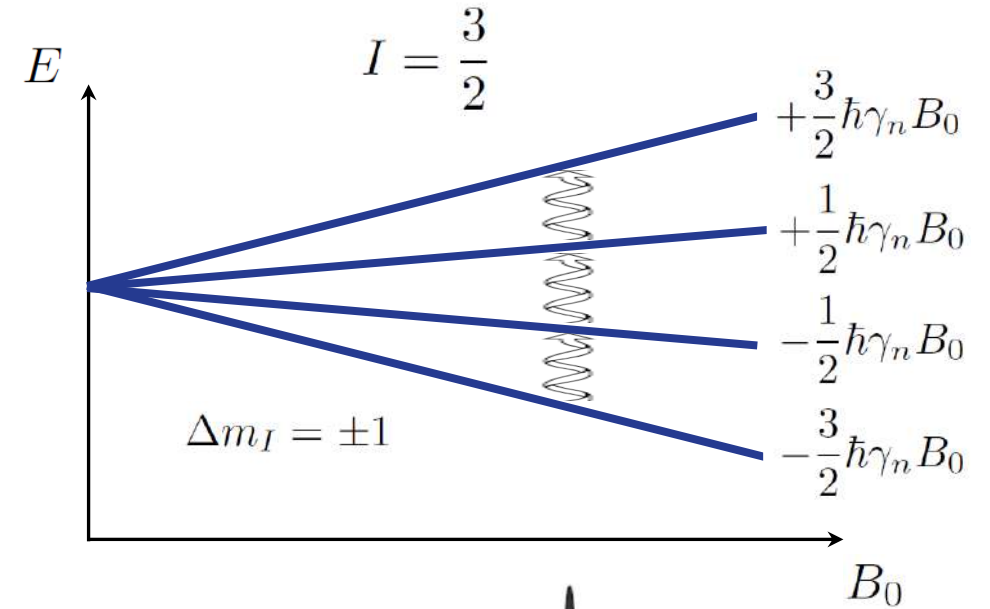


NMR Apparatus

- magnet
- RF source
- detector



Bruker NMR spectrometer

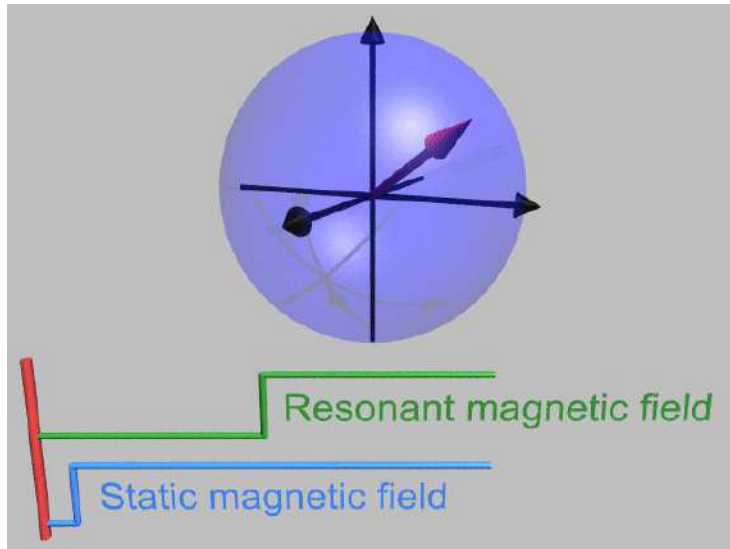


Larmor frequency: $\nu_L = \frac{\gamma_n}{2\pi} B_0$

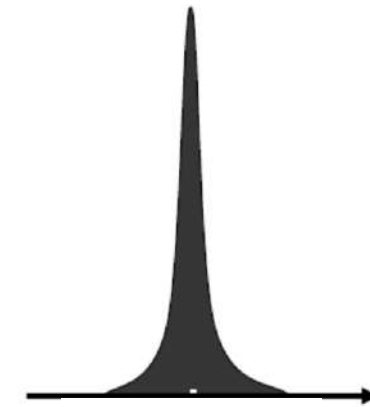
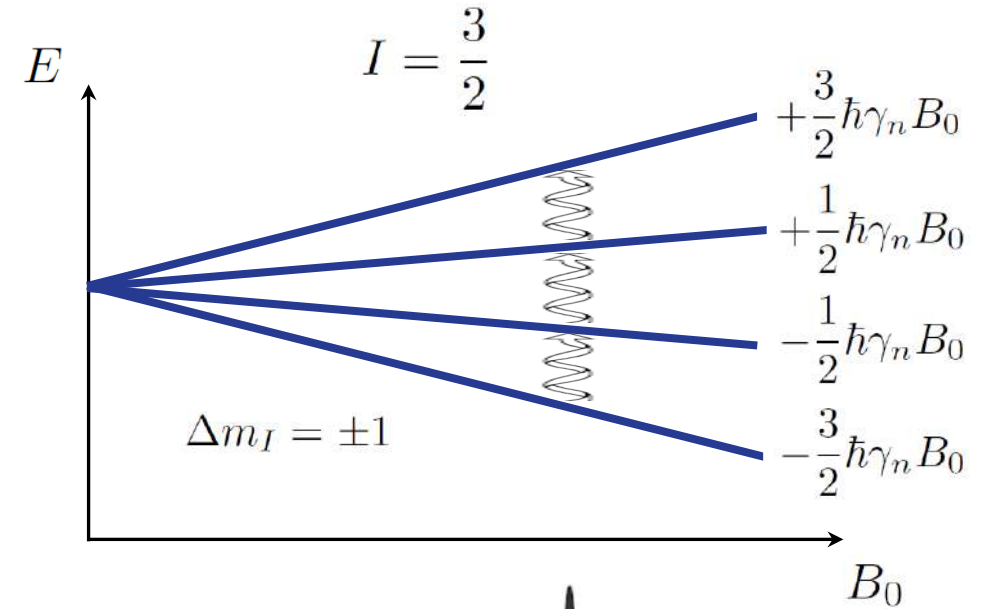
NMR Apparatus

- magnet
- RF source
- detector

$$\frac{d\vec{\mu}}{dt} = \gamma_n \vec{\mu} \times \vec{B}$$



Wikimedia Commons



Larmor frequency: $\nu_L = \frac{\gamma_n}{2\pi} B_0$

Nuclear Magnetization

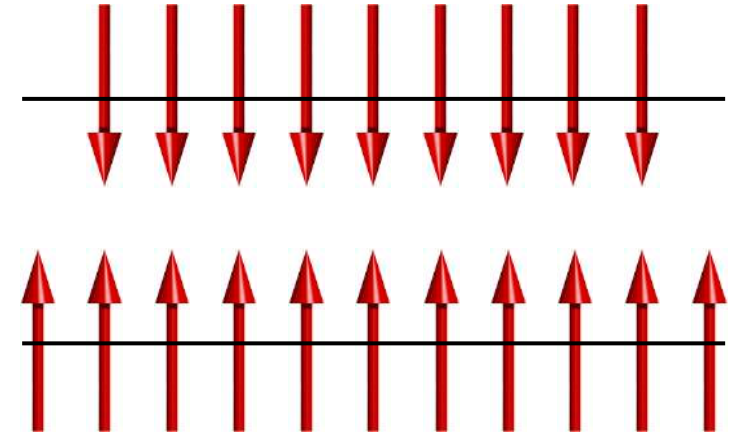
□ External field: $\vec{B}_0 \parallel z$



equilibrium
magnetization
at 1 K and 1 T

$$\frac{\hbar\gamma_n B_0}{k_B} \sim 100 \mu\text{K}$$

$$M_{mol} = \frac{N_A \mu^2}{3k_B T} B_0 \sim 10^{-4} \mu N_A \sim 10^{-7} \text{ Am}^2$$

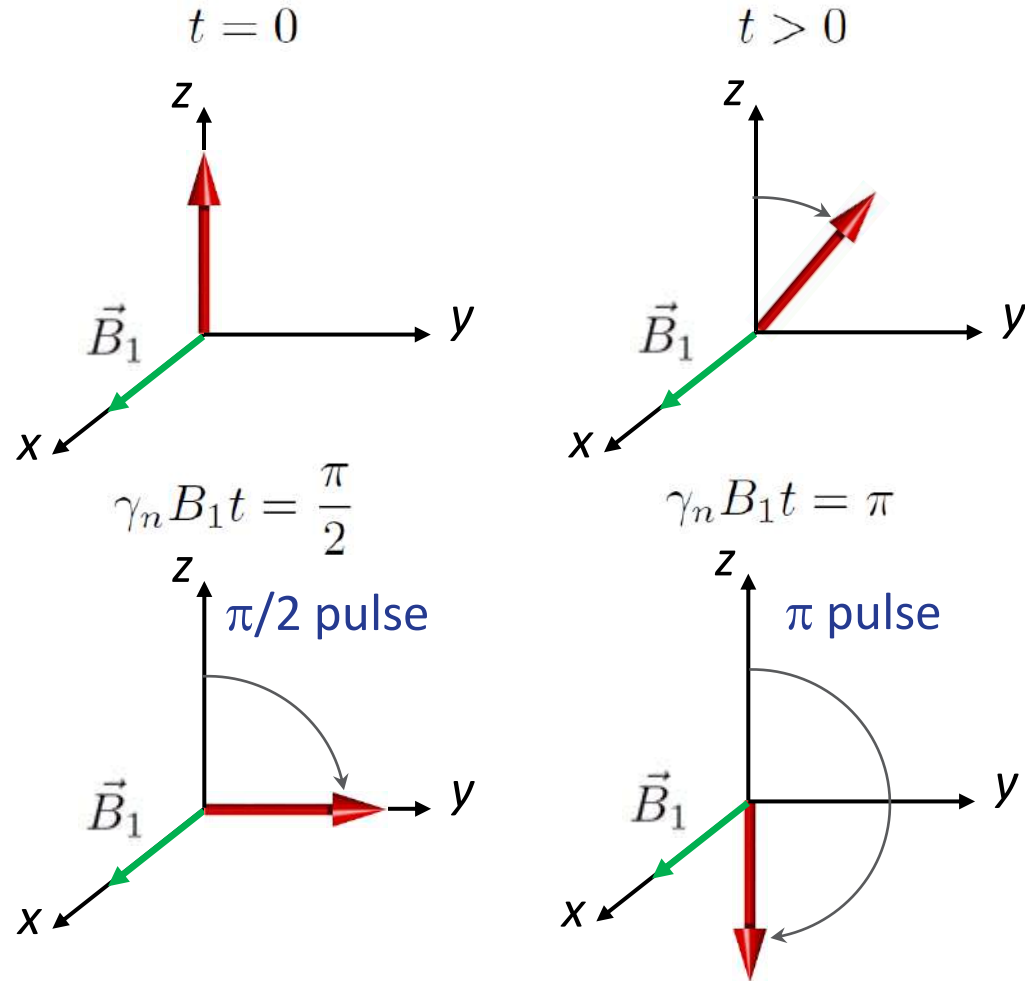


□ Requirements:

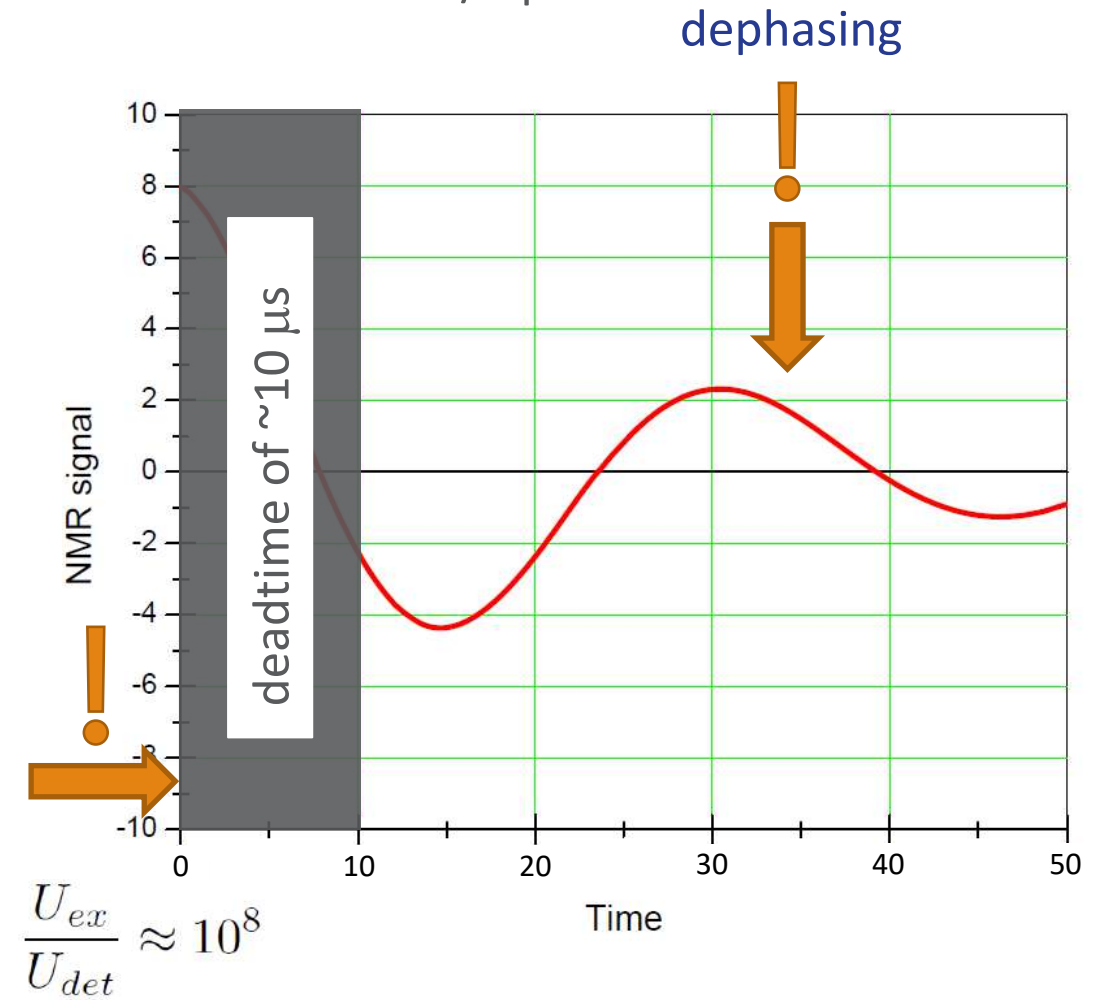
- high magnetic field (> 1 T)
- (low temperature helps)

Pulsed NMR

□ Pulsed RF field: $\vec{B}_1 \perp \vec{B}_0 \parallel z$

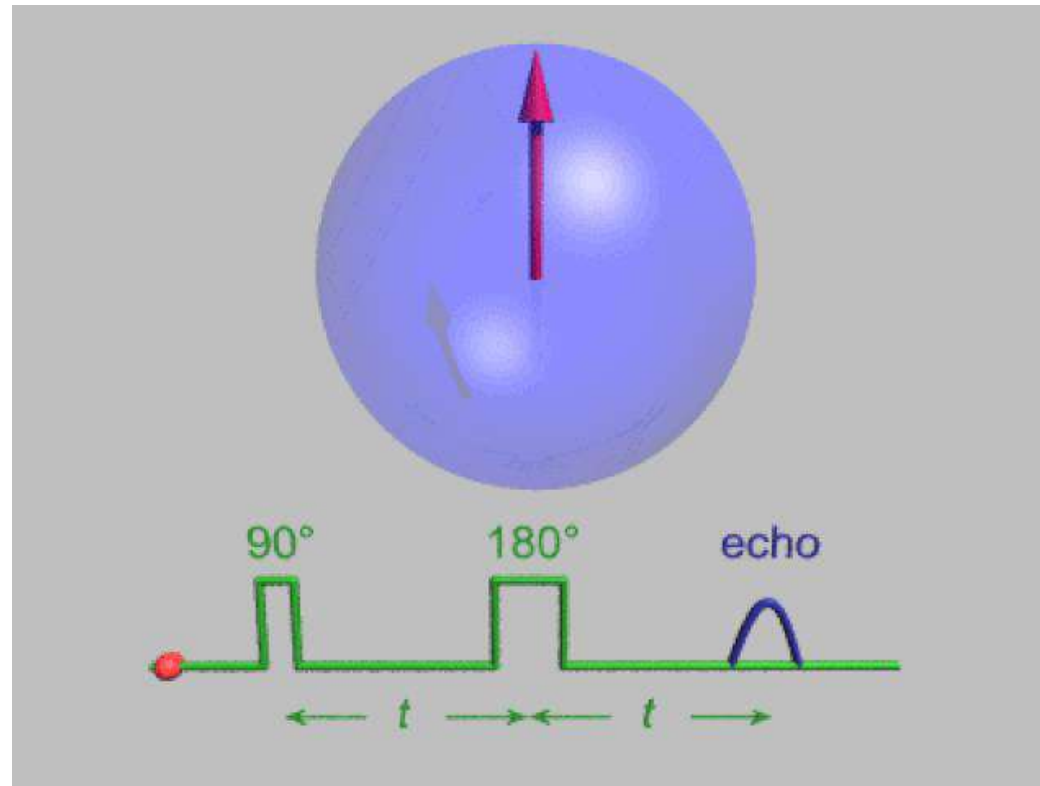


□ FID after $\pi/2$ pulse:



Pulsed NMR

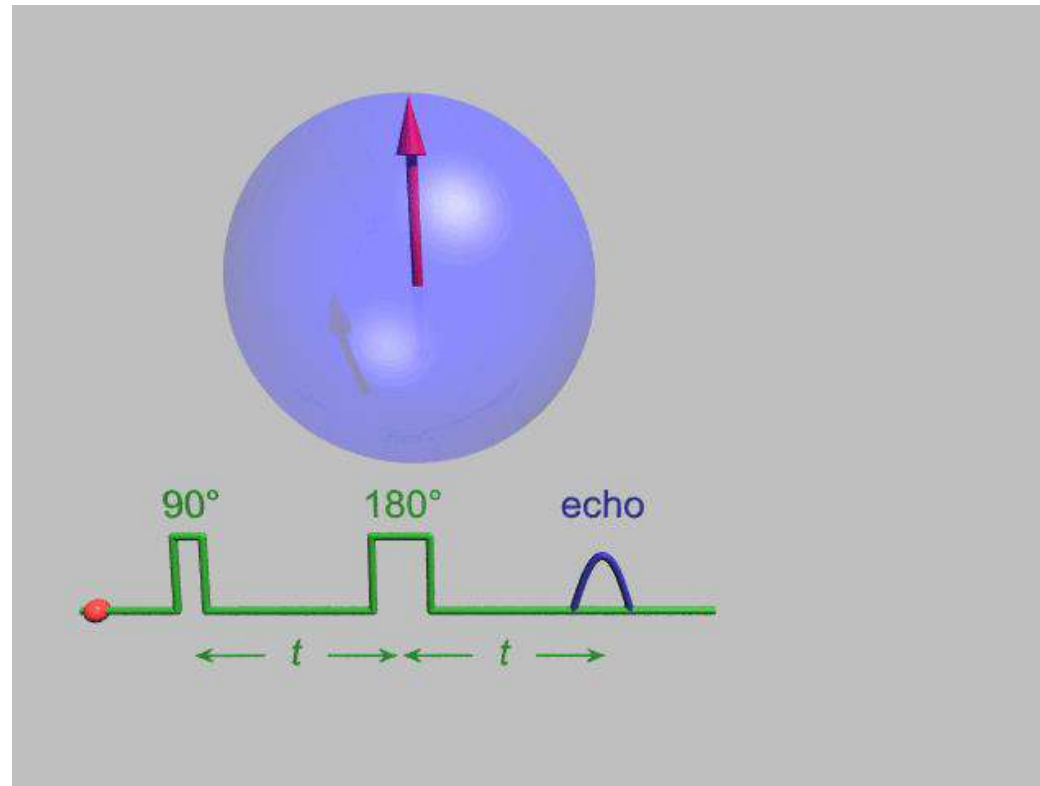
- Spin (Hahn) echo: $\pi/2 - \pi - \text{ECHO}$



Wikimedia Commons

Nuclear Spin Relaxation

- Spin-spin relaxation: T_2 relaxation



Bloch equations:

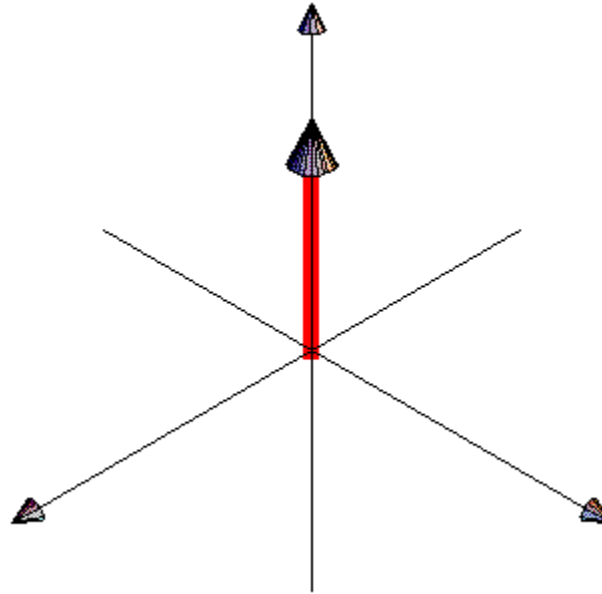
$$\frac{dM_x}{dt} = \gamma_n M_y B_0 - \frac{M_x}{T_2}$$

$$\frac{dM_y}{dt} = -\gamma_n M_x B_0 - \frac{M_y}{T_2}$$

Wikimedia Commons

Nuclear Spin Relaxation

- Spin-lattice relaxation: T_1 relaxation



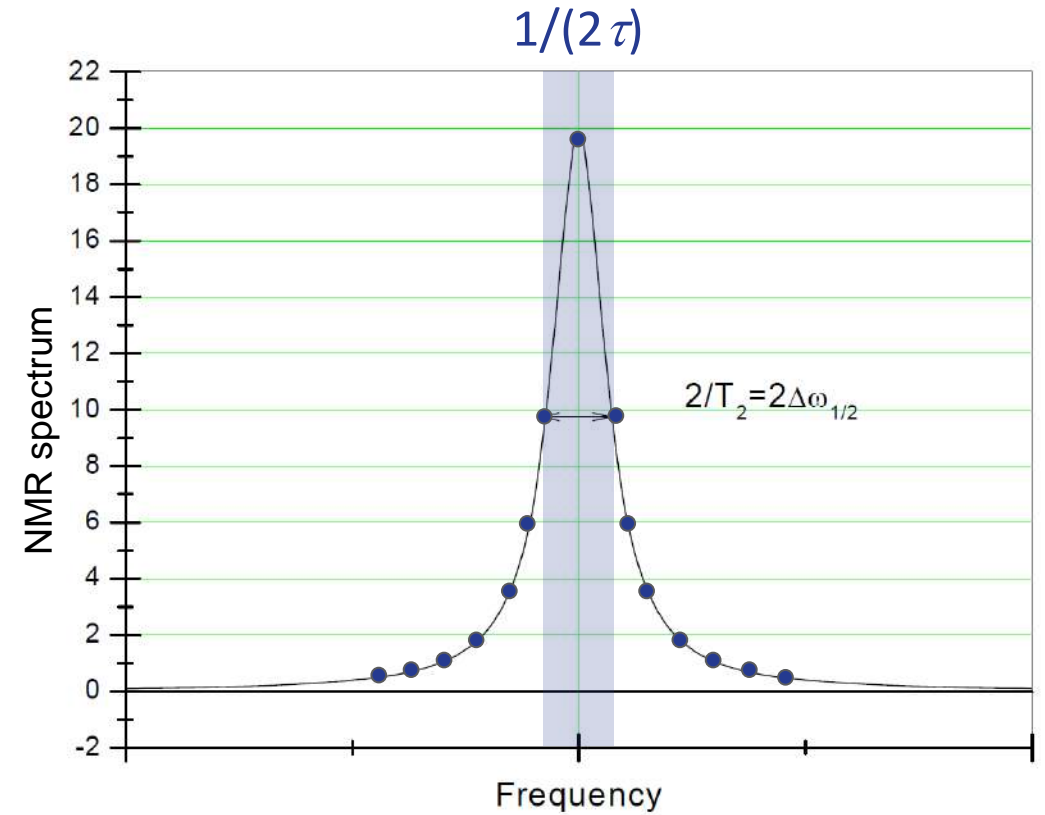
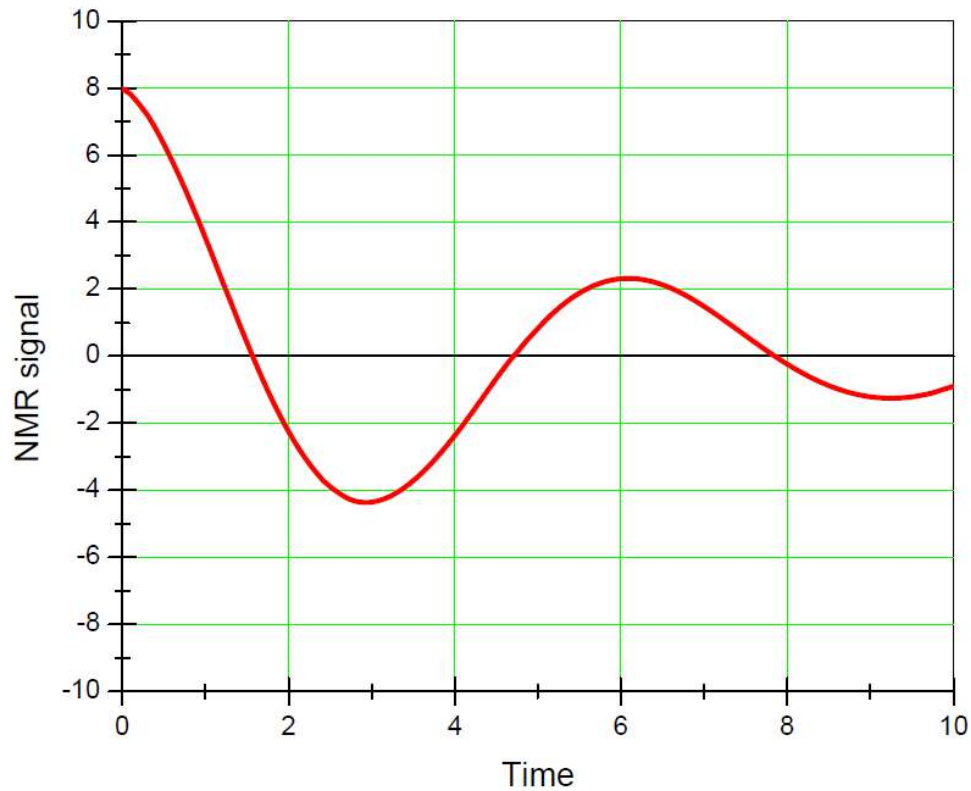
Bloch equations:

$$\frac{dM_z}{dt} = \frac{M_0 - M_z}{T_1}$$

<https://gifimage.net>

NMR spectrum

□ Fourier transform: excitation width $1/(2\tau)$



combining FTs

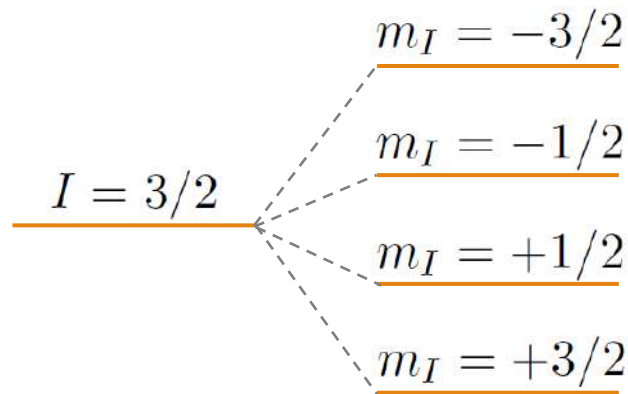


NMR Hamiltonian

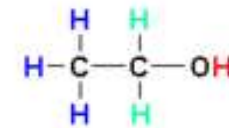
□ The Hamiltonian:

$$\mathcal{H} = \mathcal{H}_{nZ} + \mathcal{H}_{nn} + \mathcal{H}_{ne} + \mathcal{H}_{EFG}$$

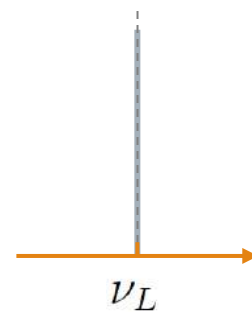
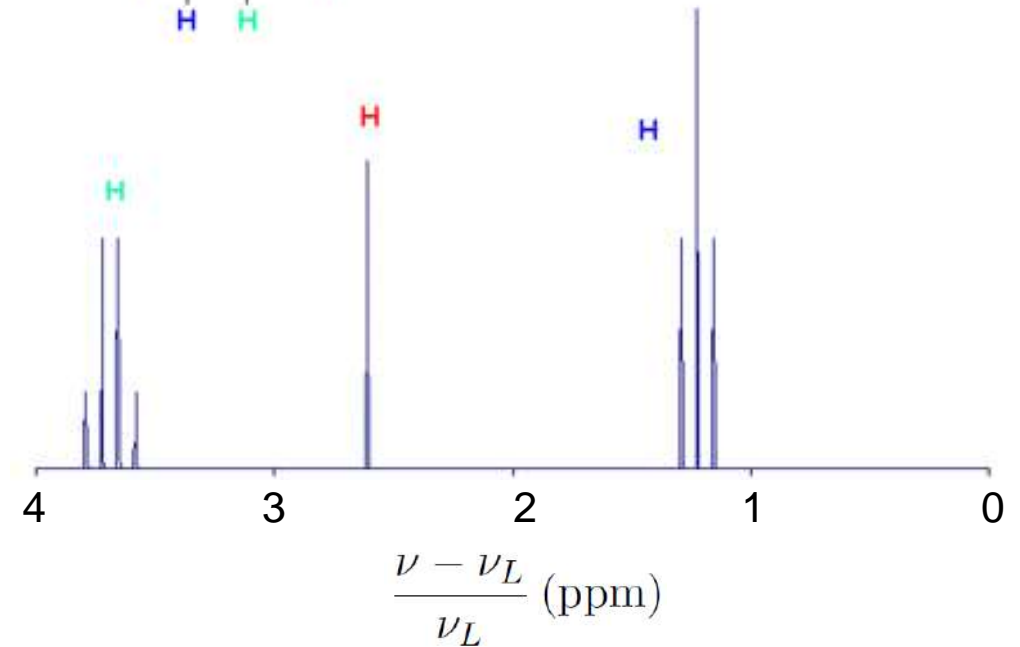
\mathcal{H}_{nZ} : nuclear Zeeman interaction
 \mathcal{H}_{nn} : nuclear-nuclear interaction
 \mathcal{H}_{ne} : hyperfine coupling
 \mathcal{H}_{EFG} : quadrupole interaction



chemical shift:
electron screening



ethanol

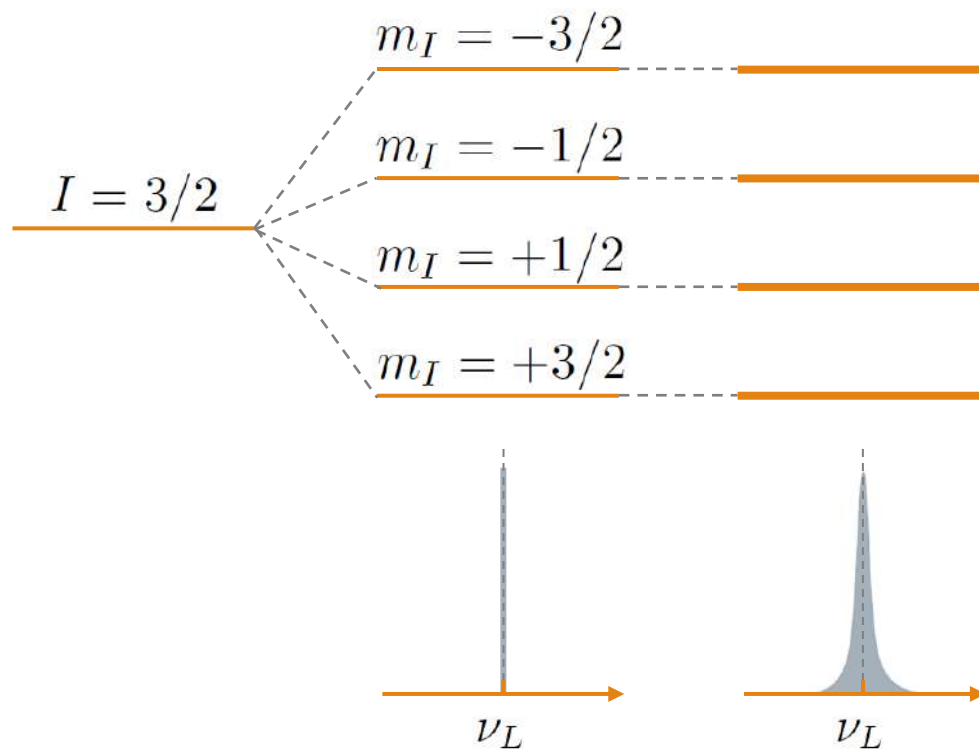


NMR Hamiltonian

□ The Hamiltonian:

$$\mathcal{H} = \mathcal{H}_{nZ} + \mathcal{H}_{nn} + \mathcal{H}_{ne} + \mathcal{H}_{EFG}$$

nuclear Zeeman interaction nuclear-nuclear interaction hyperfine coupling quadrupole interaction

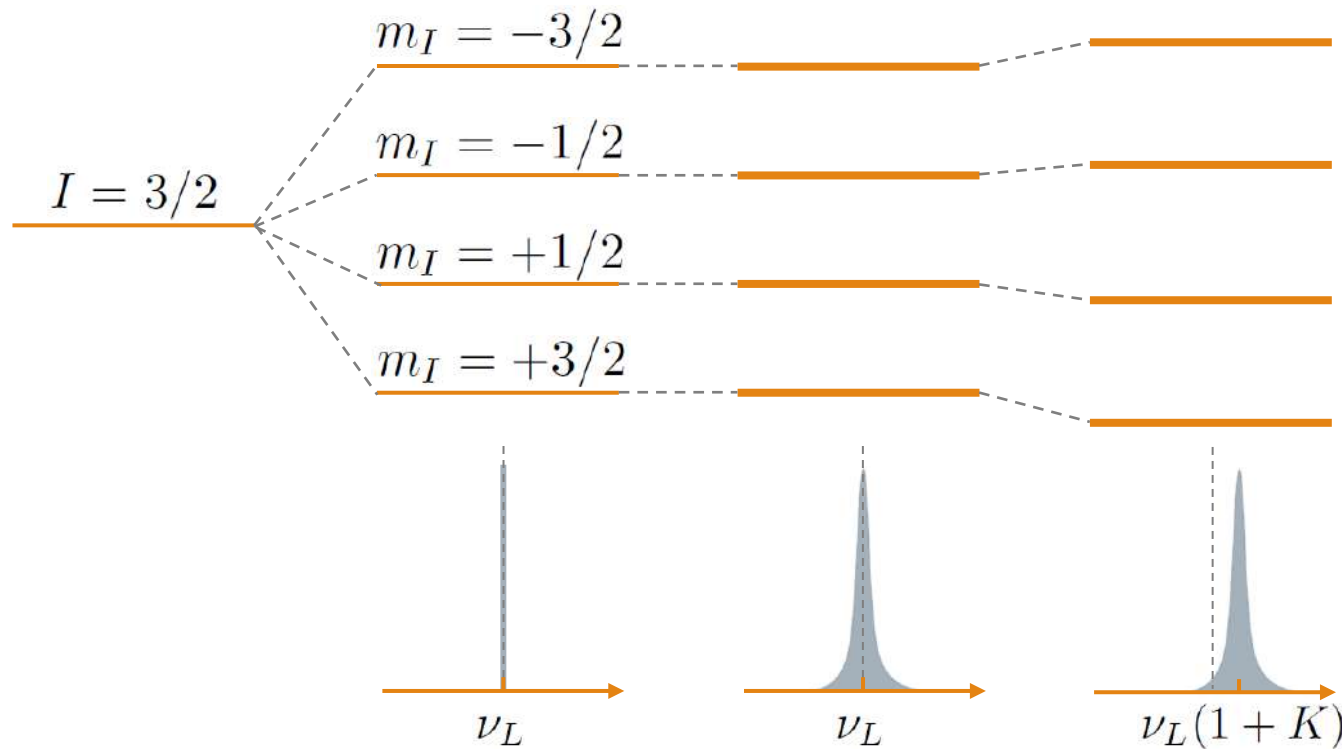


NMR Hamiltonian

□ The Hamiltonian:

$$\mathcal{H} = \mathcal{H}_{nZ} + \mathcal{H}_{nn} + \mathcal{H}_{ne} + \mathcal{H}_{EFG}$$

nuclear Zeeman interaction nuclear-nuclear interaction hyperfine coupling quadrupole interaction

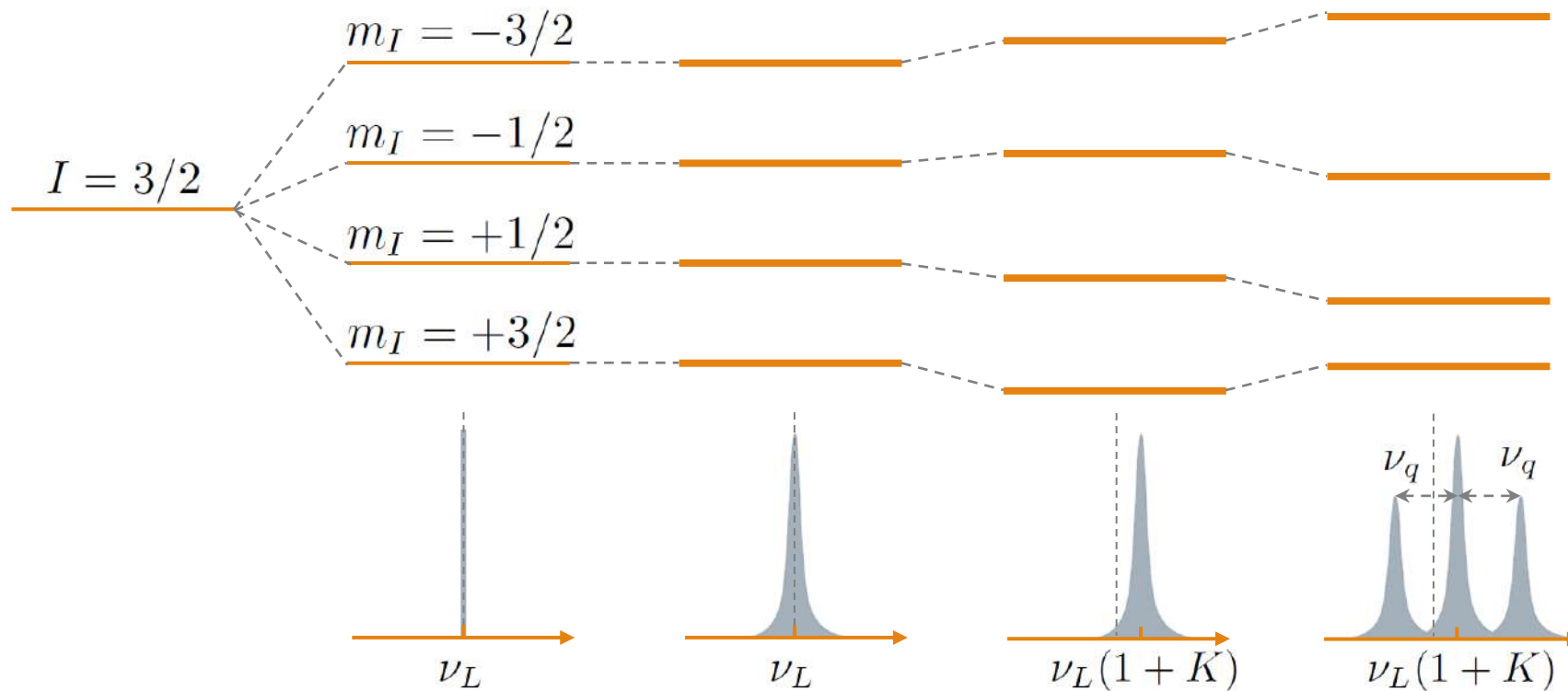


NMR Hamiltonian

□ The Hamiltonian:

$$\mathcal{H} = \mathcal{H}_{nZ} + \mathcal{H}_{nn} + \mathcal{H}_{ne} + \mathcal{H}_{EFG}$$

nuclear Zeeman interaction nuclear-nuclear interaction hyperfine coupling quadrupole interaction



NMR Hamiltonian

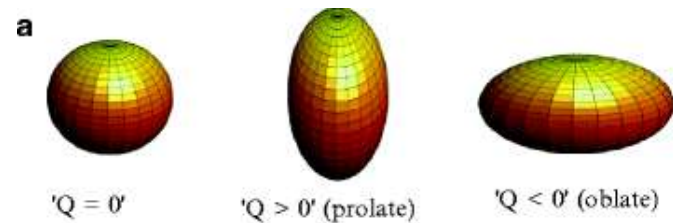
$$\mathcal{H} = \mathcal{H}_{nZ} + \mathcal{H}_{nn} + \mathcal{H}_{ne} + \mathcal{H}_{EFG}$$

□ The Hamiltonian:

□ Quadrupole interaction: $I > 1/2$

➤ nuclear quadrupole moment:

$$eQ_{\alpha\beta} = e \sum_{i \in \text{protons}} \left(3x_i^\alpha x_i^\beta - \delta_{\alpha\beta} r_i^2 \right)$$



Fernandez, Probing Quadrupolar Nuclei
by Solid-State NMR Spectroscopy:
Recent Advances

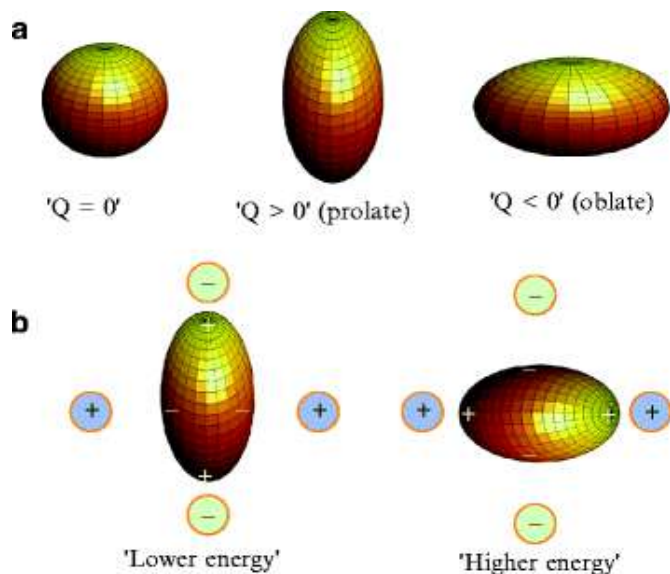


NMR Hamiltonian

□ The Hamiltonian:

$$\mathcal{H} = \mathcal{H}_{nZ} + \mathcal{H}_{nn} + \mathcal{H}_{ne} + \mathcal{H}_{EFG}$$

□ Quadrupole interaction: $I > 1/2$



Fernandez, Probing Quadrupolar Nuclei
by Solid-State NMR Spectroscopy:
Recent Advances

➤ nuclear quadrupole moment:

$$eQ_{\alpha\beta} = e \sum_{i \in \text{protons}} (3x_i^\alpha x_i^\beta - \delta_{\alpha\beta} r_i^2)$$

➤ electric field gradient: $V_{\alpha\beta} = \frac{\partial^2 V}{\partial x^\alpha \partial x^\beta}$

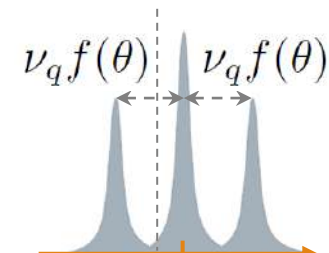
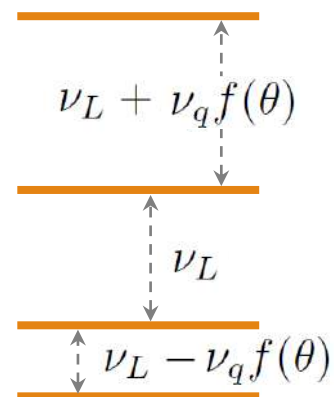
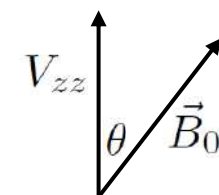
$$V(\vec{r}) = V(0) + \frac{1}{2} \sum_{\alpha, \beta = x, y, z} x^\alpha x^\beta \frac{\partial^2 V}{\partial x^\alpha \partial x^\beta}$$

➤ Hamiltonian:

$$\mathcal{H}_{EFG} = \frac{e^2 q Q}{4I(2I-1)} \left[3I_z^2 - I(I+1) + \frac{\eta}{2}(I_+^2 + I_-^2) \right]$$

$$eq = V_{zz} \quad \eta = \frac{V_{yy} - V_{xx}}{V_{zz}} \quad V_{zz} \geq V_{yy} \geq V_{xx}$$

$$\eta = 0 \quad \Delta E^{(1)} = \nu_q (3 \cos^2 \theta - 1) [3m_I^2 - I(I+1)]$$



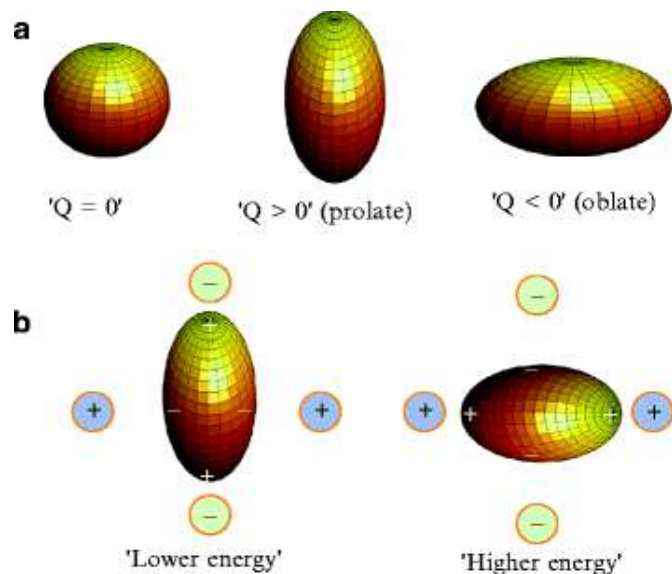
single crystal

NMR Hamiltonian

□ The Hamiltonian:

$$\mathcal{H} = \mathcal{H}_{nZ} + \mathcal{H}_{nn} + \mathcal{H}_{ne} + \mathcal{H}_{EFG}$$

□ Quadrupole interaction: $I > 1/2$



Fernandez, Probing Quadrupolar Nuclei by Solid-State NMR Spectroscopy: Recent Advances

➤ nuclear quadrupole moment:

$$eQ_{\alpha\beta} = e \sum_{i \in \text{protons}} (3x_i^\alpha x_i^\beta - \delta_{\alpha\beta} r_i^2)$$

➤ electric field gradient: $V_{\alpha\beta} = \frac{\partial^2 V}{\partial x^\alpha \partial x^\beta}$

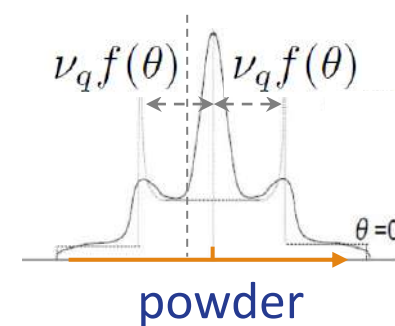
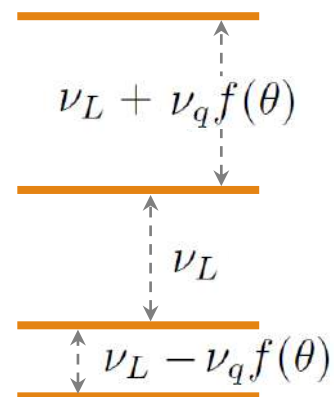
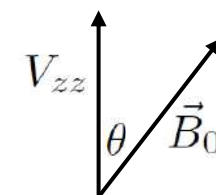
$$V(\vec{r}) = V(0) + \frac{1}{2} \sum_{\alpha, \beta = x, y, z} x^\alpha x^\beta \frac{\partial^2 V}{\partial x^\alpha \partial x^\beta}$$

➤ Hamiltonian:

$$\mathcal{H}_{EFG} = \frac{e^2 q Q}{4I(2I-1)} \left[3I_z^2 - I(I+1) + \frac{\eta}{2}(I_+^2 + I_-^2) \right]$$

$$eq = V_{zz} \quad \eta = \frac{V_{yy} - V_{xx}}{V_{zz}} \quad V_{zz} \geq V_{yy} \geq V_{xx}$$

$$\eta = 0 \quad \Delta E^{(1)} = \nu_q (3 \cos^2 \theta - 1) [3m_I^2 - I(I+1)]$$

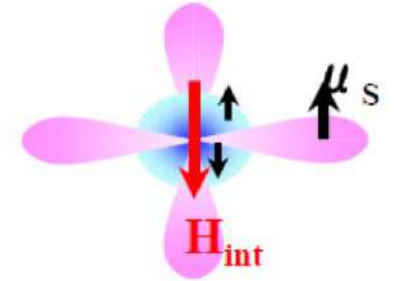


NMR: the Probe of Static Magnetism

□ Nucleus-electron (hyperfine) interaction:

- on-site hyperfine
- transferred hyperfine
- dipolar interaction
- contact interaction (metals)

$$\mathcal{H}_{ne}^i = -\hbar\gamma_n \vec{I}_i \cdot \sum_j \underline{A}_{ij} \cdot \vec{S}_j = -\hbar\gamma_n \vec{I}_i \cdot \vec{B}_i^{loc}$$



□ LRO: internal field (order parameter)

□ Fast spin fluctuations: $B_{loc} = \langle \vec{B}_i^{loc} \rangle_z = \sum_j \underline{A}_{ij} \cdot \langle \vec{S}_j \rangle_z$ $K = \frac{B_{loc} - B_0}{B_0} = \frac{\nu - \nu_L}{\nu_L}$

$$B_{loc} \ll B_0$$

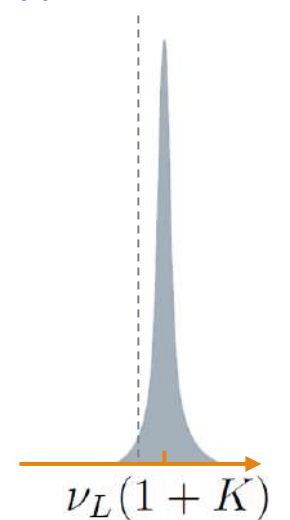


$$\nu = \gamma_n(B_0 + B_{loc}) = \nu_L(1 + K)$$

□ Paramagnet: uniform static susceptibility $\chi(q=0, \omega=0) = \mu_0 \frac{Ng\mu_B \langle \vec{S}_j \rangle_z}{VB_0}$

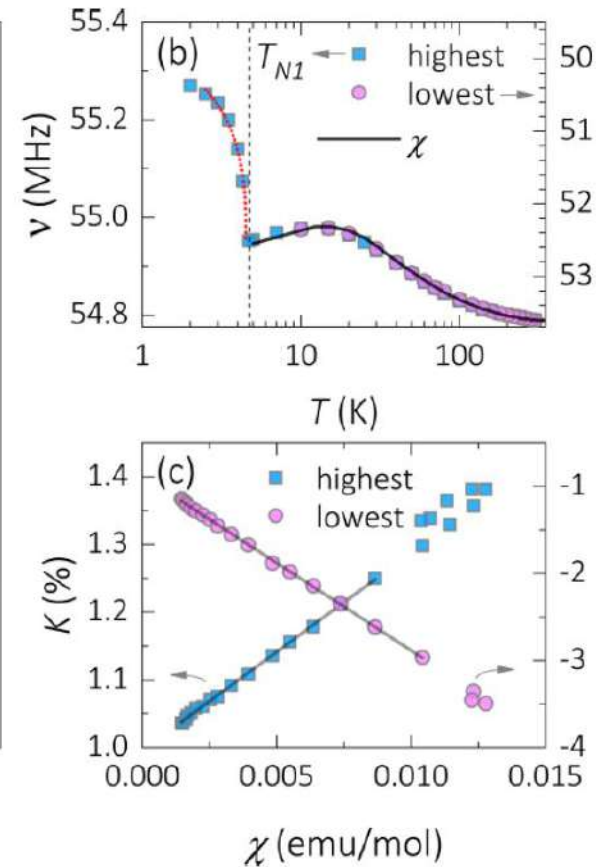
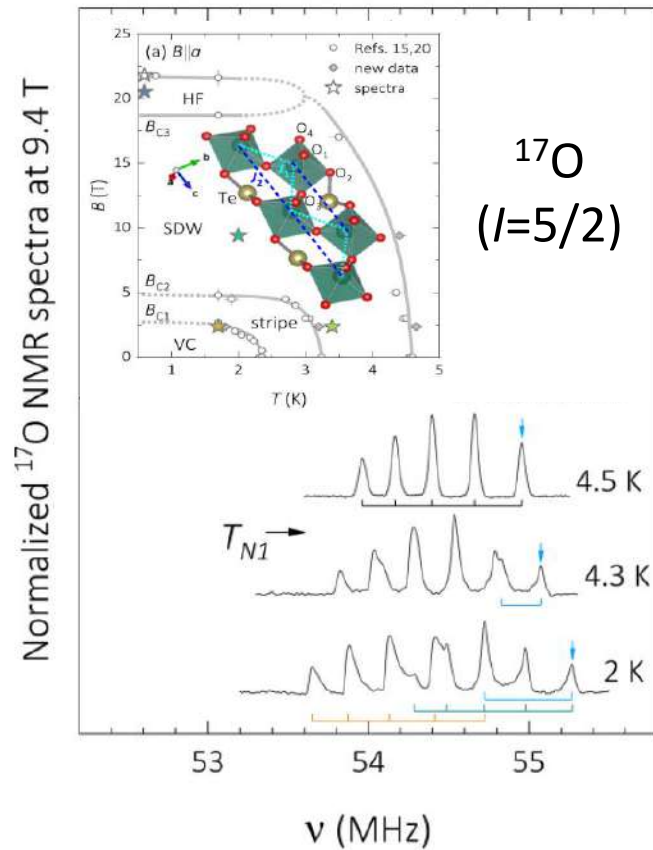
$$K = \sum_j \tilde{A}_{ij} \chi(q=0, \omega=0)$$

hyperfine shift

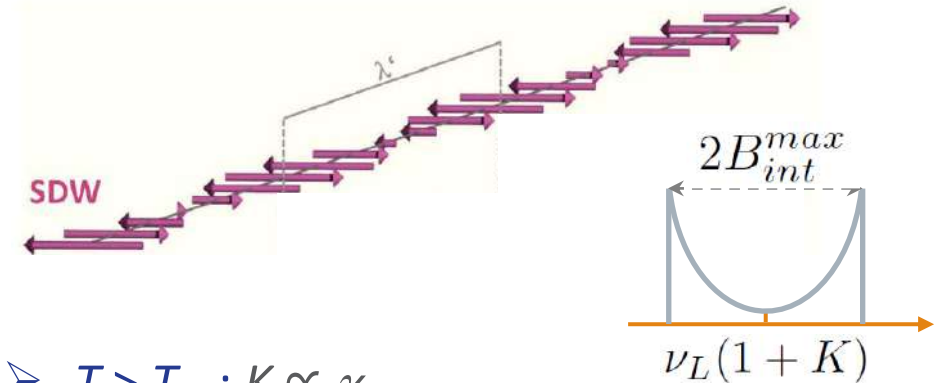


NMR: the Probe of Static Magnetism

□ Frustrated zig-zag spin chain: β -TeVO₄



➤ $T < T_{N1}$: line splitting + field distribution



➤ $T > T_{N1}$: $K \propto \chi$



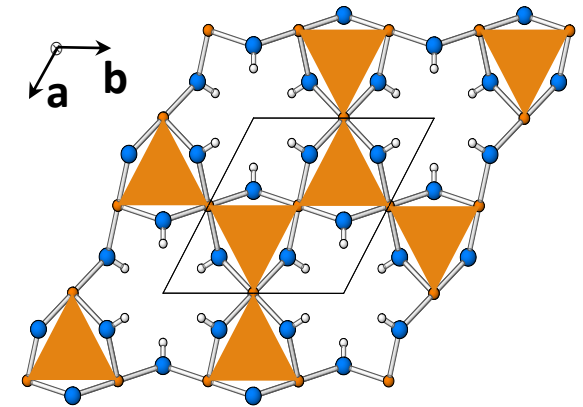
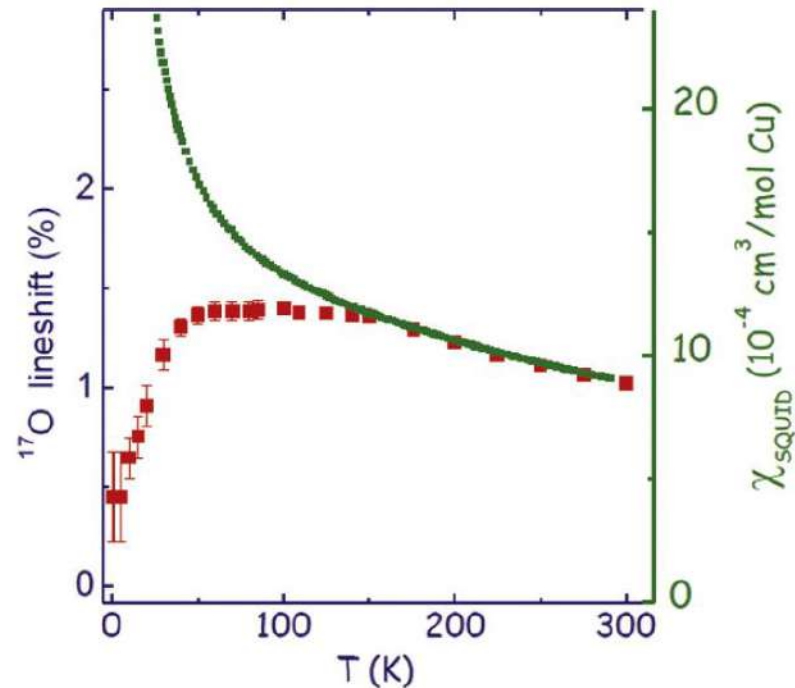
Clogston-Jaccarino plot

Pregelj *et al.*, Phys. Rev. B **105**, 035145 (2022)



NMR: the Probe of Static Magnetism

□ Intrinsic spin susceptibility in a QSL: kagome AFM $\text{ZnCu}_3(\text{OH})_6\text{Cl}_2$



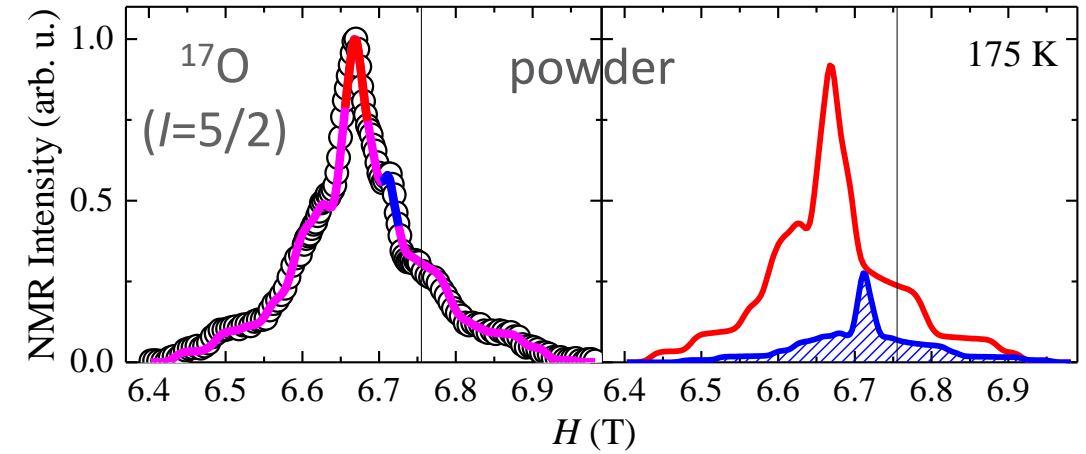
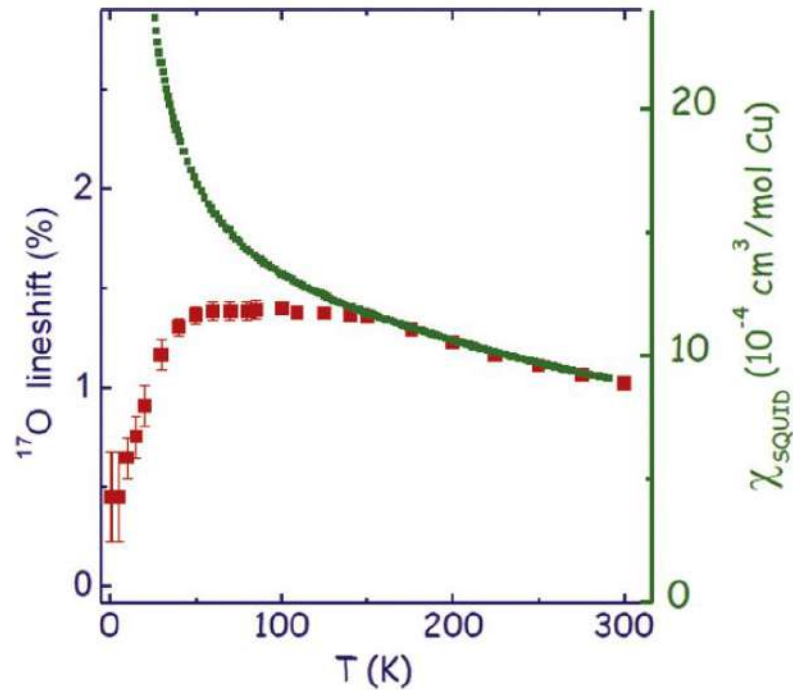
- bulk susceptibility: dominated by impurities
- local susceptibility: maximum due to spin correlations

Olariu *et al.*, Phys. Rev. Lett. **100**, 087202 (2008)



NMR: the Probe of Static Magnetism

□ Intrinsic spin susceptibility in a QSL: kagome AFM $\text{ZnCu}_3(\text{OH})_6\text{Cl}_2$



- bulk susceptibility: dominated by impurities
- local susceptibility: maximum due to spin correlations

Olariu *et al.*, Phys. Rev. Lett. **100**, 087202 (2008)



NMR: the Probe of Static Magnetism

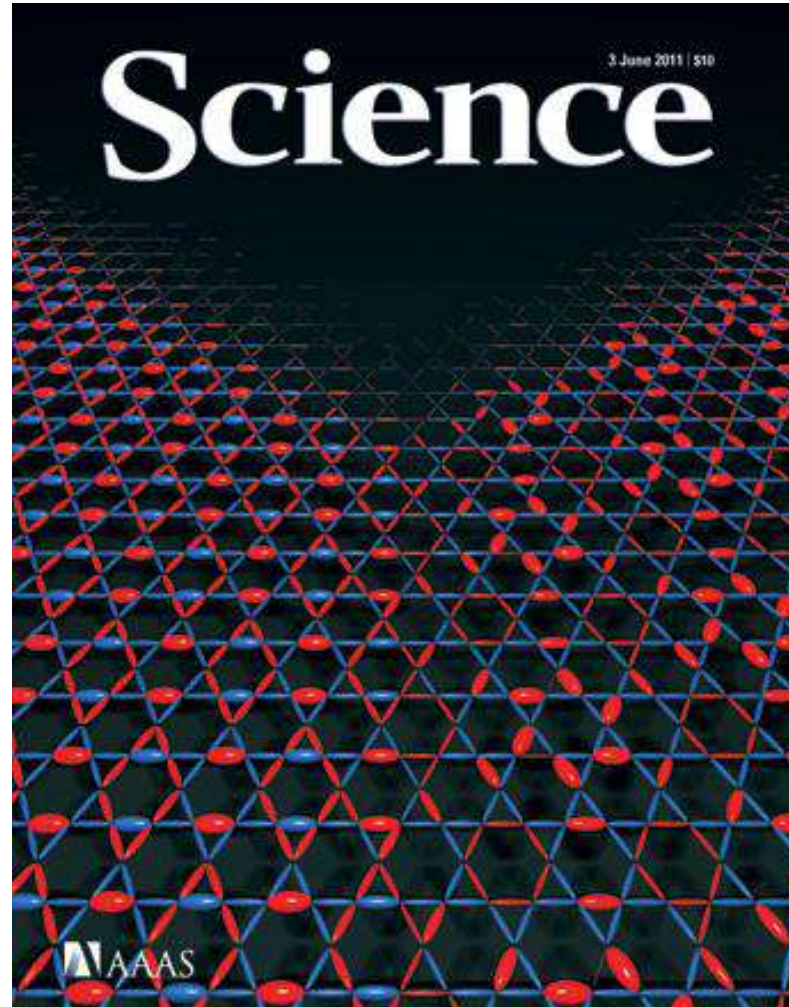
□ The nature of the GS:

gapped

topological QSL

$$c_v \propto e^{-\Delta/T}$$

$$\chi \propto e^{-\Delta/T}$$



gapless

algebraic Dirac QSL

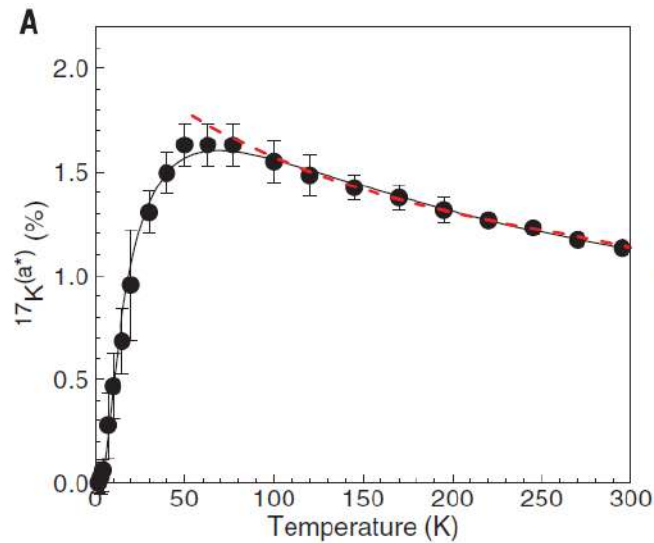
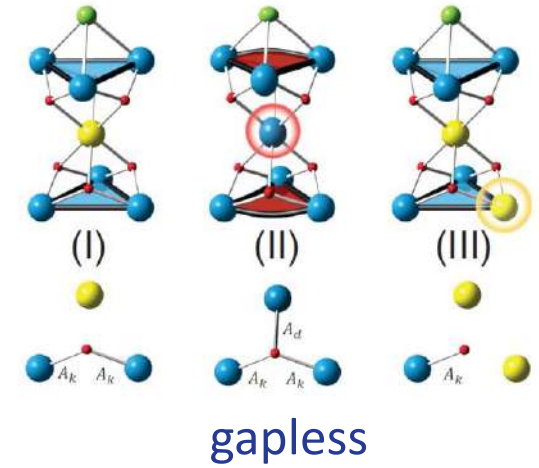
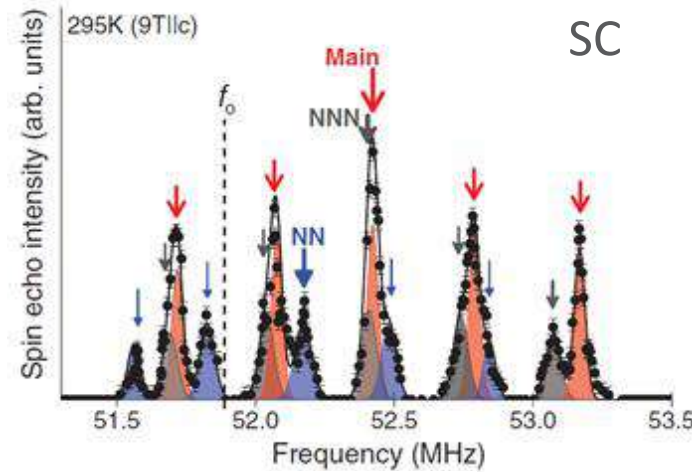
$$c_v \propto T^2$$

$$\chi \propto T$$

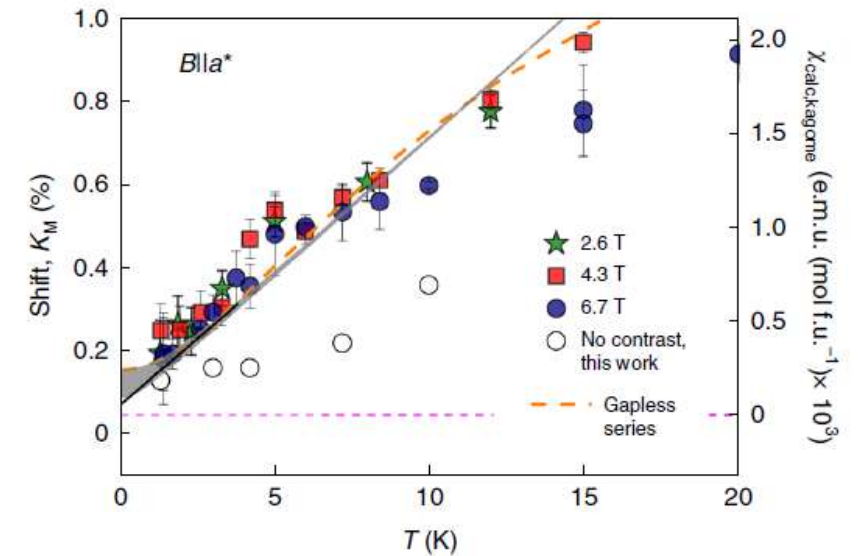
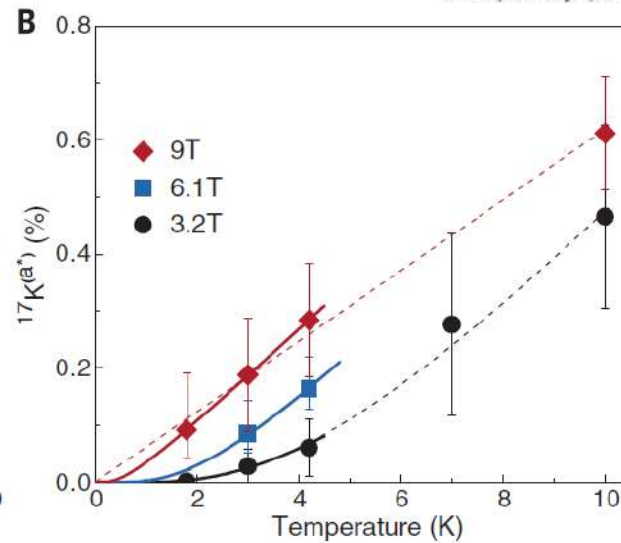
<https://www.science.org>

NMR: the Probe of Static Magnetism

□ The nature of the GS:
the problem of defects



Fu *et al.*, Science **350**, 655 (2015)

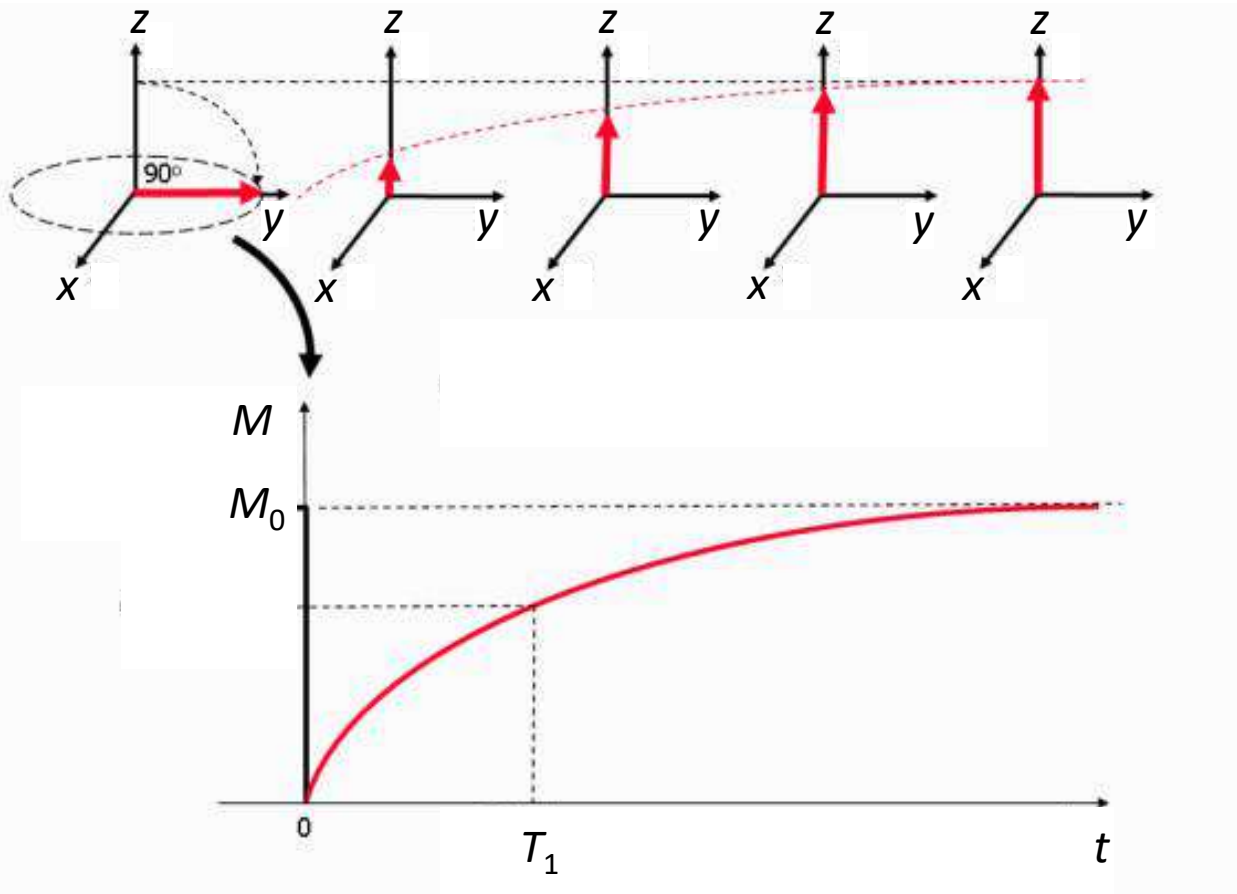


Khuntia *et al.*, Nat. Phys. **16**, 469 (2020)



NMR: the Probe of Spin Fluctuations

Fluctuations of local fields at frequency ω induce transitions between Zeeman-split levels – T_1 relaxation:



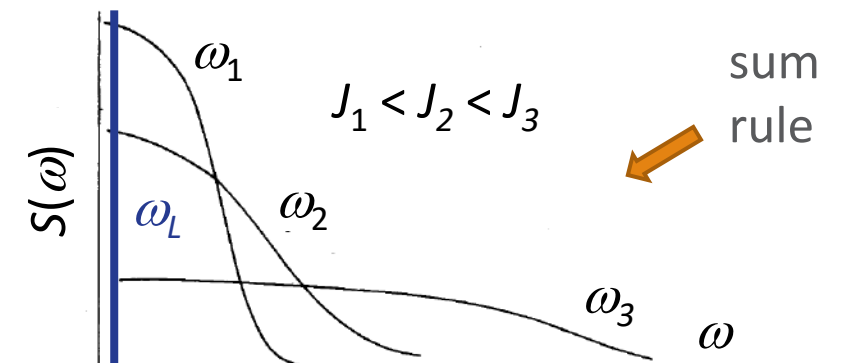
➤ exponential recovery towards equilibrium

➤ Fermi golden rule: $B_{loc}(t) \ll B_0$

$$\frac{1}{T_1} = \frac{\gamma_n^2}{2} \int_{-\infty}^{\infty} \langle B_{loc}^+(t) B_{loc}^-(0) \rangle e^{-i\omega_L t} dt$$

❖ transverse fluctuations

❖ spectral density at the Larmor frequency



NMR: the Probe of Spin Fluctuations

Fluctuations of local fields at frequency ω induce transitions between Zeeman-split levels – T_1 relaxation:

reciprocal space: $\vec{S}(\vec{q}, t) = \frac{1}{\sqrt{N}} \sum_j e^{i\vec{q}\cdot\vec{r}_j} S_j(t)$

$$\frac{1}{T_1} = \frac{\gamma_n^2}{2} \frac{1}{N} \sum_{\vec{q}, \alpha=x,y,z} [|A_{\vec{q}}|^2 S_{\alpha\alpha}(\vec{q}, \omega_L)]_{\perp}$$

$$S_{\alpha\beta}(\vec{q}, \omega_L) = \frac{1}{2\pi} \int_{-\infty}^{\infty} \langle B_{-\vec{q}}^{\alpha}(t) B_{\vec{q}}^{\beta}(0) \rangle e^{-i\omega_L t} dt$$

❖ q -integrated DSF over 1BC

❖ form factor: $|A_{\vec{q}}|^2$ $A_{\vec{q}} = \sum_j A_j e^{i\vec{q}\cdot\vec{r}_j}$
↙ scalar

imaginary dynamical spin susceptibility (FD theorem): $k_B T \gg \hbar \omega_L$

$$\frac{1}{T_1} = \frac{\gamma_n^2}{2} \frac{k_B T}{\hbar} \frac{1}{N} \sum_{\vec{q}, \alpha=x,y,z} \left[|A_{\vec{q}}|^2 \frac{\chi''_{\alpha\alpha}(\vec{q}, \omega_L)}{\omega_L} \right]_{\perp}$$

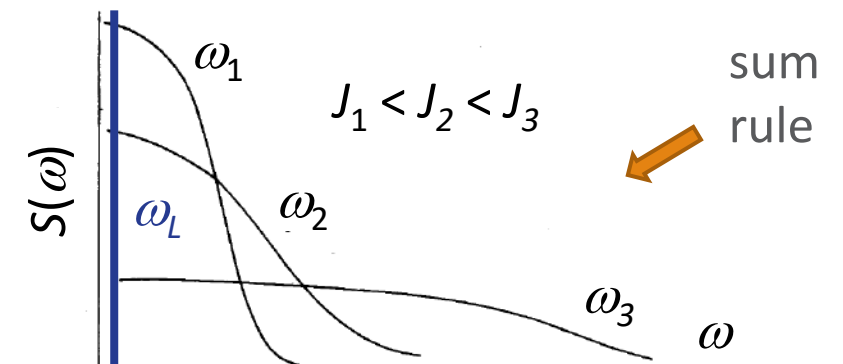
exponential recovery towards equilibrium

Fermi golden rule: $B_{loc}(t) \ll B_0$

$$\frac{1}{T_1} = \frac{\gamma_n^2}{2} \int_{-\infty}^{\infty} \langle B_{loc}^+(t) B_{loc}^-(0) \rangle e^{-i\omega_L t} dt$$

❖ transverse fluctuations

❖ spectral density at the Larmor frequency



NMR: the Probe of Spin Fluctuations

□ Redfield formula (BPP): exponentially decaying local-field correlations

$$\langle B_{loc}^+(t) B_{loc}^-(0) \rangle = \Delta^2 e^{-\nu t}$$

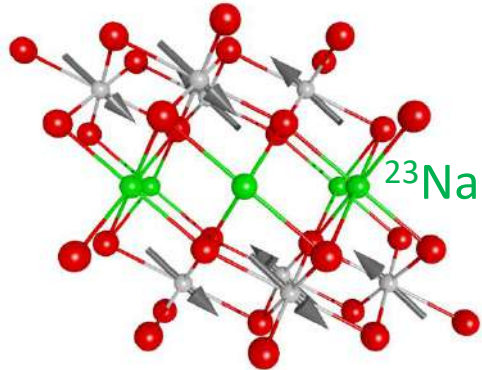
➤ critical slowing down of spin fluctuations: $T > T_N$

➤ phase transition: drastic change of excitations

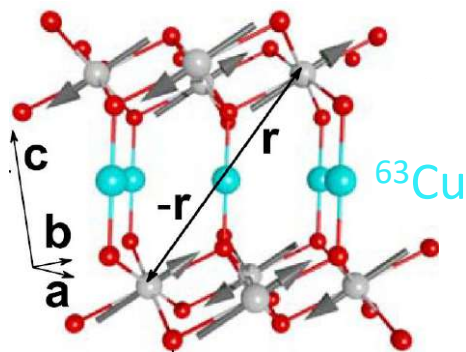
➤ filtering by the form factor:

$$A_{\vec{q}} = \sum_j A_j e^{i\vec{q} \cdot \vec{r}_j}$$

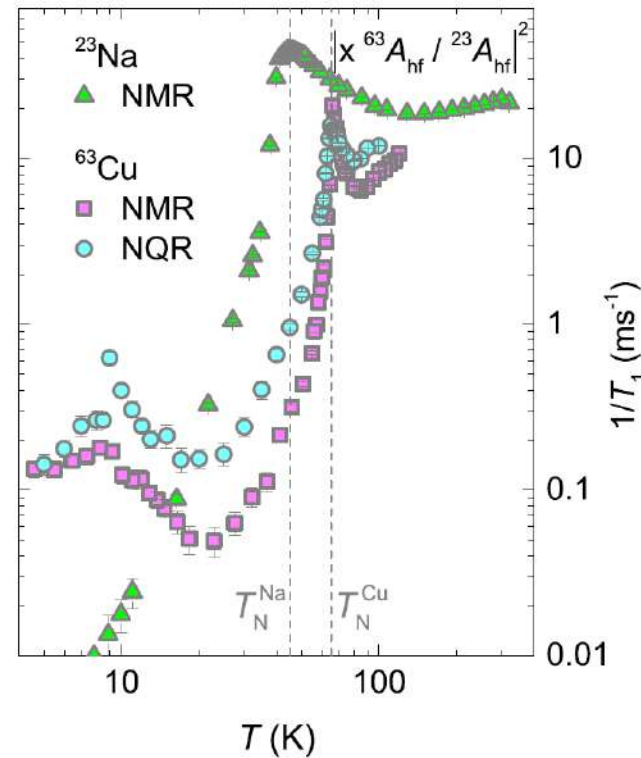
$$A_{\vec{q}_{AFM}} = 0$$



$$A_{\vec{q}_{AFM}} \neq 0$$

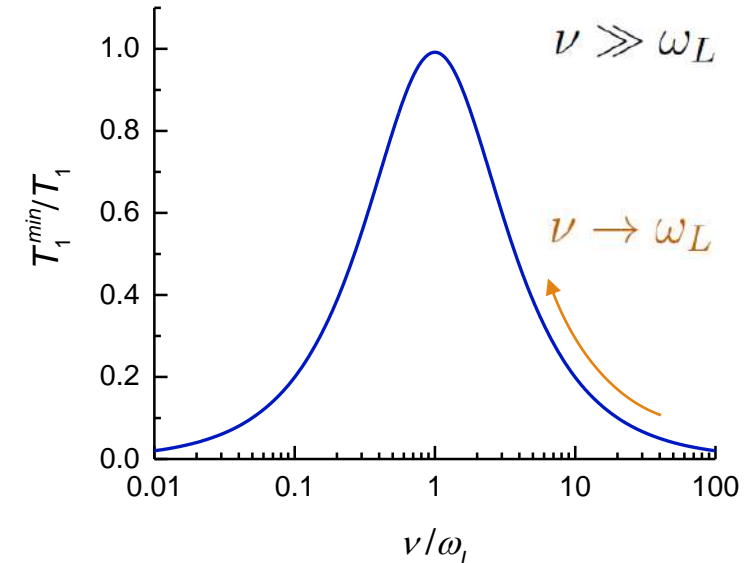


NaMnO₂ & CuMnO₂:
triangular AFM



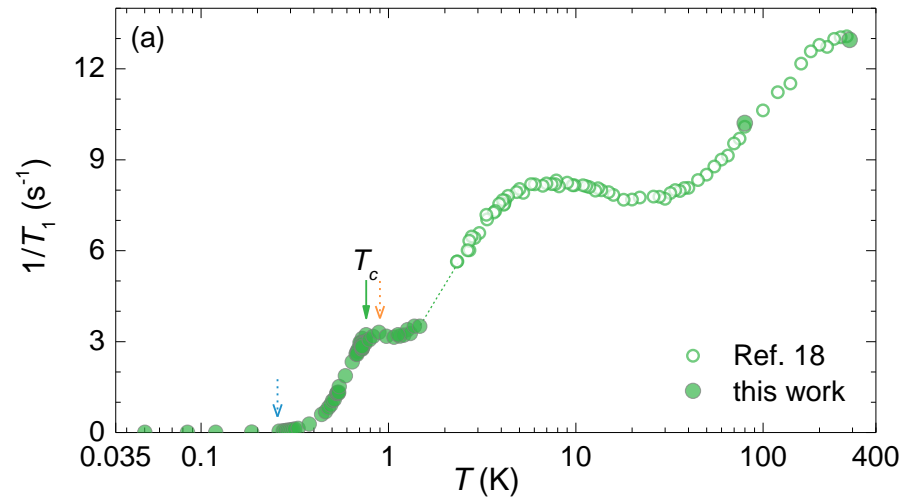
Zorko *et al.*, *Sci. Rep.* **5**, 9272 (2015)

$$\frac{1}{T_1} = \frac{\gamma^2 \Delta^2 \nu}{\nu^2 + \gamma^2 B_0^2}$$



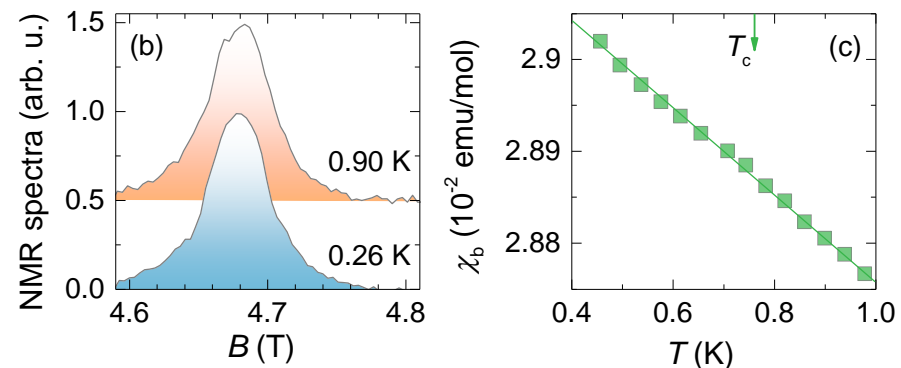
NMR: the Probe of Spin Fluctuations

□ Zn-brochantite: distorted kagome-lattice AFM with a spinon-Fermi-surface QSL GS

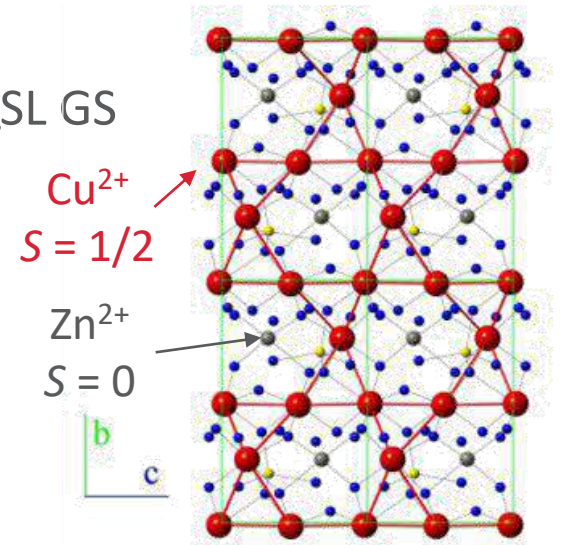


➤ NO magnetic order at $T_c = 0.76$ K

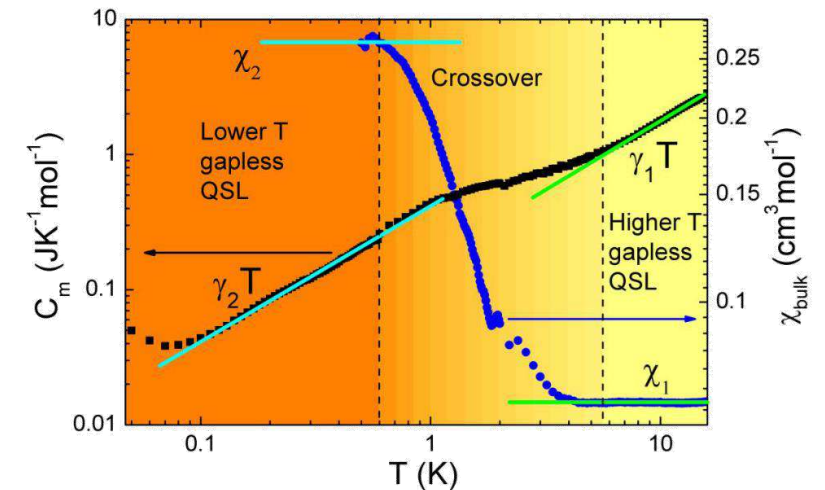
- ❖ no divergence in $1/T_1$
- ❖ no NMR broadening
- ❖ no thermodynamic anomaly



Gomilšek *et al.*, Phys. Rev. Lett. 119, 137205 (2017)



- ↓
- ❖ QSL state at $T < T_c$
 - ❖ fundamental modification of the excitation spectrum

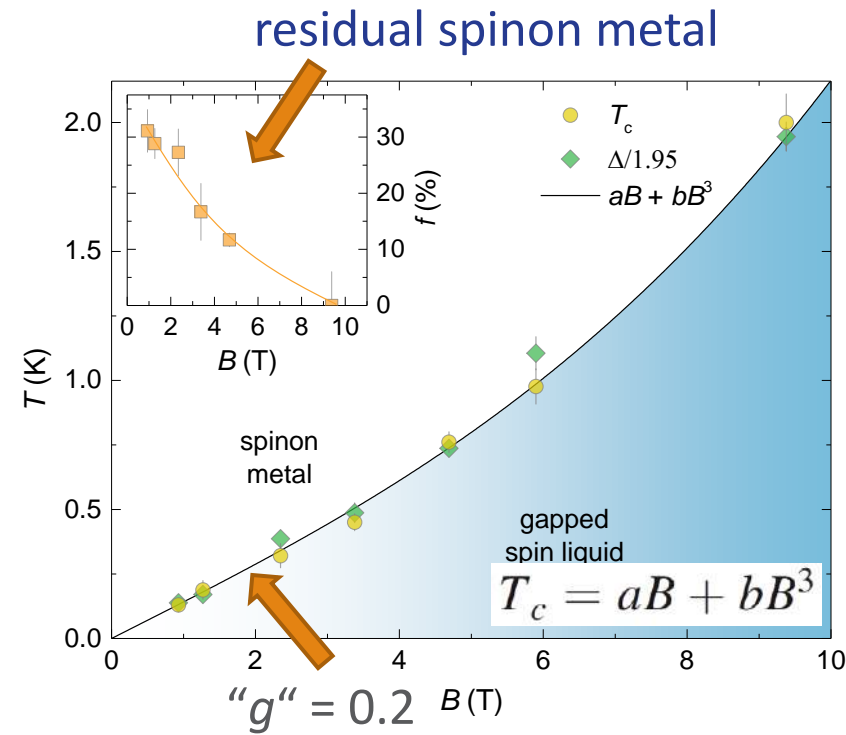
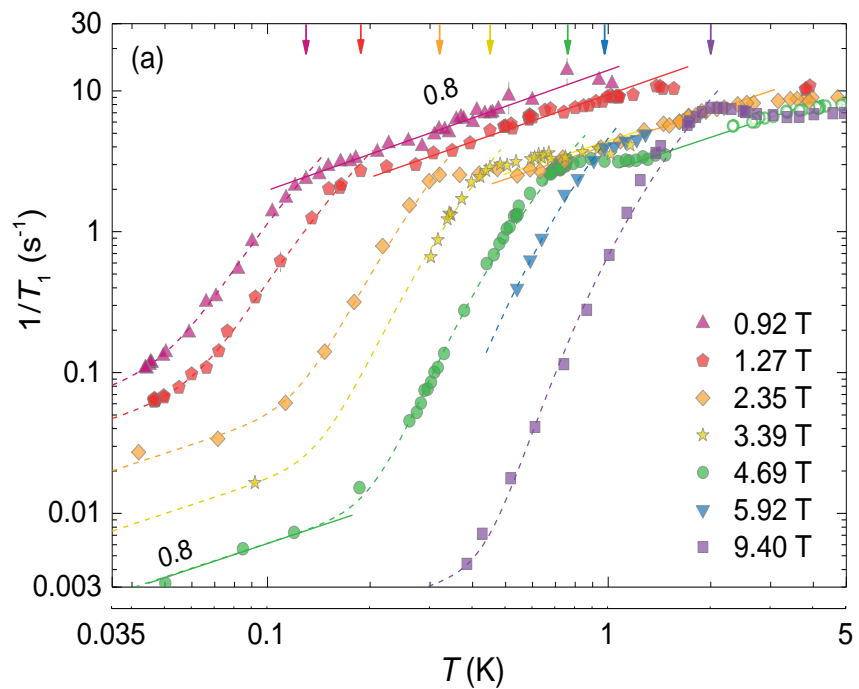
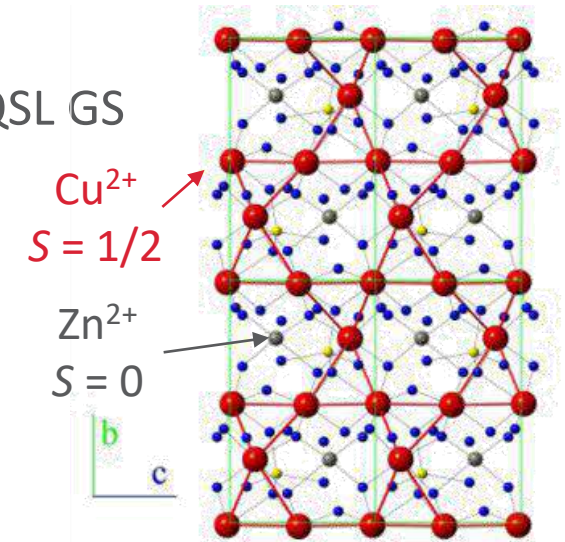


Li *et al.*, New J. Phys. 16, 093011 (2014)



NMR: the Probe of Spin Fluctuations

- Zn-brochantite: distorted kagome-lattice AFM with a spinon-Fermi-surface QSL GS
- Field-induced modification of the spinon Fermi surface below T_c



$$\frac{1}{T_1} = dTe^{-\Delta/T} + f^2 cT^\eta$$

gapped QSL

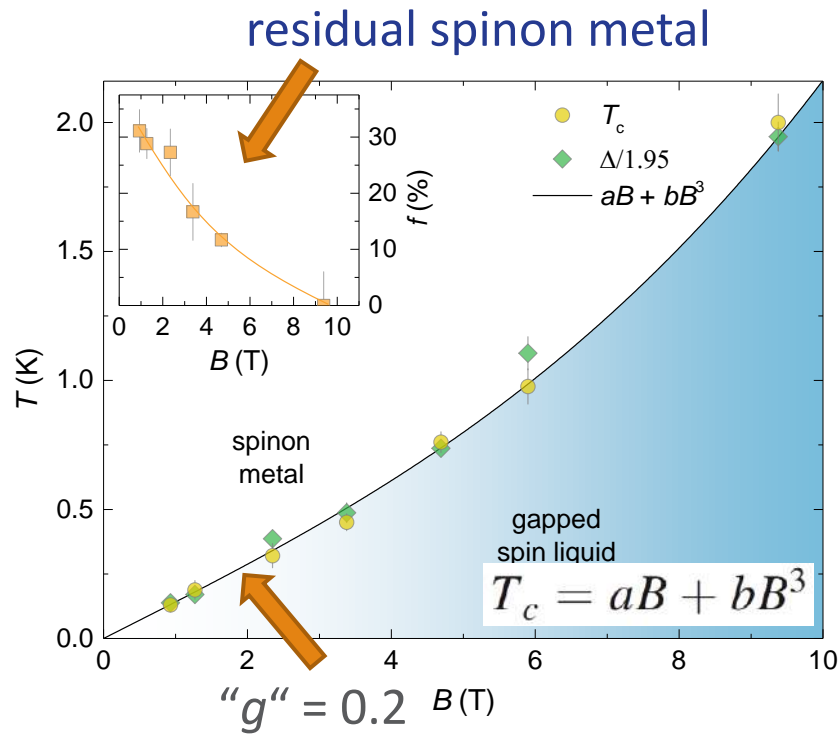
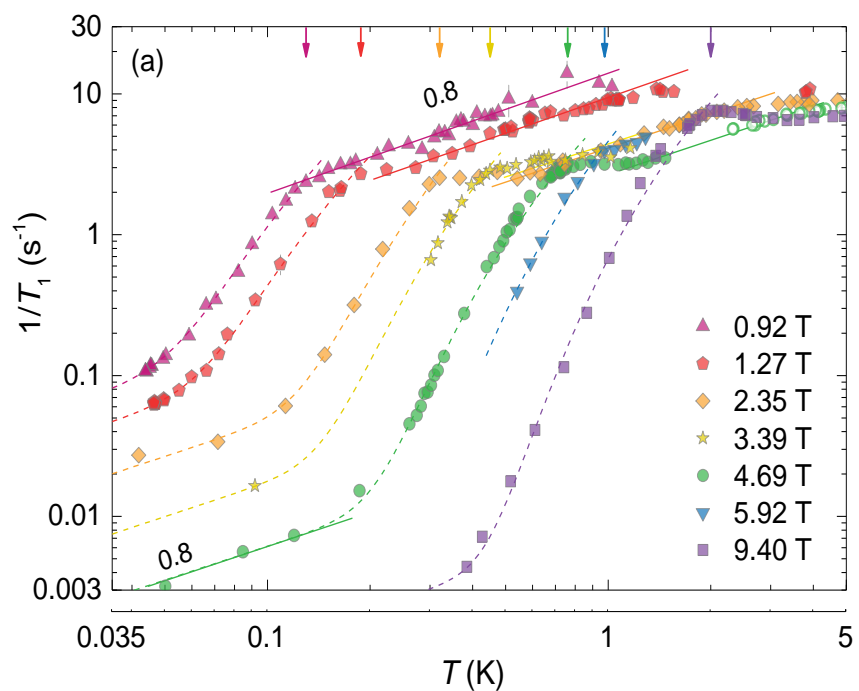
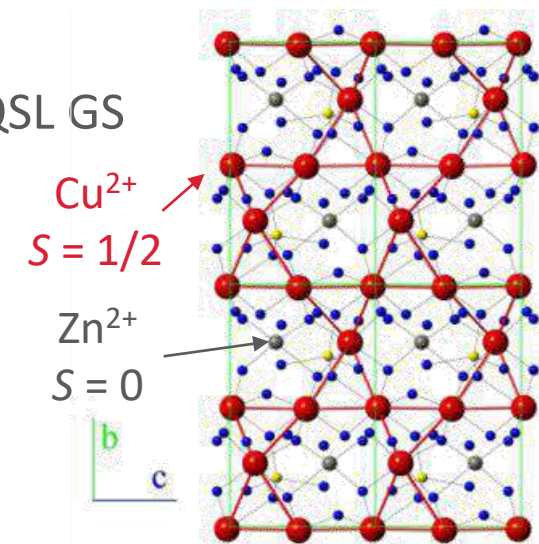
residual spinon metal

Gomilšek *et al.*, Phys. Rev. Lett. 119, 137205 (2017)



NMR: the Probe of Spin Fluctuations

- Zn-brochantite: distorted kagome-lattice AFM with a spinon-Fermi-surface QSL GS
- Field-induced modification of the spinon Fermi surface below T_c

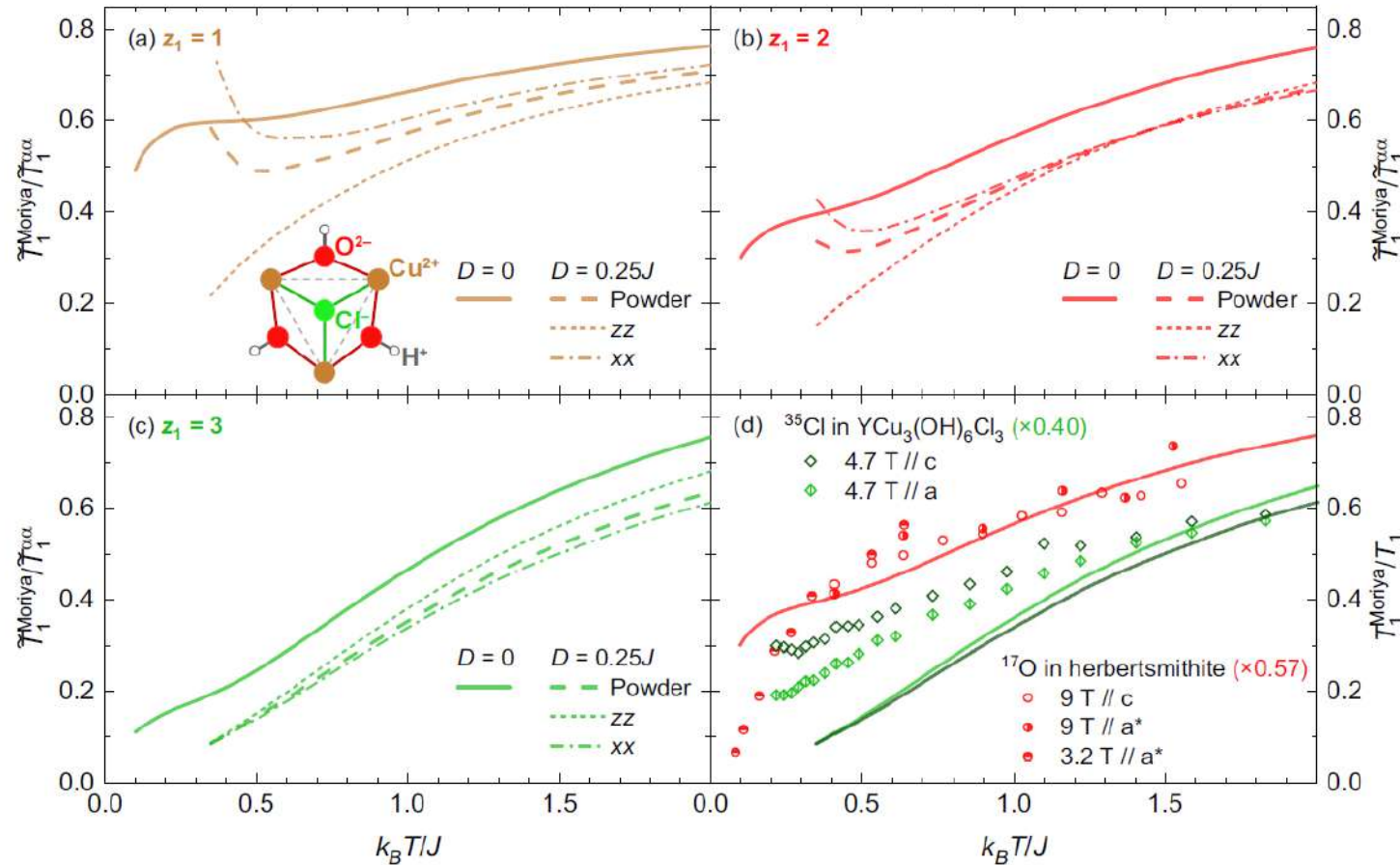


Gomilšek *et al.*, Phys. Rev. Lett. 119, 137205 (2017)



NMR: the Probe of Spin Fluctuations

□ Kagome AFM + DM interaction: T_1 -relaxation in the correlated “paramagnetic” state by FTLM



➤ Deviations from the Moriya limit: high temperatures

$$\frac{1}{T_1} = \sqrt{\frac{\pi}{3}} \frac{A^2 \sqrt{S(S+1)}}{\hbar J \sqrt{z}}$$

➤ anisotropic fluctuations due to DM interaction

➤ site-specific anisotropy



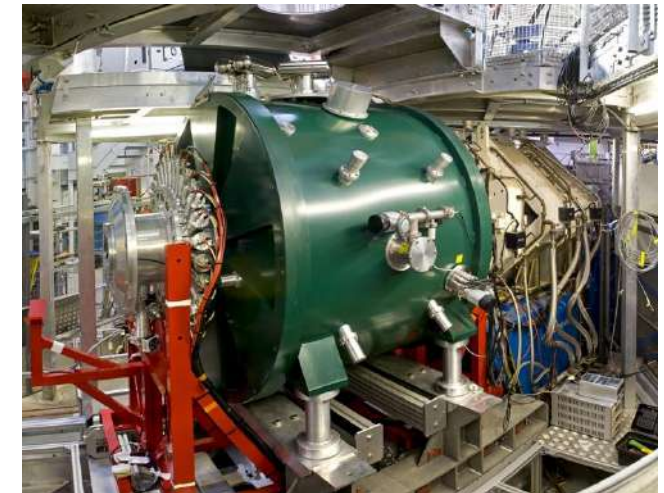
filtering of dominant chiral fluctuations by form factor

Prelovšek *et al.*, Phys. Rev. B **103**, 014431 (2021)



Outline

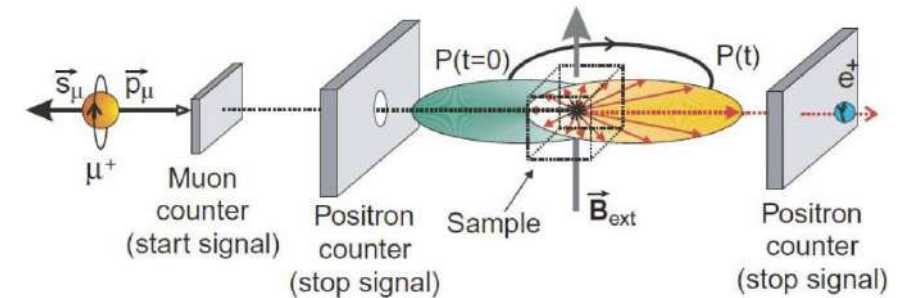
- Introduction to magnetism
- Probing magnetism: conventional bulk and scattering techniques
- Local probes of magnetism
- Electron spin resonance (ESR)
- Nuclear magnetic resonance (NMR)
- Muon spectroscopy (μ SR)
- Summary: strengths, limitations and complementarity of local probes



HIFI, ISIS, UK

Motivation for Muon Spectroscopy

- ❑ Extreme sensitivity to static and dynamic internal fields: ~ 0.1 G
- ❑ Measures fluctuations in a broad frequency range: $10^4 - 10^{12}$ Hz
- ❑ Muon can be implanted into any material
- ❑ A non-destructive technique that does not active samples
- ❑ Allows zero-field measurements



<https://www.psi.ch>

Motivation for Muon Spectroscopy



□ Range of applications:

- study of ionic diffusion in battery materials
- study of energy-storage materials
- study of reactions kinetics
- study of free-radical chemistry
- ...

CHEMISTRY/
INDUSTRY

- study of cultural heritage artefacts
- ...

OTHER AREAS

- magnetic properties of materials
- electronic properties of superconductors
- study of functional materials
- impurities in semiconductors
- ...

PHYSICS/
MATERIALS
RESEARCH



Motivation for Muon Spectroscopy



□ Range of applications:

- study of ionic diffusion in battery materials
- study of energy-storage materials
- study of reactions kinetics
- study of free-radical chemistry
- ...

CHEMISTRY/
INDUSTRY

- study of cultural heritage artefacts
- ...

OTHER AREAS

- magnetic properties of materials
- electronic properties of superconductors
- study of functional materials
- impurities in semiconductors
- ...

PHYSICS/
MATERIALS
RESEARCH

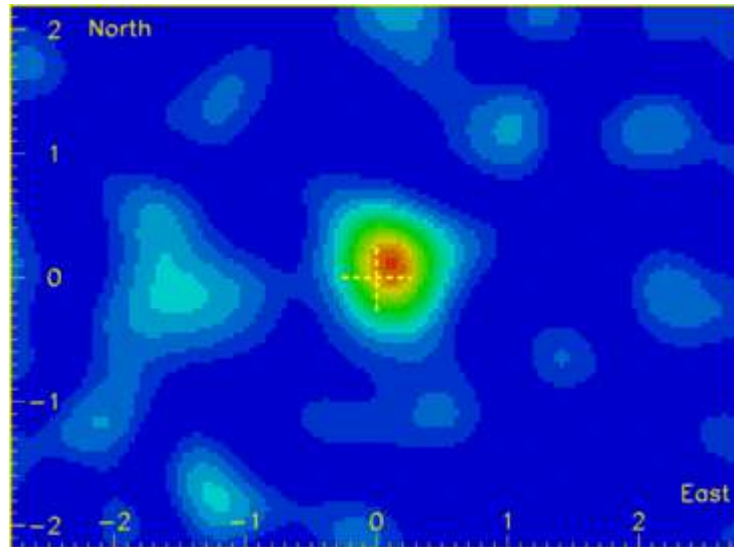


A Brief History of μ SR

- 1936: discovery of the muon as secondary radiation of cosmic rays

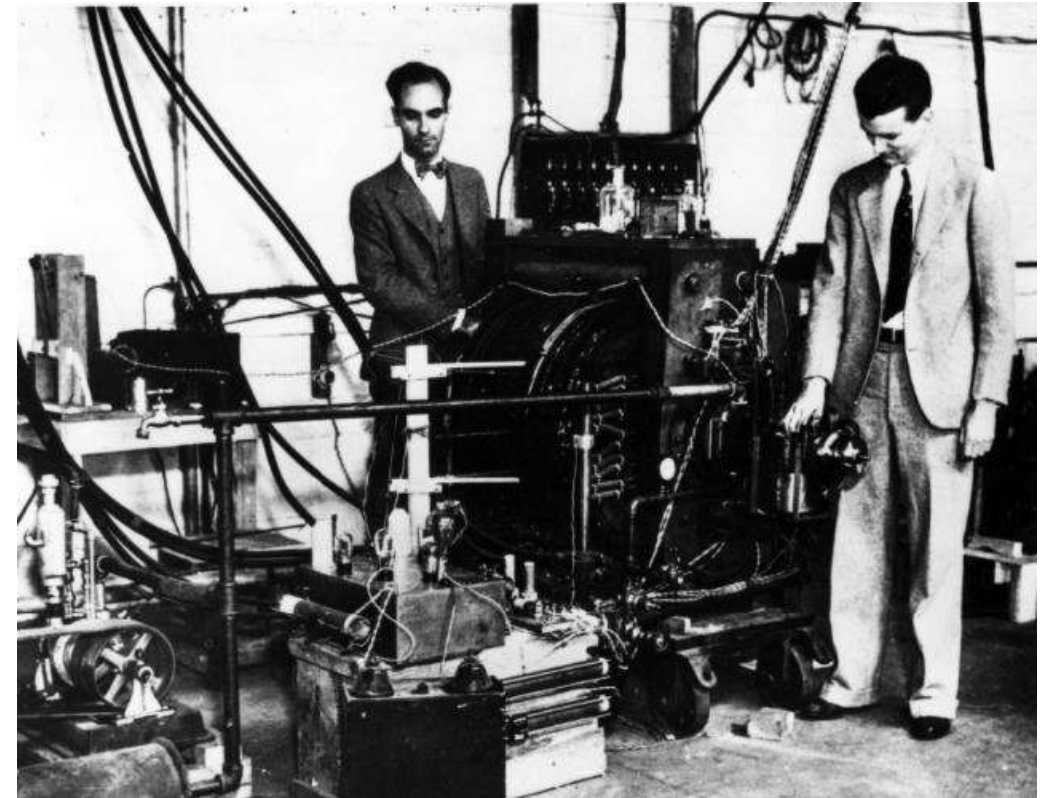
I. I. Rabi: “Who ordered that?”

cosmic ray shadow



<https://en.wikipedia.org>

Carl Anderson and Seth Neddermeyer with magnet cloud chamber



<https://digital.archives.caltech.edu>

A Brief History of μ SR

- 1936: discovery of the muon as secondary radiation of cosmic rays

Initially labeled “mesotron”



Hideki Yukawa

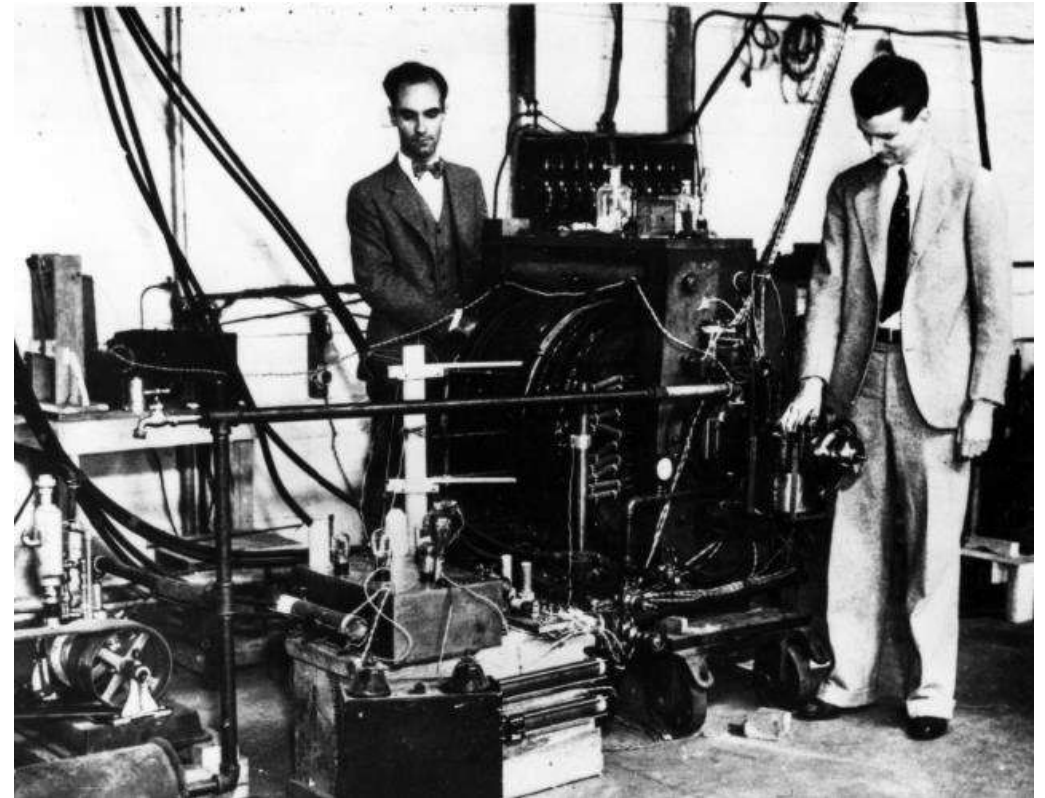
<https://en.wikipedia.org>

Anderson/Neddermeyer particle



Yukawa particle

Carl Anderson and Seth Neddermeyer
with magnet cloud chamber

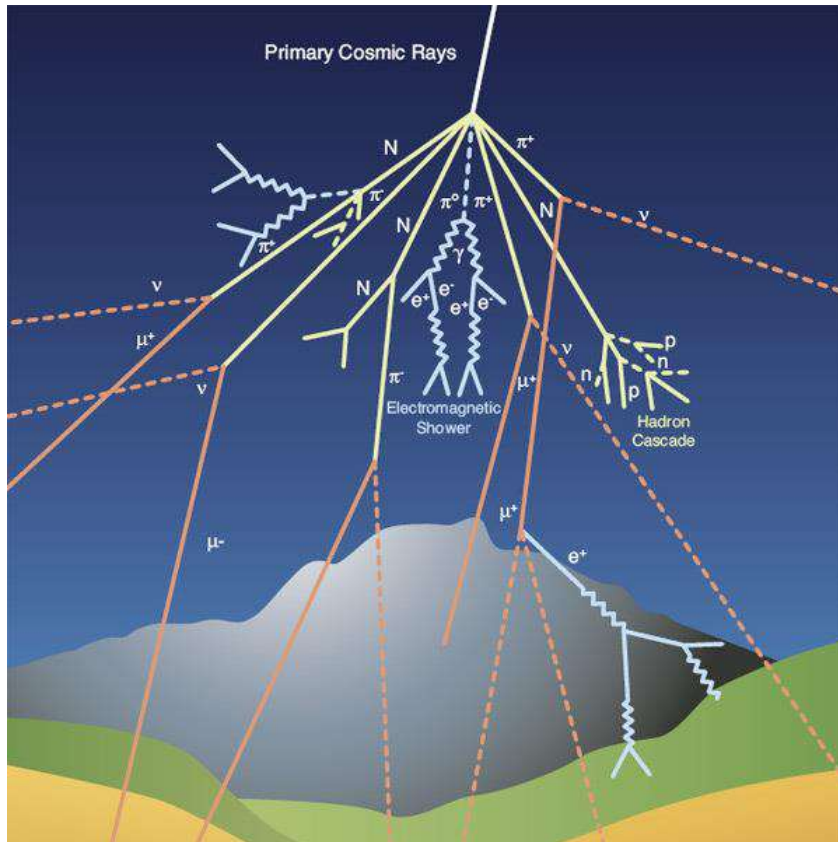


<https://digital.archives.caltech.edu>



A Brief History of μ SR

□ 1947: discovery of pions



<https://home.cern>

$$\pi^+ \rightarrow \mu^+ + \nu_\mu$$

$$\pi^- \rightarrow \mu^- + \bar{\nu}_\mu$$

$$m_\pi c^2 = 139.6 \text{ MeV}$$

$$m_\mu c^2 = 105.7 \text{ MeV}$$

$$\tau = 27 \text{ ns}$$

The Nobel Prize in Physics 1950



Photo from the Nobel
Foundation archive.
Cecil Frank Powell
Prize share: 1/1

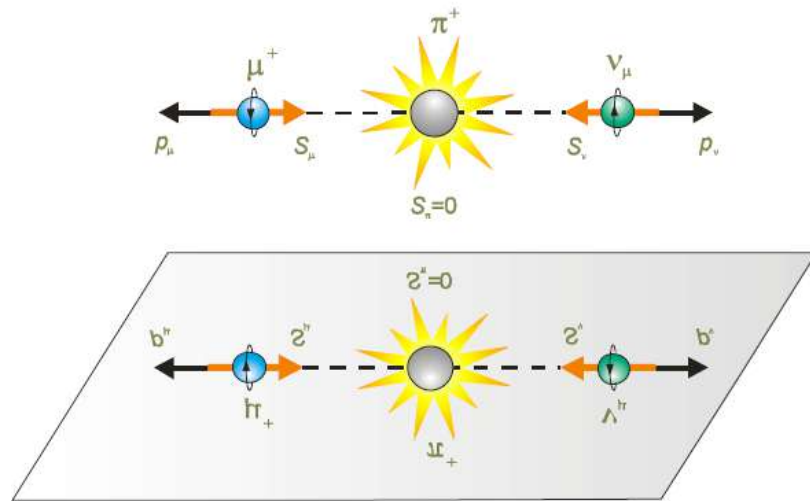
The Nobel Prize in Physics 1950 was awarded to Cecil Frank Powell "for his development of the photographic method of studying nuclear processes and his discoveries regarding mesons made with this method."

<https://www.nobelprize.org>



A Brief History of μ SR

□ 1957: discovery of parity violation in weak decay



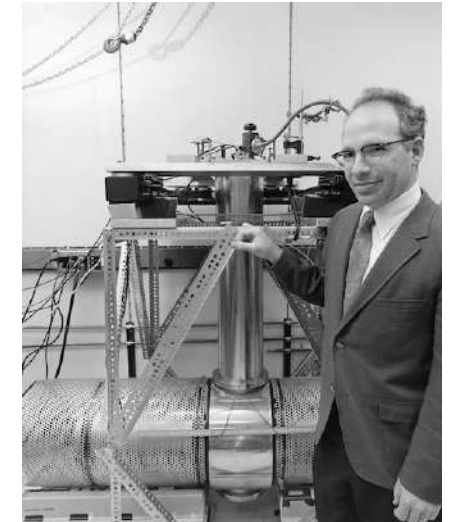
<http://cmms.triumf.ca>



muon's spin antiparallel
to its momentum



Leon M. Lederman



Richard L. Garwin

Various other materials were investigated for μ^+ mesons. Nuclear emulsion as a target was found to have a significantly weaker asymmetry (peak-to-valley ratio of 1.40 ± 0.07) and it is interesting to note that this did not increase with reduced delay and gate width. Neither was there any evidence for an altered moment. It seems possible that polarized positive and negative muons will become a powerful tool for exploring magnetic fields in nuclei (even in Pb, 2% of the μ^- decay into electrons⁹), atoms, and interatomic regions.

Observations of the Failure of Conservation of Parity and Charge Conjugation in Meson Decays: the Magnetic Moment of the Free Muon*

RICHARD L. GARWIN,† LEON M. LEDERMAN,
AND MARCEL WEINRICH

*Physics Department, Nevis Cyclotron Laboratories,
Columbia University, Irvington-on-Hudson,
New York, New York*

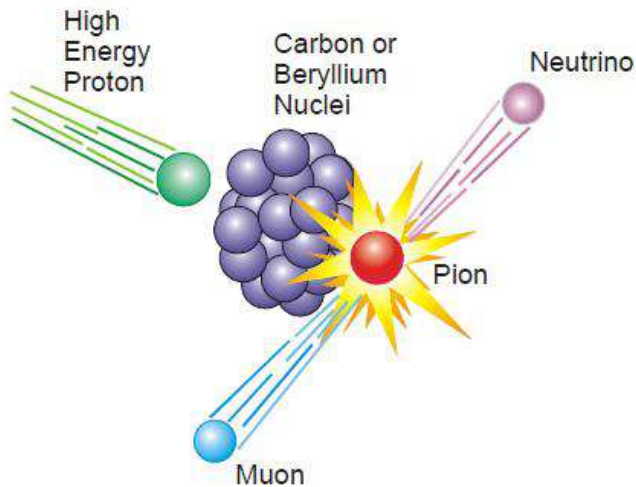
(Received January 15, 1957)



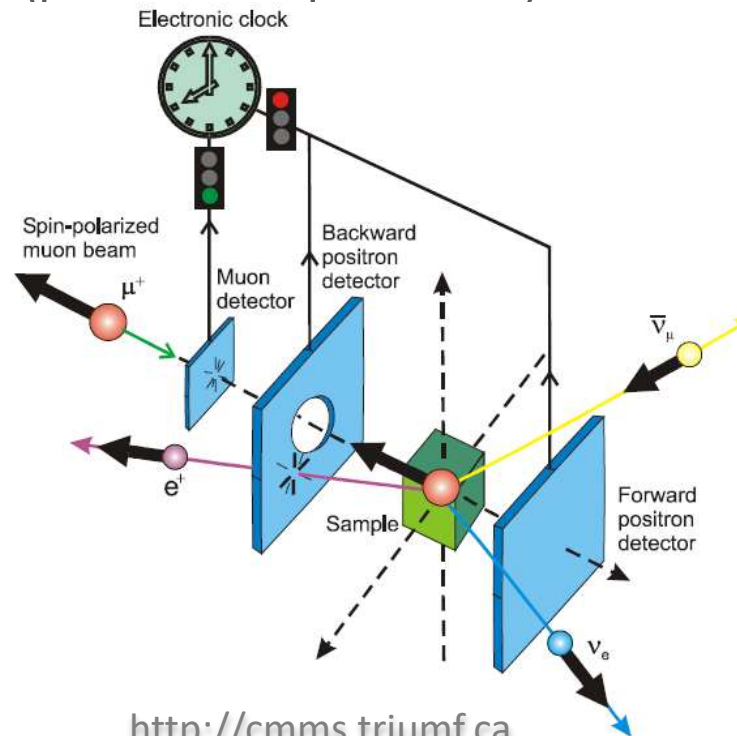
μ SR Apparatus

□ How does it work?

1. muon production (accelerator):
surface muons ($p = 29.8 \text{ MeV}/c$)

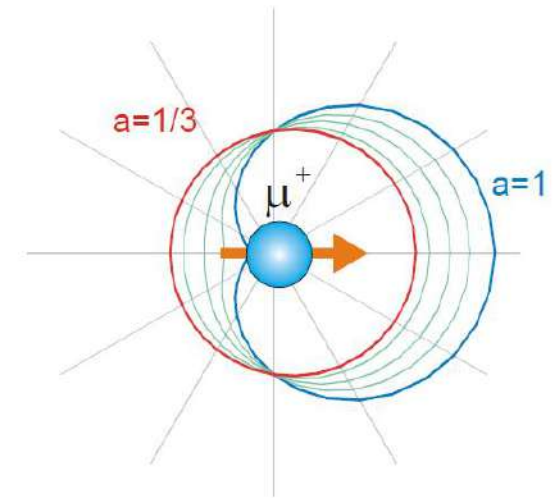
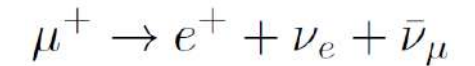


2. muon implantation: in about
100 ps up to a few tenths of mm
(polarization preserved)

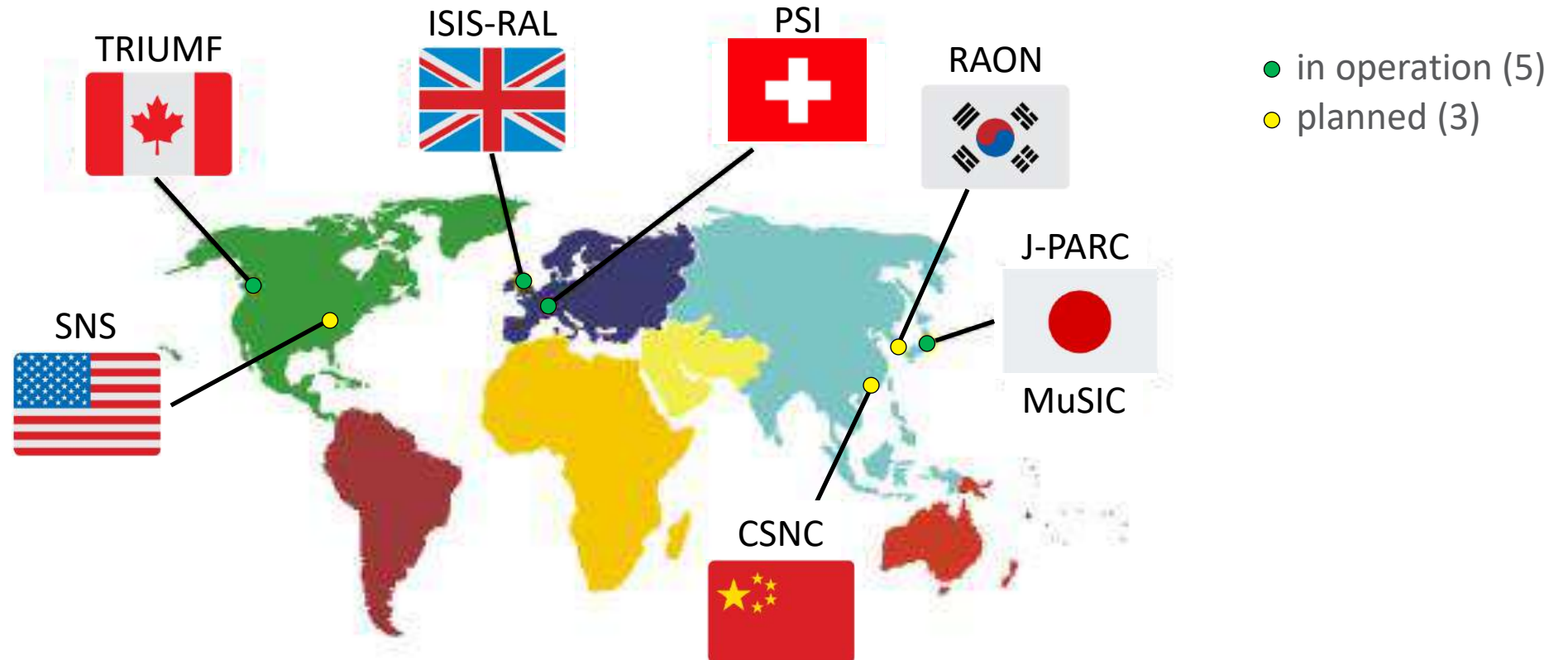


<http://cmms.triumf.ca>

3. muon decay: $\tau = 2.2 \mu\text{s}$
(parity violation)



μ SR User Facilities



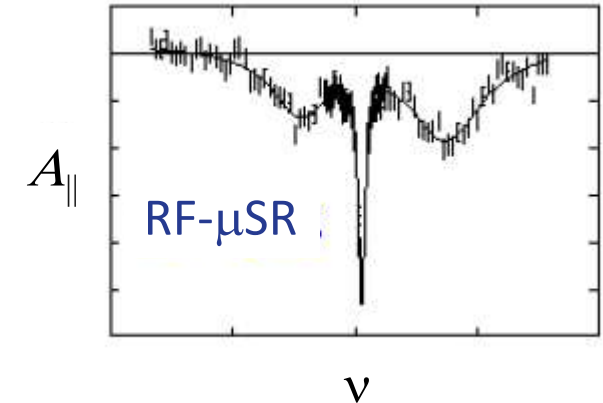
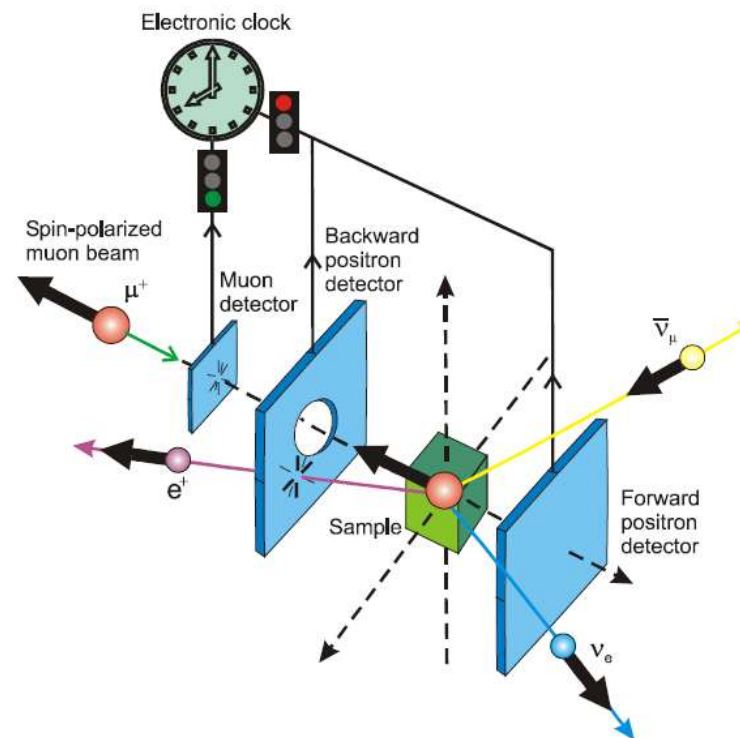
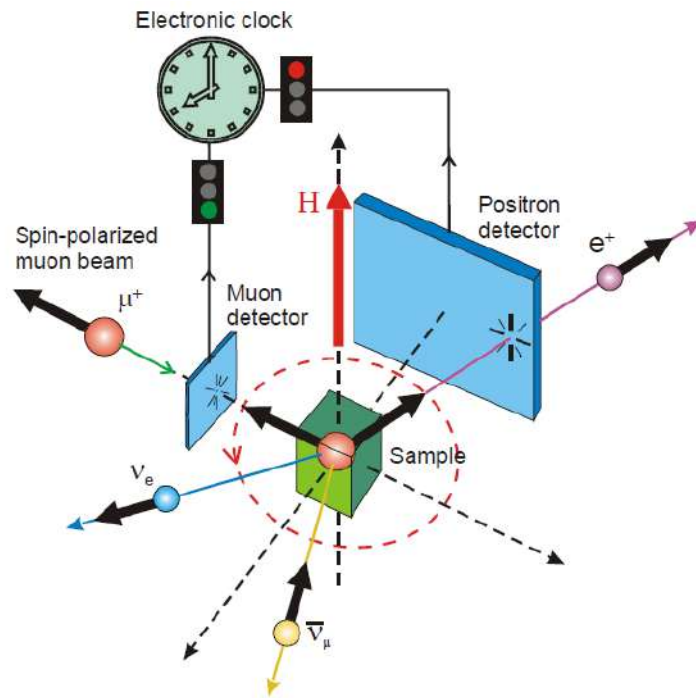
μ SR Experiments

□ μ SR = muon spin rotation/relaxation/resonance (research)

1. rotation: TF- μ SR

2. relaxation: LF- μ SR and ZF- μ SR

3. resonance: RF- μ SR,
 μ LCR, μ SE

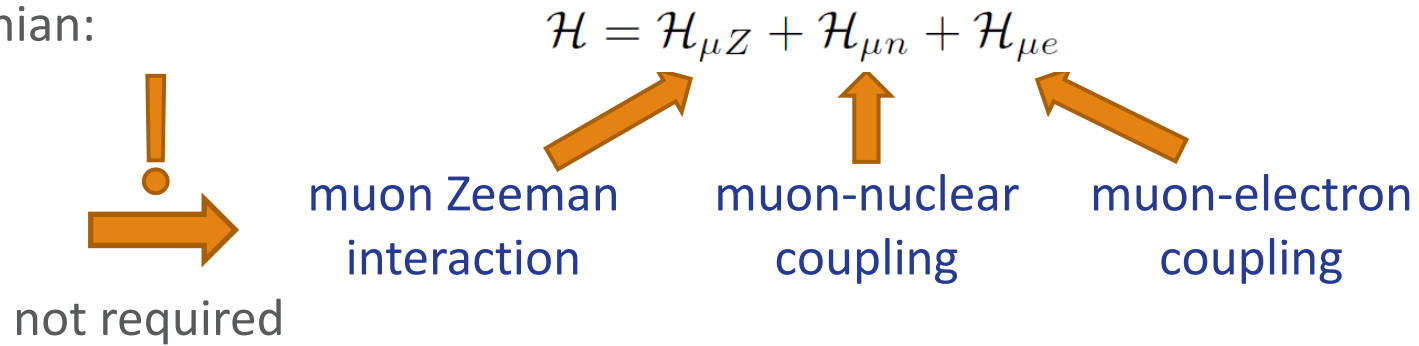


<https://muonsources.org>



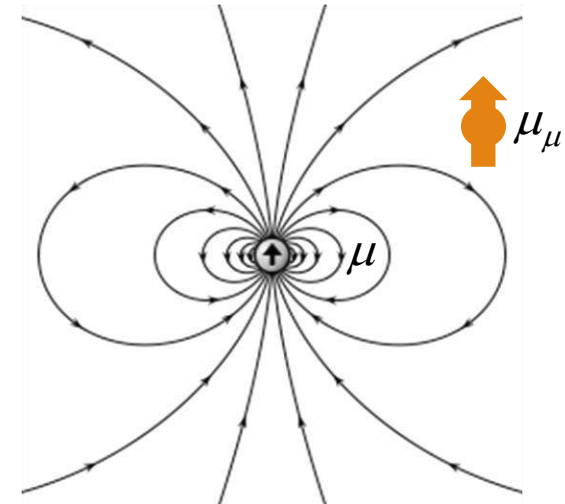
μ SR Hamiltonian

□ The Hamiltonian:



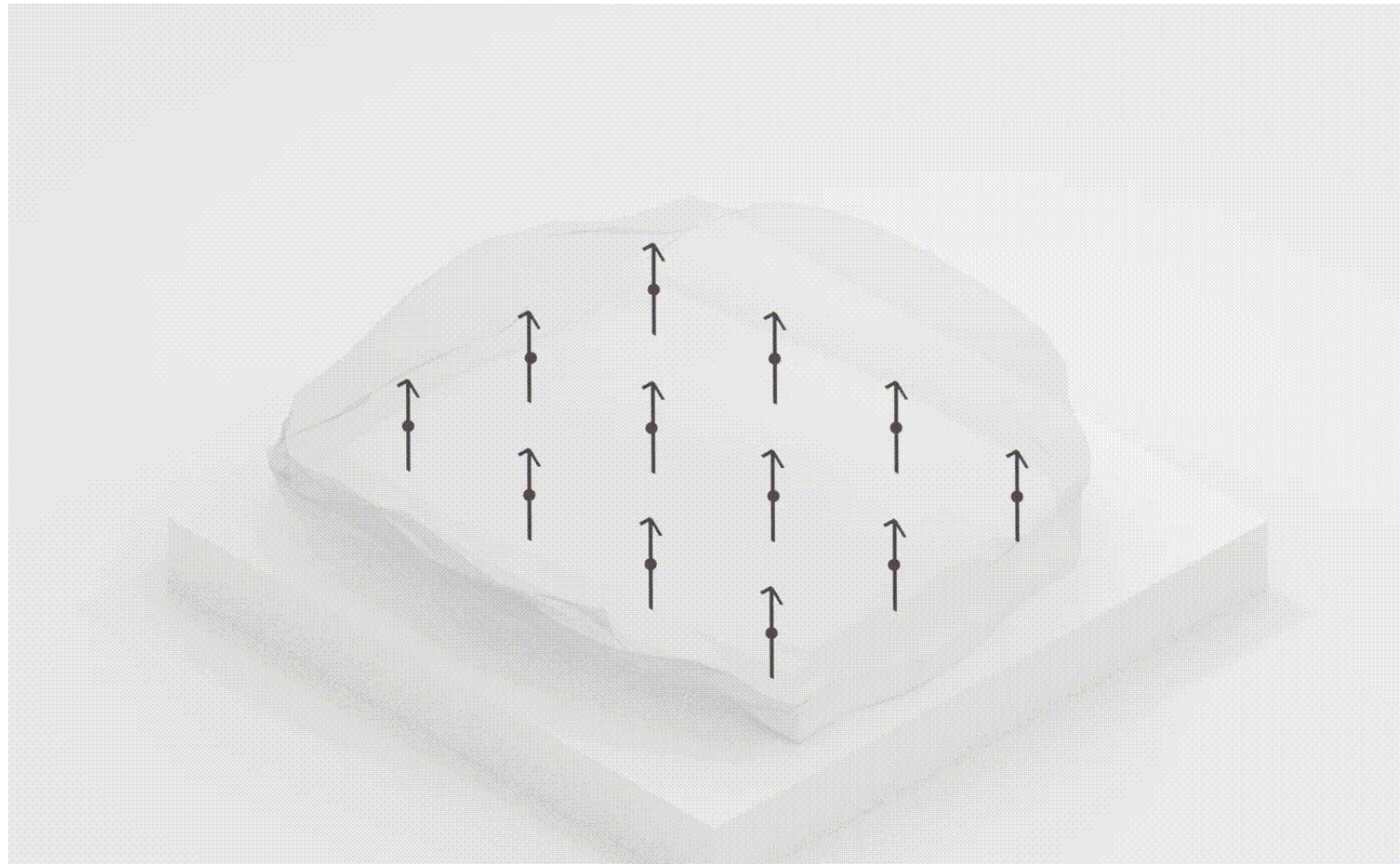
$$\mathcal{H}_{dip} = \frac{\mu_0}{4\pi} \left(\frac{\vec{\mu}_\mu \cdot \vec{\mu}}{r^3} - \frac{3(\vec{\mu}_\mu \cdot \vec{r})(\vec{\mu} \cdot \vec{r})}{r^5} \right)$$

dipole field



μ SR: Static Field

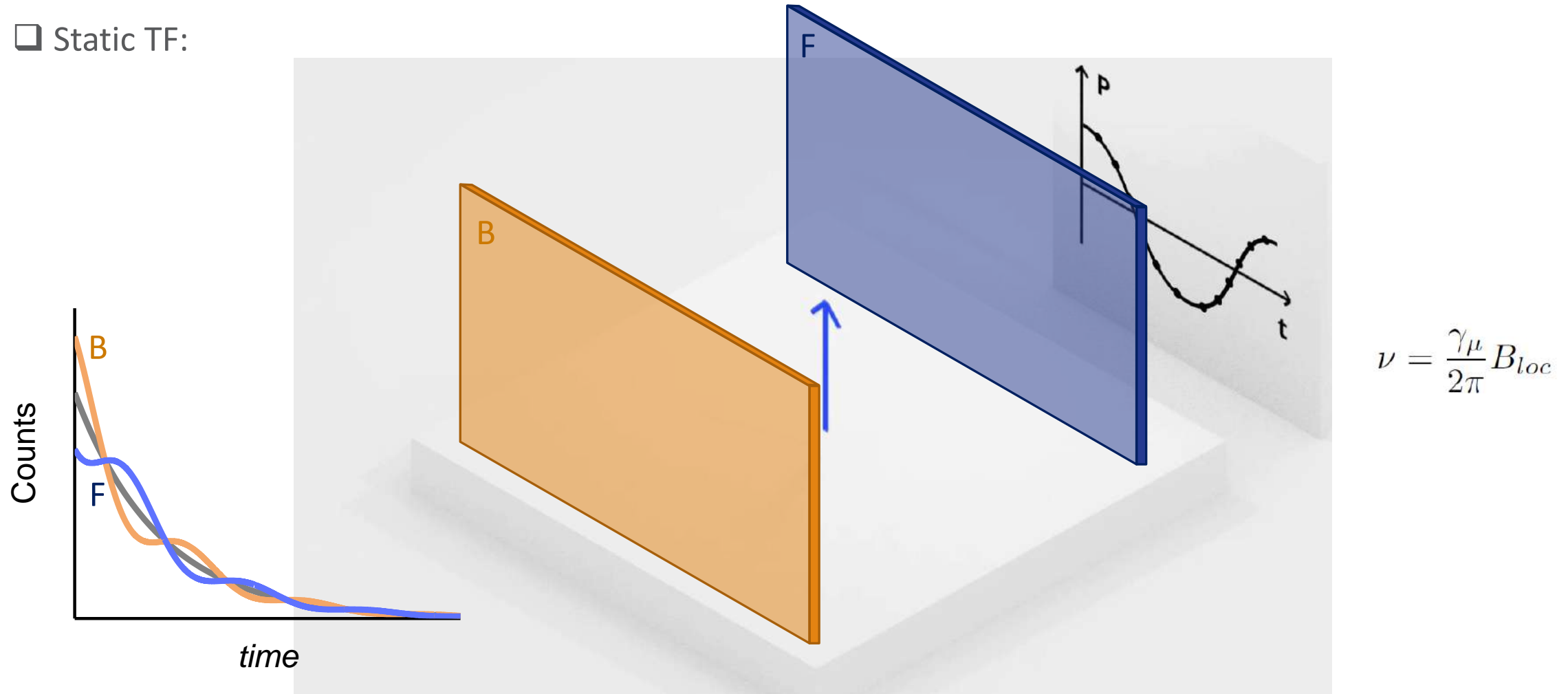
□ Static TF:



https://upload.wikimedia.org/wikipedia/commons/8/87/Muon_Spin_Resonance_%28Musr%29.webm

μ SR: Static Field

□ Static TF:



https://upload.wikimedia.org/wikipedia/commons/8/87/Muon_Spin_Resonance_%28Musr%29.webm

μ SR: Static Field

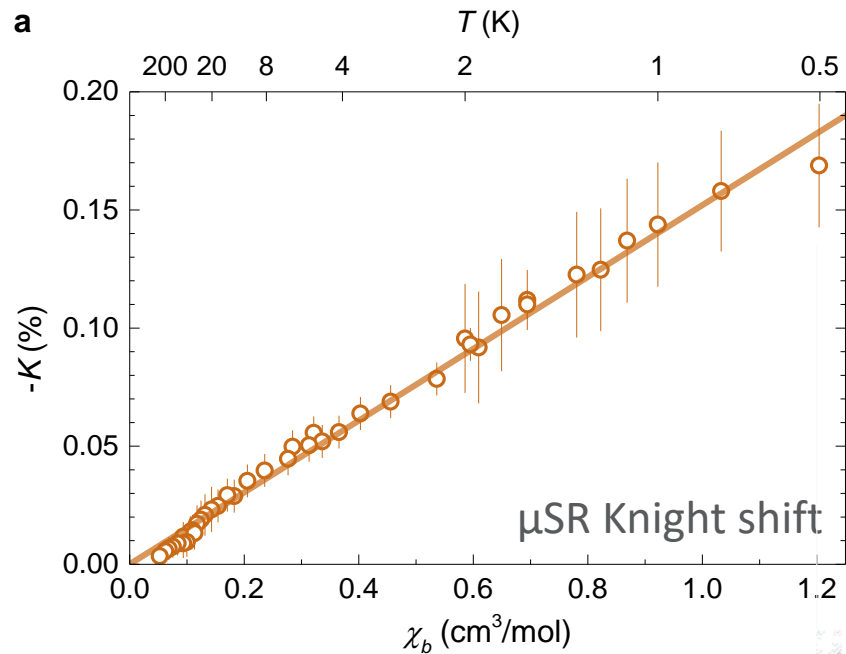
□ Static TF: frequency shift

$$B_{loc} \ll B_0$$



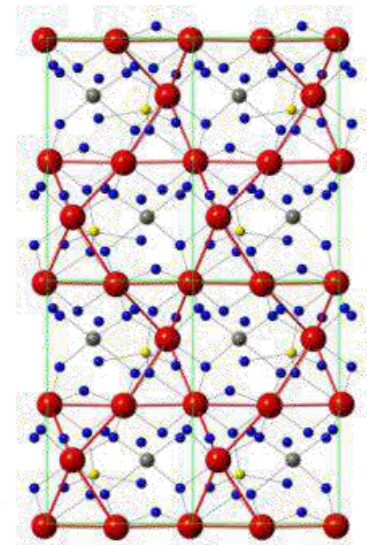
$$K = \frac{B_{loc} - B_0}{B_0} = \frac{\nu - \nu_L}{\nu_L}$$

$$K = \sum_j \tilde{A}_{ij} \chi(q=0, \omega=0)$$

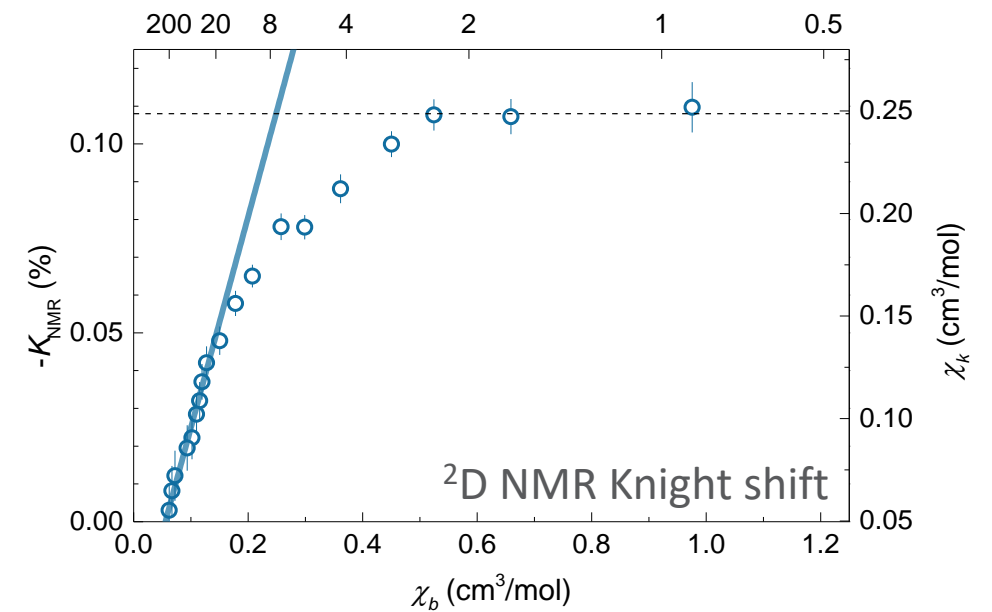


coupling to **intrinsic** and **impurity** spins

Zn-brochantite:
distorted KAFM
(spinon FS QSL)



Gomilšek *et al.*, Nat. Phys. **15**, 754 (2019)



coupling to only **intrinsic** spins



μ SR: Static Field

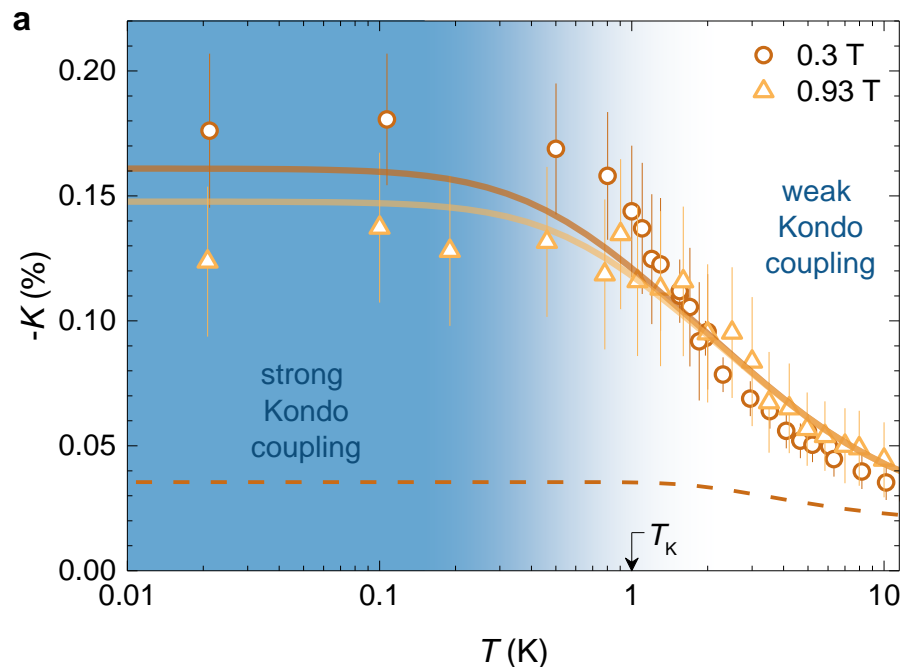
□ Static TF: frequency shift

$$B_{loc} \ll B_0$$

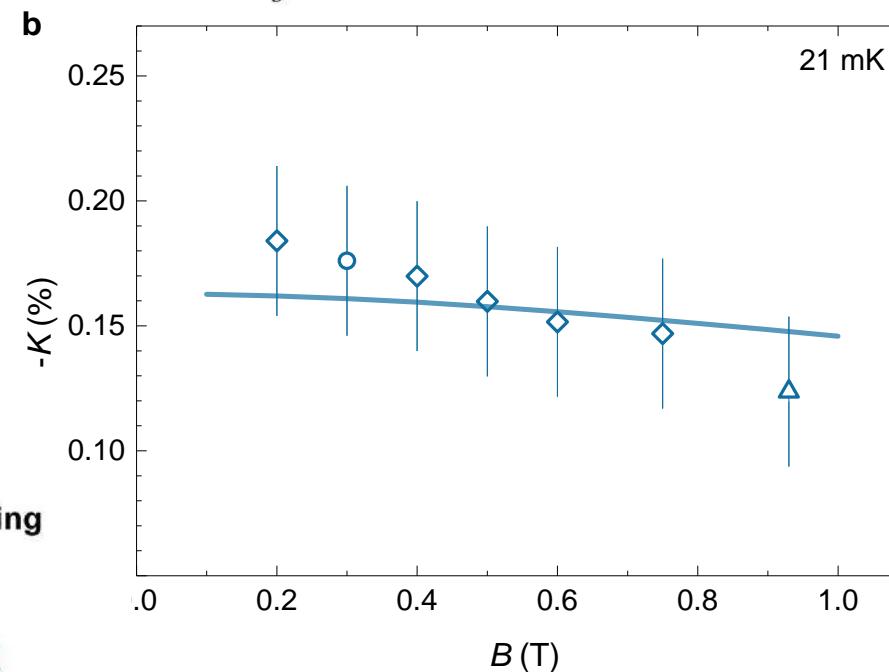
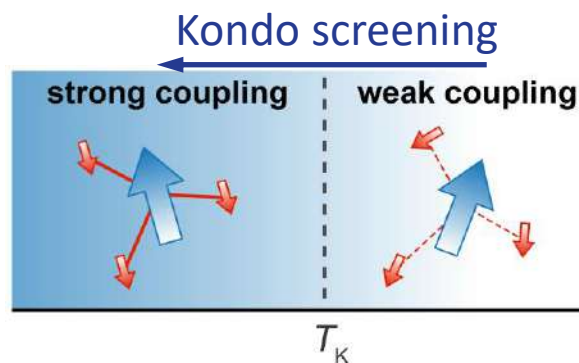


$$K = \frac{B_{loc} - B_0}{B_0} = \frac{\nu - \nu_L}{\nu_L}$$

$$K = \sum_j \tilde{A}_{ij} \chi(q=0, \omega=0)$$



Zn-brochantite:
distorted KAFM
(spinon FS QSL)



spinon Kondo effect



coupling of spinons

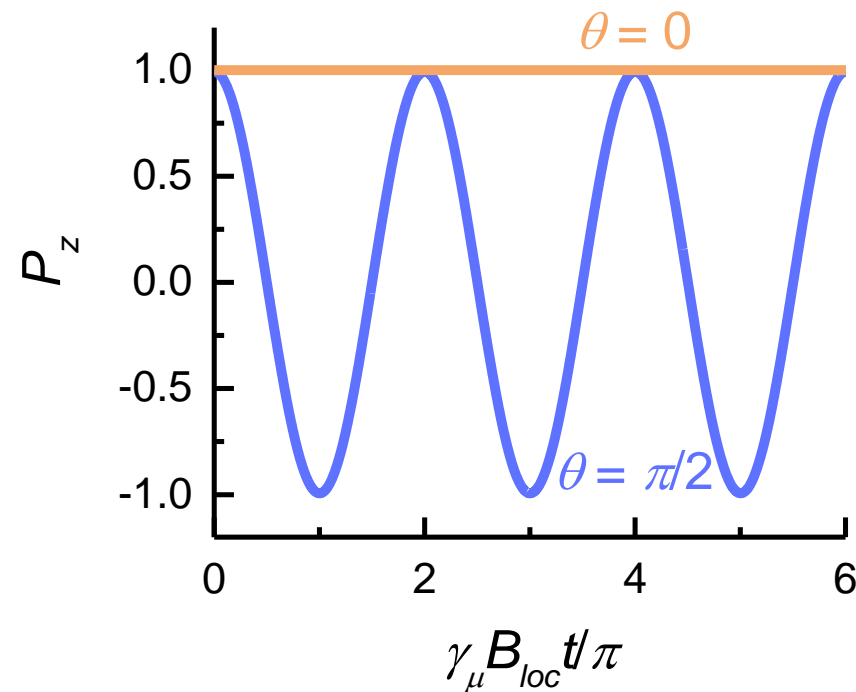
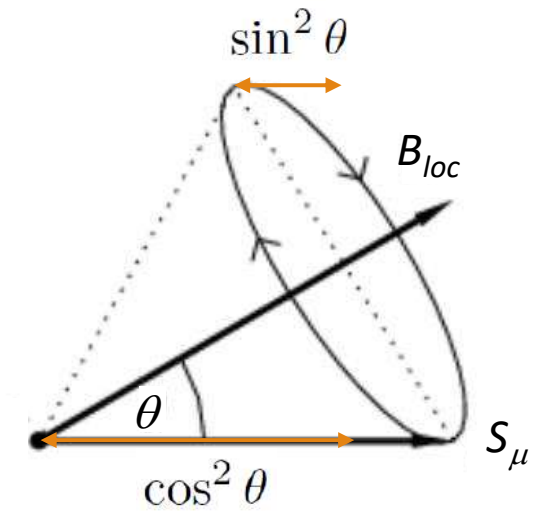
Gomilšek, AZ et al., Nat. Phys. **15**, 754 (2019)



μ SR: Static Field

□ Static local field:

$$P_z(t) = \cos^2 \theta + \sin^2 \theta \cos(\gamma_\mu B_{loc} t)$$

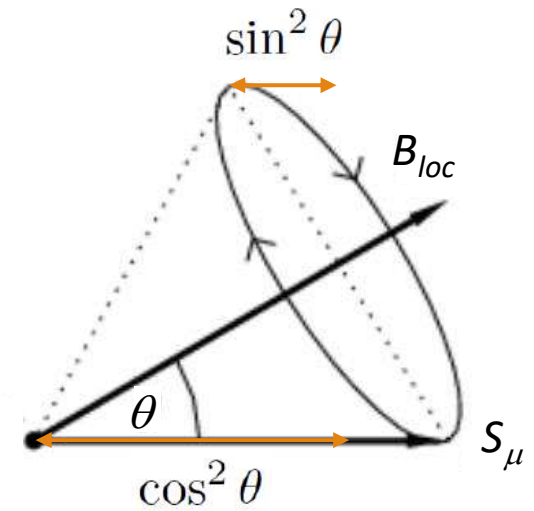
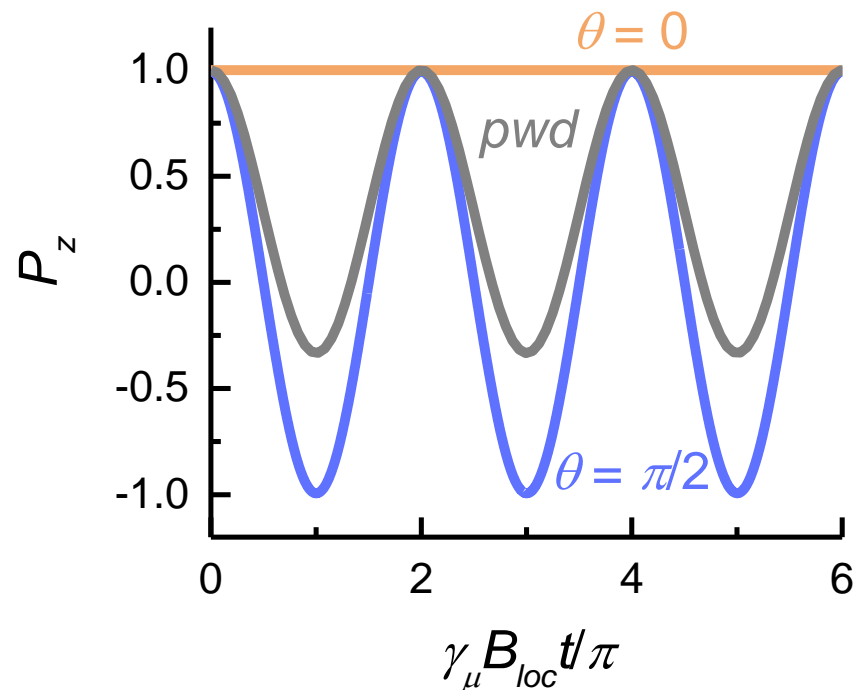


μ SR: Static Field

□ Static local field:

$$P_z(t) = \cos^2 \theta + \sin^2 \theta \cos(\gamma_\mu B_{loc} t)$$

powder \longrightarrow $P_z(t) = \frac{1}{3} + \frac{2}{3} \cos(\gamma_\mu B_{loc} t)$

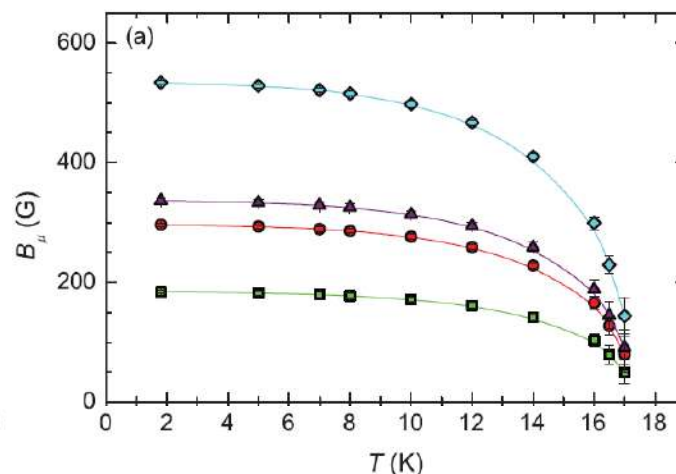
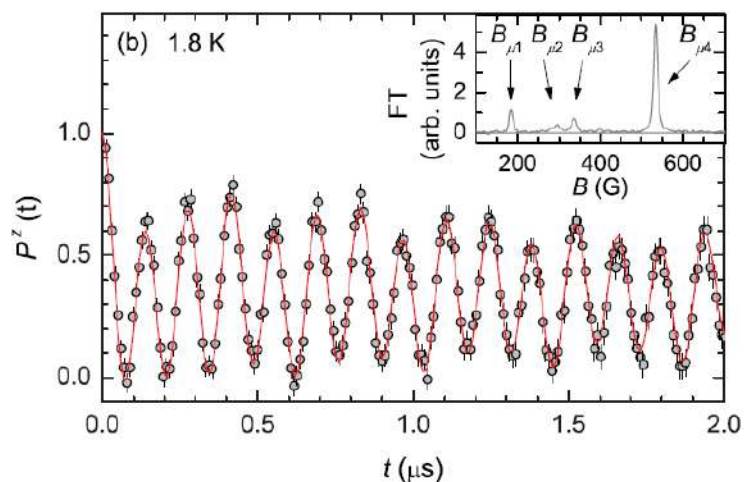
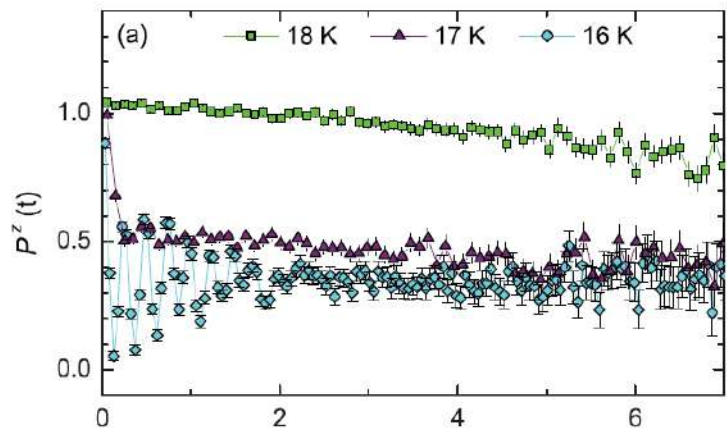
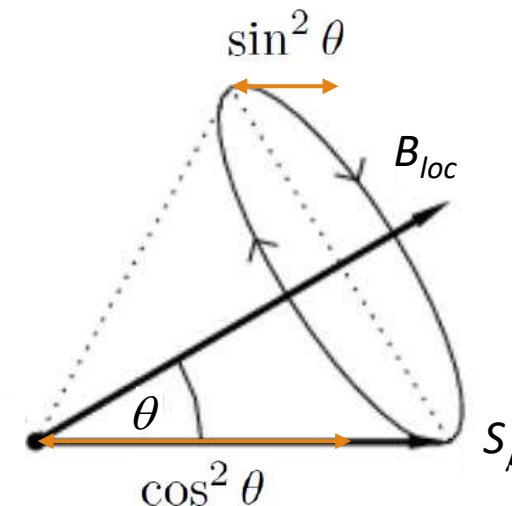


μ SR: Static Field

□ Static local field:

$$P_z(t) = \cos^2 \theta + \sin^2 \theta \cos(\gamma_\mu B_{loc} t)$$

$$P_z(t) = \frac{1}{3} + \frac{2}{3} \cos(\gamma_\mu B_{loc} t)$$



Herak *et al.*, Phys. Rev. B **87**, 104413 (2013)

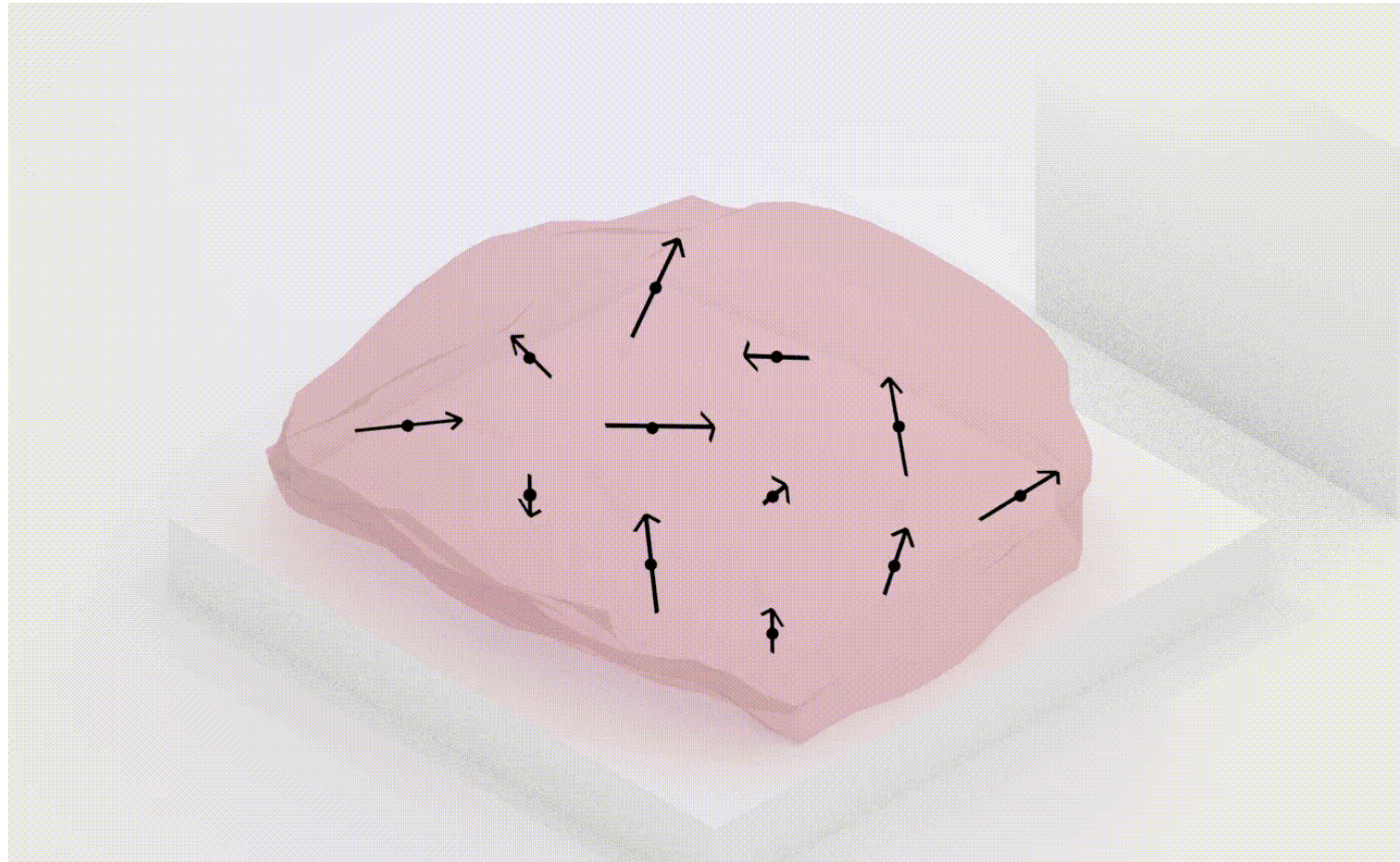
quasi-1D: CuSe_2O_5

- order parameter
- volume fraction
- FT analysis



μ SR: Static Field

□ Static-field (random) distribution:



$$\nu = \frac{\gamma_{\mu}}{2\pi} B_{loc}$$

https://upload.wikimedia.org/wikipedia/commons/8/87/Muon_Spin_Resonance_%28Musr%29.webm

μ SR: Static Field

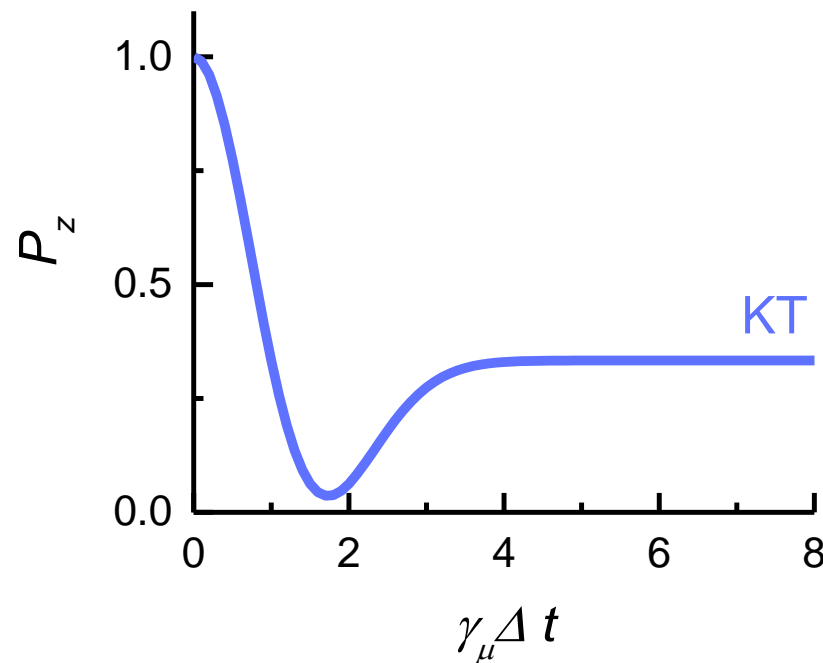
- Static-field (random) distribution:
Gaussian

$$\text{prob}(B) \propto B^2 e^{-B^2/2\Delta^2}$$



ZF Kubo-Toyabe function

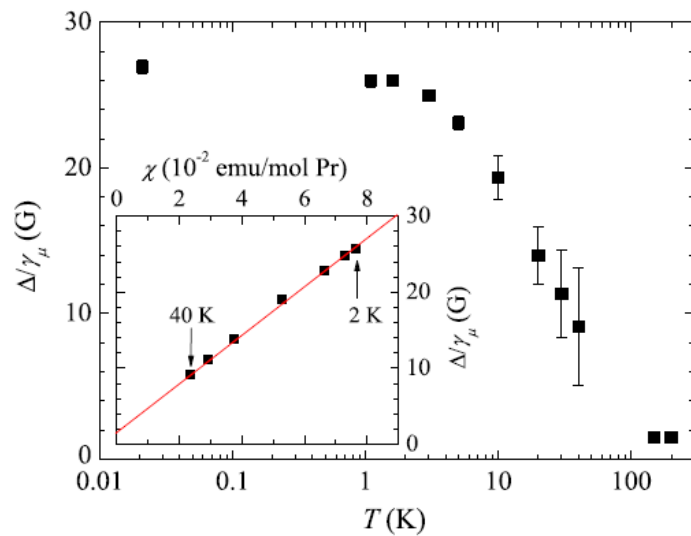
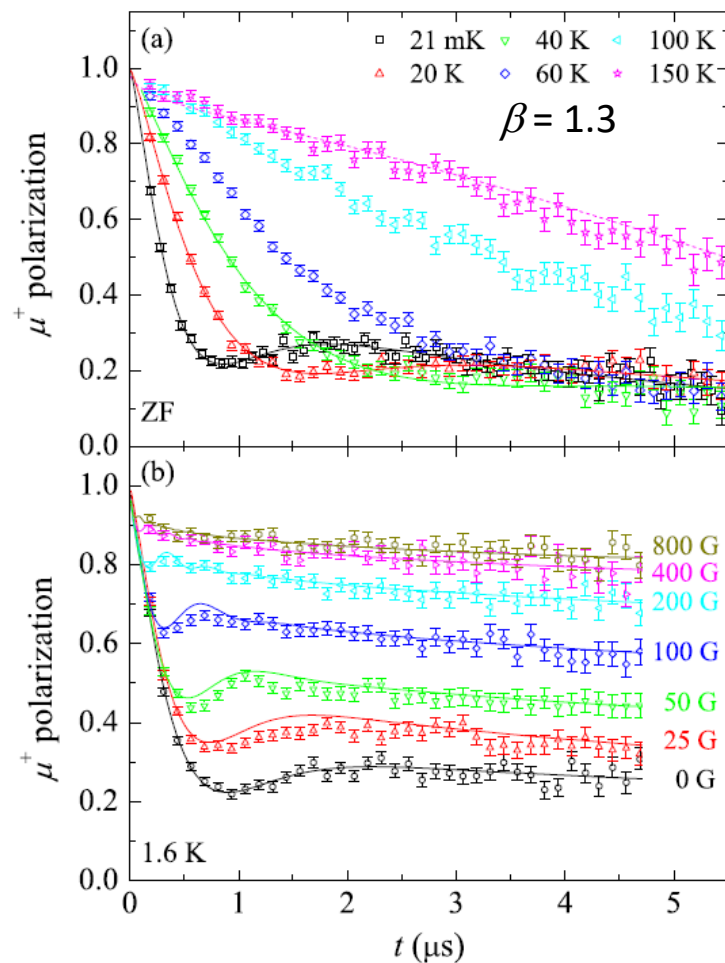
$$P_z(t) = \frac{1}{3} + \frac{2}{3} e^{-\frac{1}{2} \gamma_\mu^2 \Delta^2 t^2} (1 - \gamma_\mu^2 \Delta^2 t^2)$$



Ryogo Kubo

μ SR: Static Field

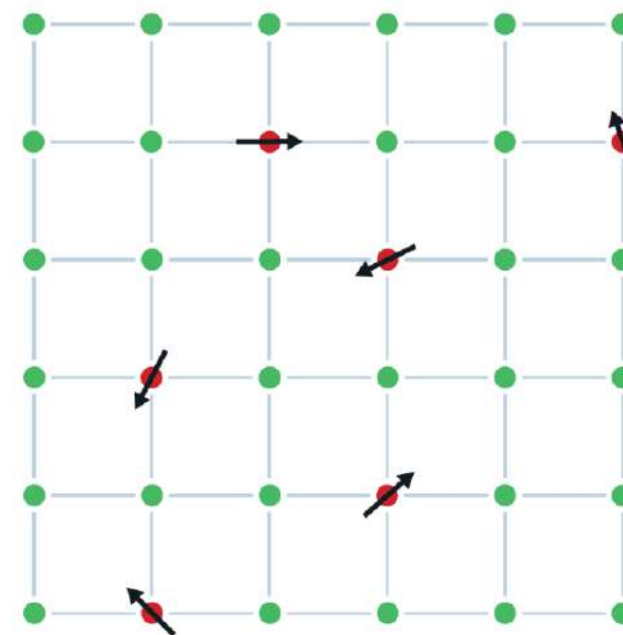
□ Voightian Kubo-Toyabe:
$$P_z(t) = \frac{1}{3} + \frac{2}{3} e^{-\frac{1}{\beta} (\gamma_\mu^2 \Delta^2 t^2)^\beta} [1 - (\gamma_\mu^2 \Delta^2 t^2)^\beta]$$



kagome lattice: $\text{Pr}_3\text{Ga}_5\text{SiO}_{14}$

- hyperfine-enhanced ^{141}Pr magnetism
- Van-Vleck paramagnet

Lorentzian ($\beta = 1$) for diluted moments: spin glass



Zorko *et al.*, Phys. Rev. Lett. **104**, 057202 (2010)

<https://www.forbes.com>



μ SR: Dynamic Fields

□ Change of the local field at frequency ν :

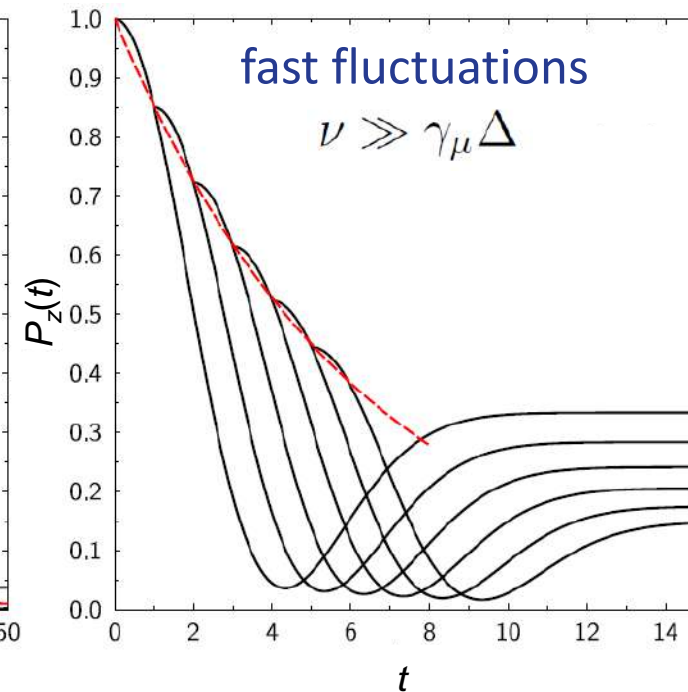
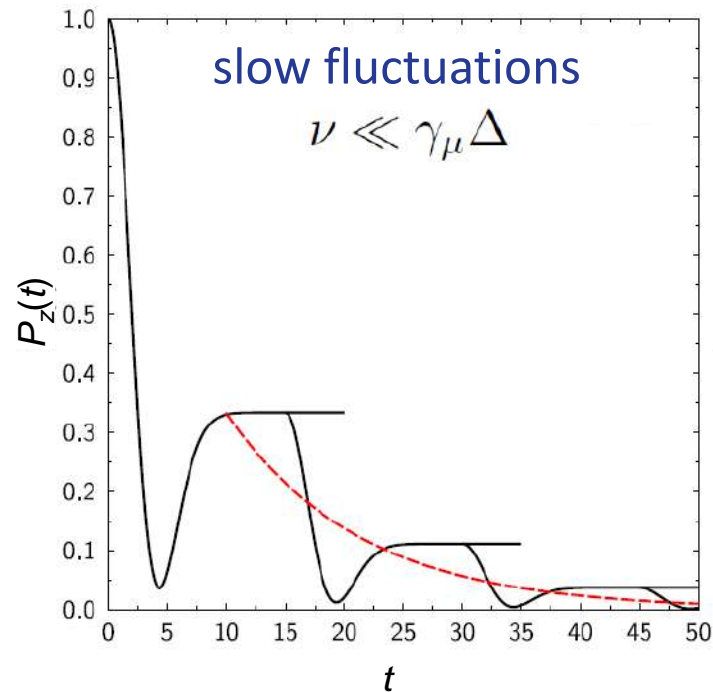
- random oscillations
- muon hopping
- elementary excitations

$$\lambda = \gamma_\mu^2 \int_0^\infty \langle B_{loc}^+(t) B_{loc}^-(0) \rangle e^{-i\omega_L t} dt$$

spectral density

$$\langle B_{loc}^+(t) B_{loc}^-(0) \rangle = \Delta^2 e^{-\nu t} \quad \longrightarrow \quad \lambda = \frac{\gamma_\mu^2 \Delta^2 \nu}{\nu^2 + \gamma_\mu^2 B_0^2}$$

!
 →
 relaxation
 of the “tail”



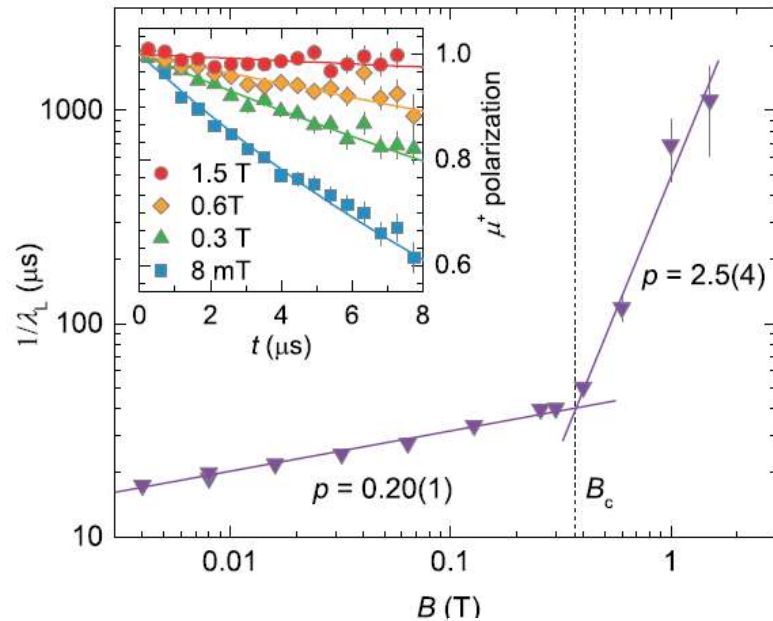
!
 ←
 exchange
 narrowing

$$P_z(t) = e^{-\lambda t}$$



μ SR: Dynamic Fields

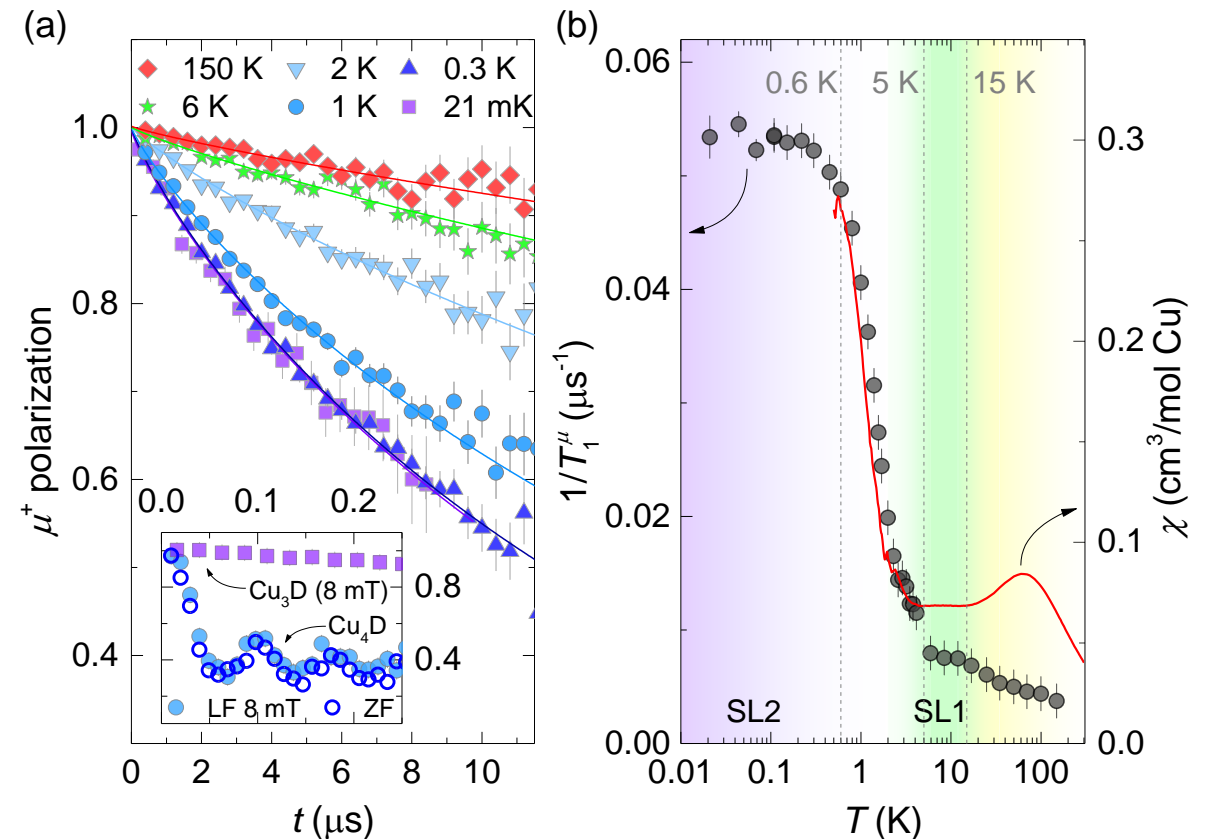
- Monotonic $P_z(t)$: fingerprint of a dynamical state (e.g., QSL)
- Field dependence of λ : energy dependence of the spectral density of fluctuations



$$S(\omega) \propto \omega^{-0.2} \longrightarrow \langle B(t)B(0) \rangle \propto t^{-0.8}$$

Gomilšek *et al.*, Phys. Rev. B **94**, 024438 (2016)

Zn-brochantite: distorted KAFM
(spinon FS QSL)



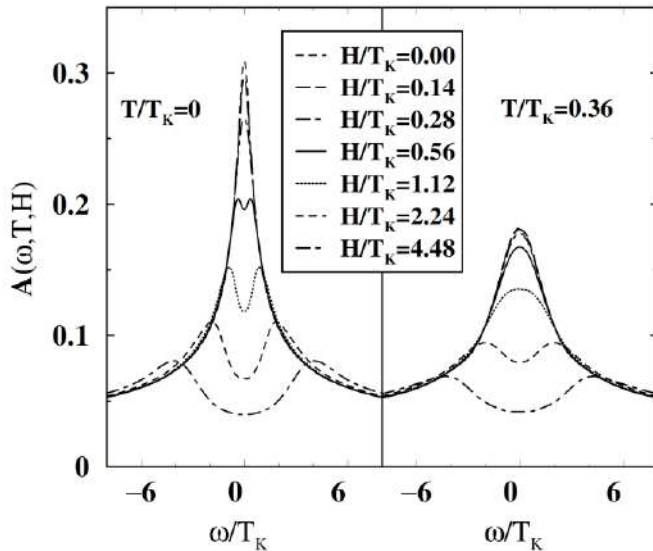
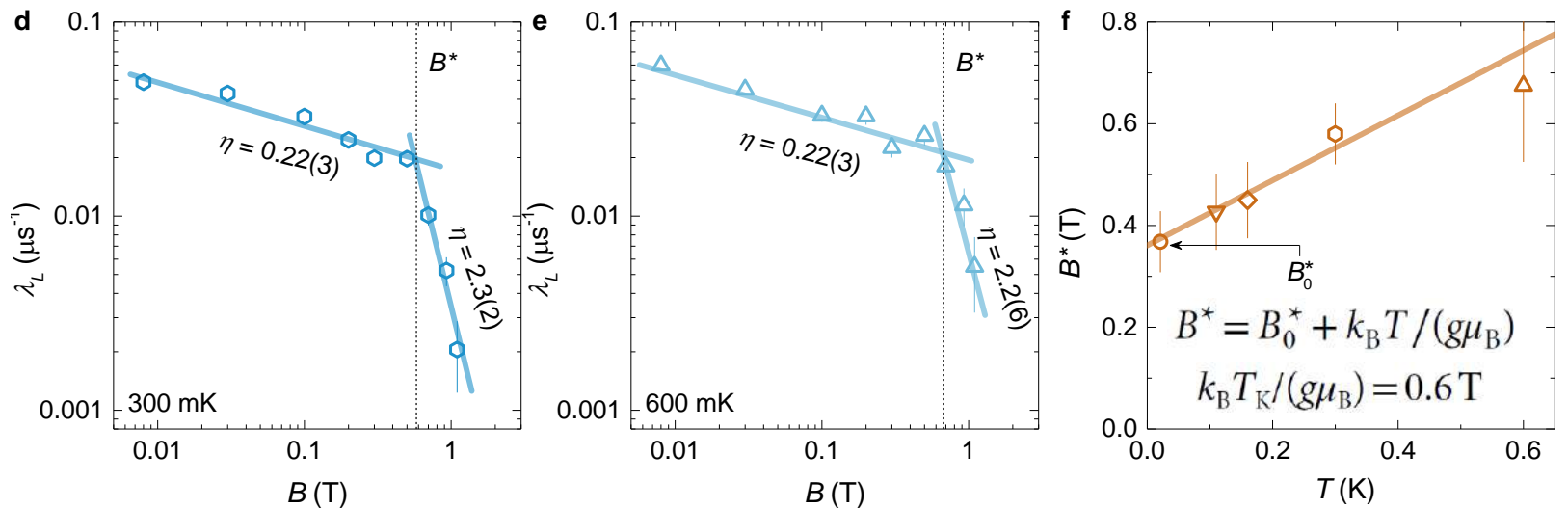
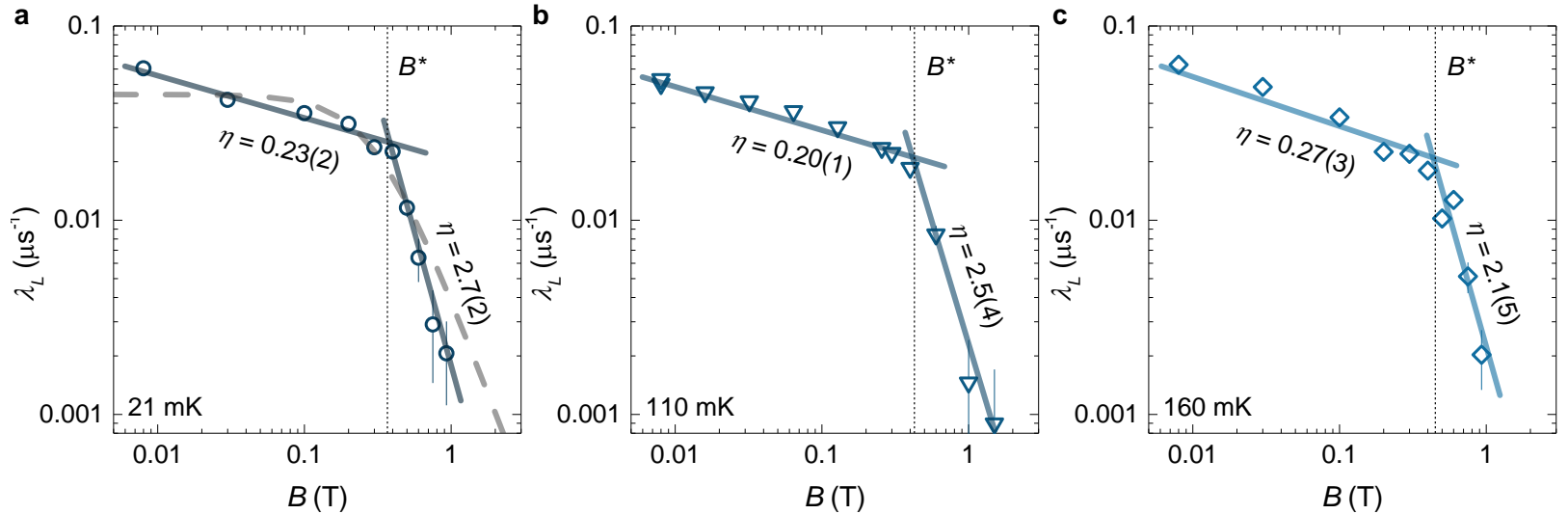
Gomilšek *et al.*, Phys. Rev. B **93**, 060405(R) (2016)



μ SR: Dynamic Fields

Changes in spin excitations:
Kondo-resonance splitting

- decrease of local DOS at the Fermi level
- finite critical field linear in T



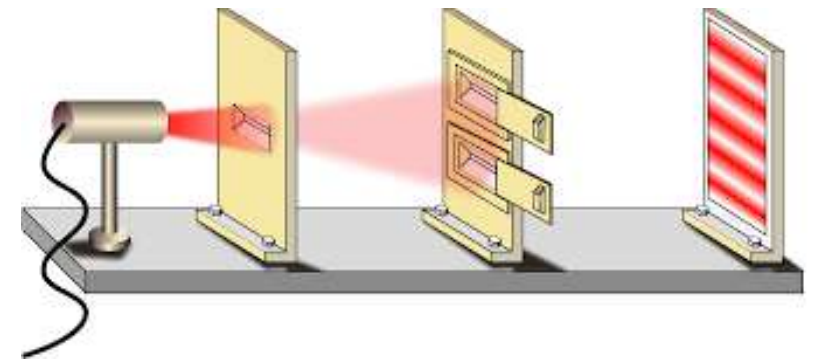
Costi *et al.*, PRL **85**, 1504 (2000)

Gomilšek *et al.*, Nat. Phys. **15**, 754 (2019)



Outline

- Introduction to magnetism
- Probing magnetism: conventional bulk and scattering techniques
- Local probes of magnetism
- Electron spin resonance (ESR)
- Nuclear magnetic resonance (NMR)
- Muon spectroscopy (μ SR)
- Summary: strengths, limitations and complementarity of local probes



Summary: STRENGTHS and LIMITATIONS



	ESR	NMR	μ SR
Sample	ESR lines not too broad (bulk samples)	many available nuclei (bulk samples)	any sample (thin-films possible, $\sim 0.01\mu_B$)
Acquisition	a few minutes	a few hours	tens of minutes
Probe location	on magnetic site	close-far from magnetism	not exactly known
Probe coupling	direct (?)	hyperfine, 0.1-10 T/ μ_B	dipolar, 0.01-0.1 T/ μ_B
Signal relaxation	only extremely "slow" relaxations can be measured	slow relaxation (infinite acq.) fast relaxation (deadtime μ s)	slow relaxation (muon decay) fast relaxation (deadtime ns)
T-range	0.35 – 1000 K (polarization decreases with T)	0.02 – 1000 K (polarization decreases with T)	0.02 – 800 K constant polarization
B-range	0.1 – 45 T finite B_0 might affect physics	1 – 45 T finite B_0 might affect physics	0 – 9.5 T inherent polarization (ZF exp.)
Perturbation	non-perturbative	non-perturbative	muon = charge defect
Cost	low cost	low cost	large-scale facilities (high cost)



Summary: Complementarity

□ Time windows: spin dynamics

➤ slow fluctuations: $\frac{1}{T_1} \propto \nu$

➤ fast fluctuations: $\frac{1}{T_1} \propto \frac{(\gamma A)^2}{\nu}$

$$\frac{A_{\text{NMR}}}{A_{\mu\text{SR}}} \sim 10 - 100 \quad \frac{\gamma_{\text{NMR}}}{\gamma_{\mu\text{SR}}} \sim \frac{1}{10}$$

➤ ESR: $\Delta B > 0.3 \text{ mT}$

↓

$$\frac{1}{T_1^{\text{ESR}}} < 100 \text{ ns}$$

➤ Combination of techniques: complementary insights

